Biochemical Mechanisms of PriA-Mediated DNA Replication Restart

By

Basudeb Bhattacharyya

A dissertation submitted in partial fulfillment of

the requirements for the degree of

Doctor of Philosophy

(Biochemistry)

at the

UNIVERSITY OF WISCONSIN-MADISON

2014

Date of final oral examination: 5/9/14

The dissertation is approved by the following members of the Final Oral Committee:

James L. Keck, Professor, Department of Biomolecular Chemistry
Michael M. Cox, Professor, Department of Biochemistry
Joseph P. Dillard, Associate Professor, Department of Medical Microbiology & Immunology
David L. Nelson, Professor Emeritus, Department of Biochemistry
M. Thomas Record, Professor, Department of Biochemistry

ABSTRACT

The mechanism by which genetic information is duplicated and transmitted to future generations in all organisms requires the coordination of several multi-protein complexes. These genome maintenance complexes generally bind and unwind duplex DNA to allow access to genomic information. In *Escherichia coli* and related bacteria, initiation of DNA replication occurs at a unique site (*oriC*) on a circular chromosome at which two replisome complexes assemble and then replicate bi-directionally away from this initiation site. However, approximately once per cell cycle, the replisomes encounter DNA damage or stalled protein complexes that prematurely force the replication machinery off the template, leaving partially duplicated chromosomes. This situation presents a potentially lethal situation for the cell and requires a sequence-independent system that reloads the replisome onto sites far removed from *oriC*. This DNA structure-dependent process of reloading the replisome is achieved through a group of proteins collectively known as the DNA replication restart primosome (RRP) and their functions are essential in bacteria. The RRP is composed of four proteins (PriA, PriB, PriC, and DnaT) that work in diverse pathways to reload the replicative helicase, DnaB, onto abandoned replication forks. PriA, a 3' to 5' helicase, is the most evolutionarily conserved member of the RRP, and it defines the dominant pathway by which replication restart occurs in bacteria. However, the lack of high-resolution structural data for PriA has hindered studies to understand how it recognizes and processes abandoned DNA replication forks. This thesis presents the first high-resolution structures of full length PriA. Models emerge explaining how PriA recognizes and remodels DNA via its intrinsic helicase activity and protein interactions that may or may not be coated with single stranded DNA binding protein (SSB). The results help to explain the results of over 30 years of biochemical experiments as well as providing novel mechanistic details of DNA replication restart.

ACKNOWLEDGEMENTS

The work presented in this thesis would not have been possible without so many people in my life and I am forever indebted for all the support given to me by so many special people over the past six years. I would first like to thank my advisor Jim Keck. Jim, your positive enthusiasm for science, and life in general, was a major reason why I joined your lab. You were always open and willing to let me be creative and explore my thesis project in ways that made me constantly look at science more completely. You fully embraced my desire to pursue outreach activities in addition to my graduate studies and I'm incredibly grateful to you for allowing me to do this.

I owe many thanks to the rest of my thesis committee: Mike Cox, Tom Record, Joe Dillard, and Dave Nelson. Along with Jim, you made me a better scientist, improving my abilities to critically analyze, challenging me intellectually, and always providing constructive feedback on better ways to approach my project. I want to give special thanks to Dave who inspired a love of teaching in me. You were always there for me since my undergraduate days, providing moral support during the times I struggled most. Your door was always open and you were always willing to talk about science or just what was going on in my life. I could not imagine the past decade without your guidance and mentorship, and for that, I am forever indebted to you.

To my lab mates in the Keck Lab—you made coming into work fun, educational, and exciting. Former Keck Lab members include Aimee Marceau, Scott Lindner, Duo Lu, and Angela Myers who were there during my first few years and helped me as I was learning new techniques. To current lab members Kelly Manthei, Chrissy Petzold, Sarah Wessel and Tricia Windgassen, thank you for being some of the best lab mates I have had, providing support and advice whenever needed. I wish you all the best in all your future endeavors.

I have been very fortunate to have worked with many students, middle and high school as well as undergraduates over the years. Teaching had healing powers for me and the contributions of working with all these students in me reaching this point cannot be understated. Special mention goes to Tiffany Thurmes, an undergraduate that I have been fortunate to work with over these past three years. Tiffany, you've made me a better teacher and I know you will make a fantastic pharmacist some day!

To my friends, thank you. Jon Mayers was always ready to discuss science or the latest fantasy leagues we participate in. Lisa Lenertz always provided great cheer and important career advice and perspectives. To Ben Spaier…we survived so much together, coaching and just exploring the country (or at least, the Midwest). To Laura and Nick George, you have been a special part of my life these past six years and I feel so fortunate to have your friendship, support, and love. Whether it was an escapade with a cat in a bathroom or learning the deeper meanings of life while drywalling two houses, I definitely could not have made it through graduate school without you. To Amber Schuh, you have meant so much to me over these past few years. I have enjoyed every moment that we got to spend together. Your smile always brightened up my darkest days and you will always have a special place in my heart.

Last, but not least, I want to thank my family. To my brother Joydeb and sister Paula…you were like a second set of parents in addition to being my siblings. Your love and support were instrumental in all my achievements and you've always been there for me. To Yu-lien Chu, you've become a sister to me and I thank you for all your support. Last, to my parents…you sacrificed your own dreams and worked hard in order to provide a better life and education for me, Joydeb and Paula. You taught me the value of hard work and sacrifice and made me what I am today. While my father passed away and my mother was not able to make it to my defense

due to ill health, I know both of you are constantly there with me and I hope I have made you proud.

TABLE OF CONTENTS

Abstract i
Acknowledgements ii
Table of Contents v
List of Tables and Figures vii
List of Abbreviations viii

Chapter 1: DNA Replication Restart 1
Abstract 2
Introduction 3
DNA Replication Restart: A Historical Perspective 4
The Replication Restart Proteins: Recognition and Remodeling of Abandoned Replication Forks 6
Proposed Models of DNA Replication Restart 18
Replication Restart in Eukaryotes 21
Future of DNA Replication Restart 22
Figures 24
References 28

Chapter 2: Structural Mechanisms of PriA-Mediated DNA Replication Restart 37
Abstract 38
Significance 39
Introduction 40
Results and Discussion 43
Materials and Methods 52
Acknowledgements 53
Figures 2.1-2.4 54
References 62
Supplemental Text Table of Contents 66
Supplemental Information (SI) Materials and Methods 67
Tables 2.1-2.3 74
Figures 2.5-2.9 77
Supplemental Information (SI) References 88

Chapter 3: Elucidating the Role of the Winged Helix Domain of *Escherichia coli* PriA 90

Abstract 91

Introduction 92

Materials and Methods 94

Results 99

Discussion 101

Figures and Tables 104

References 116

Chapter 4: Conclusions and Future Perspectives 118

Introduction 119

Final Perspectives 123

References 128

LIST OF FIGURES AND TABLES

Figure 1.1: The Physiological Importance of DNA Replication Restart (page 24)

Figure 1.2: DNA Replication Restart Pathways in *Escherichia coli* (page 26)

Figure 2.1: Structure of PriA DNA Helicase (page 54)

Figure 2.2: PriA Domain Features (page 56)

Figure 2.3: PriA/SSB Complex Structure and Function (page 58)

Figure 2.4: PriA Replication Restart Initiation Models (page 60)

Table 2.1: X-ray data collection and structure determination statistics (page 74)

Table 2.2: Oligonucleotides used in this study (page 75)

Table 2.3: Strains used in this study (page 76)

Figure 2.5: Biochemical, Cellular and Sequence Comparison of KpPriA and EcPriA (pages 77-78)

Figure 2.6: Comparison of PriA and LexA WH domains (page 80)

Figure 2.7: Comparison of the Putative PriA DNA Unwinding Wedge to Wedge Elements in other Superfamily II DNA Helicases (page 82)

Figure 2.8: DNA Unwinding by EcPriA and the Arg697Ala EcPriA Variant (page 84)

Figure 2.9: smFRET analysis of DNA binding by EcPriA and the Arg697Ala EcPriA variant (page 86)

Figure 3.1: Recognition of Abandoned Replication Forks via the N-terminus of PriA (page 105)

Table 3.1: Relevant Strains used in this Study (page 106)

Figure 3.2: PriA ΔWH is Capable of Binding a Model Replication Fork (page 107)

Figure 3.3: PriA ΔWH Displays Reduced ATPase Activity (page 109)

Figure 3.4: PriA ΔWH Maintains Robust Helicase Activity (page 111)

Figure 3.5: PriA ΔWH Displays Unique Phenotypes *in vivo* (page 113)

Table 3.2: Quantification of Phenotypic Analysis of *priA ΔWH* (page 115)

LIST OF ABBREVIATIONS

ARL: Aromatic rich loop

BPA: Bisphenol A

CRR: Cysteine rich region

CTD: C-terminal domain

DBD: DNA binding domain

DSB: Double stranded breaks

dsDNA: Double stranded DNA

FP: Fluorescence polarization

HD: Helicase domain

ITC: Isothermal titration calorimetry

RRP: Replication restart primosome

SAXS: Small angle X-ray scattering

SSB: Single stranded DNA binding protein

SSB-CT: SSB C-terminal tail peptide (WMDFDDDIPF)

ssDNA: Single stranded DNA

WH: Winged-helix domain

Chapter 1

DNA Replication Restart

This chapter represents a publication in preparation:

Bhattacharyya B, Wessel SR, Windgassen T, Lopper ME, Sandler SJ, and Keck JL. DNA Replication Restart. *Critical Reviews in Biochemistry and Molecular Biology, in preparation*

Abstract

DNA replication is a complicated, orchestrated dance of multi-protein complexes that perform the essential process of transmitting genetic information to subsequent generations. Common themes are present across all kingdoms of life: initiation through site-specific replication protein complex binding (replisome); translocation and replication of the genome of both leading and lagging strand templates in a direction-specific manner; and termination of replication that includes removal of the replisome and final processing of DNA products. While the general processes achieve similar results, the diversity of genomic structures provides unique challenges to faithful DNA replication. Case in point, bacterial chromosomes such as those present in *Escherichia coli* and related bacteria possess a circular chromosome with one origin of replication (*oriC*) where DNA replication is initiated. Bacterial DNA replication rarely occurs without some interrupting event that has the potential to dislodge the replisome. Such an event is potentially lethal for the cell and requires housekeeping processes to reload the replisome. DNA replication restart serves the purpose of reloading the replicative helicase which leads to subsequent loading of the rest of the replisome. Coordinated by a group of proteins known as the Replication Restart Primosome (RRP), diverse abandoned replication forks that occur as the result a wide array of DNA replication disruption events can be successfully processed. The focus of this review covers the RRP proteins PriA, PriB, PriC, and DnaT from *E. coli* and related gram negative organisms, their genetic and biochemical contexts, recent structural work, and insights into their broader placement in genome maintenance processes.

Introduction

Transfer of genetic information to successive generations is an essential life process. DNA replication achieves information transfer by a coordinated effort of multi-protein complexes that deal with a unique helical, directional, and double stranded template in a highly regulated fashion. Core activities of these protein complexes, known as the replisome, are conserved across kingdoms and include initiating genome duplication, unwinding duplex DNA, movement along DNA substrates, and replication of the template via nucleotide incorporation. While the core actions of initiation, elongation, and termination possessed by these protein complexes is conserved across kingdoms, obvious variations and differences do exist among diverse organisms in how they regulate DNA replication, deal with unique chromosome structures and topologies, and overcome DNA damage or other events that require DNA repair mechanisms.

DNA replication in the model organism *Escherichia coli* has been extensively studied and has provided a basic understanding of the diverse mechanisms of genome duplication employed by all organisms, including humans. In *E. coli*, DNA replication is initiated at a unique sequence known as the origin of replication (*oriC*). Duplex DNA at *oriC* is melted by the initiator ATPase DnaA that forms a nucleoprotein filament (1, 2). Exposure of single-stranded DNA (ssDNA) at the origin allows for loading of the replicative helicase DnaB with the aid of the helicase loader DnaC (3-6). Additional exposed ssDNA on the lagging strand template is quickly coated by single-stranded DNA binding protein (SSB) (7). Loading of DnaB leads to spontaneous loading of the replicative polymerase III holoenzyme (PolIII HE), a complex of 10 proteins that uses the power of ATP hydrolysis to duplicate the genome, as well as the primase DnaG which allows for replication initiation on the lagging strand and replication through formation of Okazaki fragments (8-10). Together, these proteins form the core replisome.

Replication proceeds bi-directionally away from *oriC* by two sets of replisomes until encountering *ter* sites coated with Tus protein, leading to dislodging of the replisomes (11). Newly synthesized daughter strands are processed and split creating two new daughter chromosomes.

DNA replication does not occur in a vacuum free from obstacles and replisome progression is often impeded by damage to the template or even normal metabolic functions of the cell, such as transcription protein complexes that occur concurrently with DNA replication, but move at a rate a magnitude slower (12). Encounters with such obstacles can cause the replisome to stall (pause) or collapse (abandonment of the replication fork). For *E. coli*, stalling and/or collapse of the replication fork is potentially lethal because of the circular nature of the chromosome and the reliance of a singular site for replication initiation—partially replicated chromosomes are deadly. Much speculation has been drawn to the importance of restarting replication from abandoned replication forks. The occurrence of such catastrophic events is difficult to measure, with one estimate of fork collapse occurring once per cell cycle (13). Recent *in vitro* work has also identified the ability of *E. coli* to withstand and even bypass complications related to replication fork stalling/collapse (14). Regardless of the rate these events occur, *E. coli* has evolved distinct mechanisms and pathways to reload the replisome on sites far removed from *oriC*, suggesting a dedicated need for the existence of such systems and highlighting the role of DNA replication restart as a general genome housekeeping process.

DNA Replication Restart: A Historical Perspective

DNA replication restart proteins were originally referred to as the primosome assembly proteins, a name which referred to a multi-subunit complex that synthesized RNA primers used by DNA polymerases to replicate DNA (15). Historically, this protein complex was purified

using DNA replication as a measure of activity using the ΦX174 phage DNA as the substrate (16-18). The ΦX174 chromosome is a ssDNA circle that contains a novel two hairpin structure called the Primosome Assembly Site (PAS) (19, 20). In these experiments, ΦX174 ssDNA was coated with SSB and incubated with PriA, PriB, PriC and DnaT, which were sequentially loaded and referred to as the pre-primosome. This pre-primosome could then associate with a complex of DnaB and DnaC (DnaB/C) such that a DnaB hexamer, but not DnaC, would load onto the pre-primosomal complex DNA. This protein complex could then translocate around the ΦX174 chromosome, transiently associating with DnaG, which would synthesize RNA primers for PolIII HE. Thus, the replication restart proteins were originally called the ΦX174 primosomal proteins because they allowed for priming of DNA synthesis of the ΦX174 genome *in vitro*. From this work, it was hypothesized that they would be part of the replisome in the host cell, priming lagging strand synthesis. This particular hypothesis was not ultimately supported as subsequent studies revealed that DnaB, DnaC, and DnaG have roles in core DNA replication processes of initiation and elongation. It is clear now that PriA, PriB, PriC and DnaT form a special group of proteins in *E. coli* for DNA replication restart and have since been renamed the replication restart primosome (RRP). There are important similarities and differences between the DnaA mediated system and the RRP mediated process in their loading of DnaB. While both processes recognize the proper DNA substrate on which to load DnaB, they differ in sequence mediated (DnaA) vs. structure mediated (RRP) mechanisms for recognition and initiation of DnaB loading. Thus the RRP can act anywhere on the chromosome at any time, while DnaA only acts at *oriC* during a certain stage of the cell cycle. While the RRP can also recognize the PAS as stated above, this should not be confused with sequence specific DNA binding as this site probably forms a molecular mimic of the D-loop and replication fork like structures

normally recognized by PriA.

The Replication Restart Proteins: Recognition and Remodeling of Abandoned Replication Forks

At its core, the RRP serves to reload the replicative helicase DnaB in order to restart DNA replication on sites far removed from *oriC*. In order to do this, the RRP must be able to both recognize a diverse set of abandoned replication forks as well as remodel the substrate to provide a ssDNA platform for DnaB to bind. Since their discovery in the early 1970s, extensive biochemical and genetic studies have elucidated much of the mechanisms employed by PriA, PriB, PriC, and DnaT to achieve this goal. Recent high resolution structures have validated these studies and provide new insights in the mechanism of DNA replication restart. The focus of this review will center on the gram negative replication restart system observed in *E. coli* and related bacteria and a description of the proteins and their genetic contexts follows.

PriA

Originally called " n' " or "Replication Factor Y," PriA is a 3' to 5' superfamily 2 (SF2) helicase. PriA is capable of recognizing nucleic acid intermediates that possess a 3' hydroxyl. Such structures are products of the repair mechanisms that deal with events leading to replisome ejection and include D-loop, R-loop and abandoned replication forks (21). PriA was originally thought to bind to substrates where the gap size between the 3' OH group and the fork junction was small (less than 5 nucleotides in length), though recent work has shown that PriA is capable of binding larger gap sizes (22, 23).

The gene for PriA was first identified using reverse genetics (24, 25). It was somewhat surprising, however, when the first deletion/insertion null mutants (*priA1::kan* and *priA2::kan*)

made on the chromosome were found to be viable (24, 26). It had been anticipated that *priA* would be an essential gene because of its presumed role in priming lagging strand synthesis during replication of the chromosome.

Studies of PriA phenotypes and suppressors gave rise to the understanding of PriA's role in replication restart. Many phenotypes have been described for *priA* mutants. They are very slow growing and are rich media sensitive (27). Analysis of single cells in a population show that a portion of the cells are filamented (even in the presence of suppressors of filamentation), induced for the SOS response and display a Par^- phenotype (Figure 1.1) (24, 26, 28). The combination of filamented cells even in the presence of a *sulA* or *sulB* suppressor mutation (suppressors of SOS inhibition of cell division) has been diagnostic for defects in replication restart (28-31). *PriA2::kan* null mutants are as recombination deficient and sensitive to UV irradiation as *recB21 recC22* mutants (32, 33). This observation was particularly surprising since *priA* null mutants have never been isolated in a screen for recombination deficient mutants, but the reason for this may be that they do not grow well on rich media and accumulate suppressors rapidly. PriA mutants are unable to properly replicate certain plasmids that use a PAS and require the RRP for DNA replication initiation, such as derivatives of ColEI (27, 34). PriA is capable of performing inducible and constitutive Stable DNA Replication (iSDR or cSDR) (27), which are special forms of initiation of DNA replication that are *oriC* and DnaA-independent (35). Many of the *priA* null mutant phenotypes (SOS^H, UV^S and poor plasmid replication) are similar to a *polA* mutant (36) suggesting that they may function in related pathways. PriA is required for repair of double strand breaks (DSB) (37, 38), UV-induced restriction alleviation (39) and resumption of DNA replication after UV-irradiation (40, 41). Lastly, the absence of PriA leads to higher frequency of transposition of *Tn7* into hotspots because this transposon seems to target stalled

replication forks for transposition (42).

In *E. coli*, the PriA protein is 732 amino acids long and was proposed to contain two major domains: an N-terminal DNA binding domain (DBD, amino acid residues 1-181) and a C-terminal helicase domain (HD, amino acid residues 182-732). The structure of the first 105 amino acids from *E. coli* PriA was previously determined by X-ray crystallography in the presence of a nucleotide (43-45). This structure revealed a mechanism for PriA's ability to recognize the 3' OH hydroxyl present in D-loop and abandoned replication forks, the primary substrates that PriA recognizes *in vivo*. The second part of the N-terminal DBD was also determined to be a DNA binding element that binds double stranded DNA (dsDNA). Both portions of the DBD were shown to work cooperatively, a common theme found in the functioning of PriA's various domains (44).

The HD makes up the majority of PriA's structure and contains the core helicase motifs present in SF2 family helicases. These motifs are responsible for binding and hydrolysis of ATP (Walker A motif) through a magnesium coordinated (Walker B motif) enzymatic mechanism. Energy from ATP hydrolysis drives DNA unwinding and translocase activities. Several studies have suggested the presence of a second, weaker nucleotide binding site (46-49) and PriA inhibitor studies propose that the inhibitor was binding at this second site (50), but the high resolution structures of PriA have yet to identify this second site (43-45, 51).

Extensive genetic studies have been performed on the conserved lysine (K230) residue of the Walker A motif that coordinates the γ-phosphate of ATP. The mutant *priA300* (K230R) abolishes ATPase, helicase and translocase activities of PriA. Despite loss of enzymatic function, this mutant behaves much like the wild type protein in *in vivo* and *in vitro* replication restart. It is able to load the RRP on ΦX174 ssDNA or replication structures *in vitro* (52) and

does not display any *priA* null mutant phenotypes *in vivo* (52-54). This suggests that ATPase, helicase, and/or translocase activity of PriA are not necessarily required for its replication restart function in all cases and that there are other pathways by which replication restart can occur. Mu replicative transposition has a requirement for the helicase activity *in vivo* and *in vitro*, while the predominant PriA/B pathway (discussed in depth below) does not (22, 31, 55). Mutants encoding PriA K230A and PriA K230D variants have also been studied *in vitro* and *in vivo*. Basic biochemical characterization and its ability to complement *priA2::kan* on the chromosome in a ColE1 plasmid transformation assay show that the *priA K230A* mutant is very similar to the *priA K230*R mutant (52). However, the *priA K230D* mutant is different in that a ColEI vector containing this mutant allele cannot replicate in a *priA2::kan* mutant (52). However, full complementation is achieved with *priA1::kan* with *priA K230D* cloned on a *priA*-independent vector (derivative of R1) (56). Therefore *priA K230D* may have a specific defect in replication of ColEI plasmids that does not relate to its ability to function in replication restart.

A defining motif of PriA is the presence of a cysteine rich region (CRR). This unique feature contains eight cysteines that coordinate zinc with the motif $CXXCX_nCXXCX_nCXXCX_nCXXC$ and exists in the middle of the second RecA-like fold of the helicase domain. Genetic studies of the CRR have provided mechanistic models for PriA activity, and mutants in this region display a range of phenotypes. Three mutants, C446G, C446/9G and C477G display PAS-dependent ATPase activity like or very similar to $PriA^+$ depending on the specific DNA substrate used but have greatly reduced ability to promote assembly of an active primosome (57). Only the C477G mutant had any helicase activity at all, and this could be stimulated with addition $ZnCl_2$ (57). A C446/9A double mutant can bind a D-loop in a gel mobility shift assay, but the shift is to a species of a different mobility than wild

type (56). On a plasmid, this double mutant has no ability to complement *priA1::kan*. PriA C439Y and PriA C446Y are plasmid encoded *priA* mutants that were first isolated for their temperature dependent SOS expression in a *priA2::kan* strain (58). Biochemical characterization of these variants revealed that they were able to bind PAS ssDNA, but were unable to assemble a primosome suitable for DNA replication. The reason for this is that they were unable to interact with PriB as detected by gel mobility assays. The requirement for PriB in this DNA replication assay could be eliminated if excess DnaT were used in the reaction, an observation that was also found to be true for wild type PriA. This result suggested that PriB was needed to facilitate formation of a PriA-DnaT complex (see PriB section for further explanation) and may be why *priA* and *dnaT* mutants have similar phenotypes. When *priA* C446Y was transferred to the chromosome, it behaved as a *priA* null mutant at 30, 37 and 42°C (unpublished results). Lastly, *priA301* (C479Y) was isolated as a suppressor of a lethal phenotype exhibited by overexpression of the *recF*, *recO* and *recR* (*recFOR*) genes from a plasmid (31). Preliminary analysis indicates that suppression was a combination of suppressing the negative effects of *recF* overexpression and lowering the plasmid copy number. This latter phenotype has also been used to isolate mutants in *priB* (59) and a mutant in *dnaC* (*dnaC1331*) that has a *priB*-like phenotype (60). Like *priA300*, *priA301* has little or no phenotype as a single mutant except a slightly lower plating efficiency for *Mu* phage (31). However, a defect in this *priA* mutant can be seen when coupled with other mutations. As with *priA300*, when *priA301* is coupled with a *priB* mutation, the double mutant behaves like a p*riA2::kan* mutant (31). When coupled with an *rnhA* mutant, the *priA300* mutant is able to do constitutive stable DNA replication, but the *priA301* mutant cannot (61). When coupled with a *priC* mutation, *priA301* increases the basal level of SOS expression significantly whereas addition of a *priA300* did not (31). Taken together, these studies support

the idea that the CRR is important for coupling helicase and ATPase activities and for interactions with other proteins.

The pattern of synthetic lethalities and suppressors for *priA* null mutants has been informative in understanding a more detailed analysis of PriA's role in the cell. PriA mutations are synthetically lethal with several mutations that affect initiation and elongation of DNA replication: *polA12*, *dnaA46* (34); extra *datA* sites (62), *holD* (63) and $gyrB^{ts}$ (64). The *datA* and *dnaA46* synthetic lethal phenotype may be due to the observation that these mutants either lead to unstable replication forks (62) or asynchronous initiation events (65). PriA mutations are synthetically lethal in mutants that fail to resolve Holliday junction intermediates, with chromosomes that have been recombinationally or topologically linked, or that affect nucleoid structure: *recG, ruvC, ftsK* (28), $gyrB^{ts}$ (64), $parE^{ts}$ (66) and *rdgC* (67). It should be noted that in some cases there are contradictory reports in the literature (*i.e., ruvC* and *recG*) for whether certain combinations of genes are synthetically lethal with *priA* mutations. This may reflect strain backgrounds or conditions used to measure the viability. In some cases, the presence of a *sulA* or *sulB* suppressor in the strain background can marginally increase the viability of the *priA2::kan* mutant (26, 28). Lastly, *recFOR* mutants that fail to load RecA at gaps are also synthetically lethal with *priA2::kan* mutations (68).

Novel point mutants of *priA* have also been isolated as suppressors of the UV sensitive phenotype of a *recG* null mutant (called *srgA* for suppressor to *recG*) (69). These suppressor mutations map in or around the highly conserved helicase motifs. The PriA proteins from two such mutants, *srgA1* (also called *priA306*) and *srgA2*, were purified and shown to have less ability than wild type PriA to unwind the nascent lagging strand at a partial replication fork *in vitro* (70). Thus, it is proposed that wild type RecG counters PriA helicase activity by binding to

a substrate that PriA could bind and use its helicase activity to negatively impact the DNA repair capacity of the cell. Supporting this hypothesis, other work has shown that PriA will bind to some replication fork structures and unwind the yet to be replicated portion of the duplex. RecG can compete with PriA for binding of these substrates (71). In opposition to this model, however, *priA300* only weakly suppresses the UV^S phenotype of *recG* mutants (72) and *srgA1* does not impart the same negative phenotypes as *priA300* when combined with a *priB* mutation (31). Hence, the mechanism of suppression of *srgA* mutants may require more than just the diminution of PriA helicase activity. It may also require some other subtle change in PriA yet to be determined.

Combination of synthetically lethal mutations can also reveal parallel pathways for accomplishing similar functions in the cell or processes that in the absence of one function increases the frequency at which other functions are required. Both of these scenarios are true for *priA* and its synthetic lethalities. The lethal combinations (*ruvABC*, *recG*, *ftsK, gyrB, holD, rep*) mentioned above seemed to be easiest explained by the latter category, since replication fork arrest is known (*gyrB^{ts}, holD, rep*), or supposed (*ruvABC, recG, ftsK*) to be increased in these backgrounds. Certain lethalities are overcome by a suppressor of *priA2::kan* that maps in *dnaC* called *dnaC809*, while others are not (*holD, rep* (63, 73)). These synthetically lethal combinations were used to define parallel pathways of replication restart; *priA* null mutations are co-lethal with mutations in *priC* or *rep.* These are not suppressed by *dnaC809* and suggest that PriC and Rep are required in the *dnaC809* suppressor pathway (73). Supporting this idea are biochemical observations that show that PriC and Rep *in vitro* can load DnaB on to replication fork structures (74). These suppressors and pathway models will be explained in more detail below.

PriB

PriB, originally called " n ", was first identified using reverse genetics (75). In *E. coli*, the protein is 104 amino acids, and it interacts with PriA, DnaT, ssDNA and potentially SSB (58). Biochemical and structural data supports PriB forming a dimeric structure with the core protein forming an oligonucleotide-oligosaccharide binding (OB) fold and is structurally similar to SSB (76). PriB has no intrinsic biochemical function on its own but is capable of both stimulating PriA helicase activity and stabilizing protein-protein interactions required for replication restart, processes mediated via ssDNA (77-79).

In vivo, PriB may be particularly important for replication restart that occurs after repair of DSB. Two lines of evidence support this idea. First, *priB* mutations are synthetically lethal with *dam* mutations (80). *dam* mutants are known to have more DSB than wild type cells (81, 82). Second, this lethality is suppressed by the introduction of a *mutH* mutation that fails to make the incision event during mismatch repair (80). One case where PriB seems to be important for a restart function in the absence of PriA is during cSDR. It was shown that *priB* is required in a *dnaC809,820* mutant that negates the need for PriA, DnaT and PriC during this process (61). It is possible that during the assembly of the replisome, PriB's role in this process may be different from that in normal replication restart because the replisome is being loaded at an R-loop instead of at *oriC*. Alternately PriB may differentially interact with DnaC809,820 (vis-à-vis $DnaC^{+}$) in the absence of ssDNA to stabilize or destabilize a complex of the mutant DnaC with DnaB. This complex interaction between *priB* and *dnaC* is further substantiated by studies that show that a novel mutation, *dnaC1331*, causes a decrease in plasmid copy number and increases amounts of SOS expression and filamentation in a *priA300* mutant similar to a *priB* mutation (60, 80). PriB is also important for resumption of DNA synthesis after UV treatment (83).

Mutations in *priB* are synthetically lethal with *priC* mutations, which was the first clue that there are multiple pathways for replication restart *in vivo*. The synthetic lethal phenotype of a *priB/priC* double mutation can be partially suppressed by a *priA2::kan* suppressor, *dnaC809* (E176G) (84). This *priBC dnaC809* triple mutant was used as a starting strain to select another growth suppressor. This one mapped once again in *dnaC* and was called *dnaC809,820* (E176G/K172N). Thus, there is a redundancy in function between *priB* and *priC* that can be compensated for by novel mutations in *dnaC*. It has also been shown that *priB* is essential in the viability of a *holD* mutant and a $gyrB^{ts}$ mutant on rich media (63, 64).

PriC

PriC, originally " n" " was first identified during studies of ΦX174 DNA replication and has no enzymatic function on its own outside of replication restart (78). In *E. coli,* PriC is 175 amino acids long and has been shown to interact with SSB, DNA, and with DnaB (85, 86). The SSB interaction occurs at a prototypical SSB binding site on PriC and is stabilized by residues R121 and R155. Abolishing this interaction by altering either of these residues or by altering the C-terminus of SSB (to which PriC binds) eliminates DnaB loading *in vitro* and *in vivo*.

PriC has also been shown to bind DNA primarily through the C-terminal portion of the protein. While it is able to bind both ds- and ssDNA, PriC preferentially binds to ssDNA with a site size of 7-9 nucleotides (86). This observation fits relatively well with the *in vitro* data that suggests PriC is most active on stalled forks with a gap >5 nucleotides between nascent leading strand and the fork junction (22). This DNA binding also appears to induce an oligomeric state of the protein that is mediated by the N-terminal region of the protein, although the role of this oligomerization in mediating replication restart has not been determined (87). The interaction

between PriC and DnaB has not been fully investigated, but it is predicted that this plays a role in recruiting the helicase to the stalled fork.

Structurally, PriC consists of 5 alpha helices, with a short loop connecting α-helix 1 and α-helix 2 (unpublished). These helices are arranged in a loose bundle. The SSB binding site is shared between helices 4 and 5. On the opposite face of these helices is a conserved region of positively charged residues, and this is predicted to be the site of ssDNA binding (unpublished data).

The genetics of *priC* are at an early stage. The most studied mutant is a null mutant (*priC303::kan*). Like the *priB* null mutation, the *priC* null mutation has no phenotype by itself and is synthetically lethal with a *priB* mutation. However, *priB* and *priC* mutants can have different phenotypes. For example, where *priB* mutations have novel phenotypes with *rep* and *priA300* mutations, *priC* mutants are unaffected. Another is that *rnhA dnaA* null mutants absolutely require *priB* in all situations (even strains with *dnaC809* or *dnaC809,820*), and these strains do not require *priC*. A third is that *priC* (and not *priB*) mutations are synthetically lethal with certain $dnaA^{ts}$ mutants (88). This lethality can be suppressed by either making the strain *dnaA*-independent with an *rnhA* mutation or in some cases by a *dnaC809,820* mutation.

It was determined in genetic studies of *E. coli* that PriC functions with the Rep helicase in a replication restart pathway independent of PriA and the other restart proteins. The dependence of the Rep helicase in the PriC-Rep pathway is seen by the fact that both PriC and Rep are required for *dnaC809* suppression of *priA2::kan* mutant phenotypes which can be relieved by the addition of a *dnaC* mutation, *dnaC809,820* (73, 84). Following this discovery, it was demonstrated that PriC is able to mediate the loading of DnaB on to a stalled fork structure in the absence of other restart proteins (22). This non-dependence on other restart proteins requires

that the fork contain no nascent lagging strand and a gap of greater than 5-nt on the leading strand. When lagging strand DNA is present, the action of either Rep or PriA (both 3' to 5' helicases) is required to facilitate DnaB loading by unwinding the nascent lagging strand DNA (89).

DnaT

DnaT, originally known as protein "i," is a 179 amino acid protein necessary for PriA-dependent replication restart (22). DnaT appears to function in recruiting DnaB-DnaC to the primosome by binding PriB in the PriB-PriA-ssDNA complex (58, 78, 79, 90). However, excess levels of DnaT have been shown to bypass the requirement for PriB in ΦX174 complementary strand DNA replication *in vitro* (58). DnaT has no enzymatic activity on its own and is not found in all bacterial species that contain PriA. Currently, no high resolution structure of the protein has been determined and the role of DnaT in the primosome remains poorly understood. DnaT is thought to consist of two domains (a large N-terminal domain and smaller C-terminal domain) and exists in a monomer-trimer equilibrium (91-93). Homotrimerization has been shown to be highly cooperative, with no dimer observed in solution (91-93). The isolated *E. coli* N-terminal domain (amino acids 1-161) forms a dimer and has led to a trimerization model where the third monomer associated through contacts between the C-terminal domains of all three monomers (91). DnaT from *Klebsiella pneumonia* has been seen to bind ~25 nucleotides ssDNA as a trimer through the highly conserved C-terminal domain (94). The N-terminal domain of *K. pneumonia* DnaT (amino acids 1-83) has been proposed to be important in PriB binding and trimerization, but not ssDNA-binding (93). Both monomer and trimer states have been implicated in functioning in primosome assembly, but more work is needed to determine the functional DnaT state (78, 92).

The *dnaT* gene was first identified by the *dnaT1* mutation in *E. coli 15T*` (95). This was a dominant, temperature sensitive, conditional lethal mutation that arrested DNA replication and thus DnaT was thought to be involved with termination of DNA replication (hence the designation "T"). However, no such role has been demonstrated. The *dnaT1* mutation was identified to be a change from an arginine to a cysteine at position 152 (30). When this mutant allele was cloned onto a pACYC184 derivative and was transferred to both a wild type strain of *E. coli* K-12 and one with a *dnaT* null allele, it was found to fully complement the *dnaT* null mutant and show no mutant phenotype in the wild type. Hence, *dnaT1* is only temperature sensitive and dominant negative in *E. coli* 15T.

Given *dnaT*'s role in replication restart and the fact that the only mutation defining the gene was a dominant temperature sensitive lethal mutation in *dnaT*, it was of interest to see if a *dnaT* null mutation could be constructed. This was accomplished by making an in-frame deletion of codons 87-92, called *dnaT822* (30). This mutation causes a phenotype that is identical to *priA2::kan* and suppressed by *dnaC809* (like *priA2::kan*). This observation supports the model that like the other replication restart genes *priA*, *priB* and *priC*, *dnaT* was not required for normal DNA replication and is only required for replication restart. The fact that its phenotype was very similar to a *priA* null mutant and was suppressed *dnaC809* suggested that, like PriA, it was only required for the PriAB and PriAC pathways and not required for the PriC-Rep pathway. The *dnaT* gene is located just upstream of *dnaC* (96, 97), and therefore it is tempting to speculate that the two proteins interact, but no such specific interaction has yet been documented.

Regulation of Replication Restart Proteins

Very little is known about the regulation of the RRP genes. They are spread throughout the chromosome. One might expect that they would be part of the DNA damage inducible SOS response, but there is no evidence to support this hypothesis (98). This observation, coupled with apparently constitutive transcriptional regulation, suggests that DNA replication restart is a process that should be available to treat DNA damage associated with log phase growth and not just after high levels of DNA damage. *priA* and *rep* are in transcriptional units by themselves, whereas the other RRP genes are part of operons. The *dnaT* and *dnaC* genes are in a single operon with two other genes of unknown function. *priC* is in a operon with *ybaM* (also of unknown function). Interestingly, *priB* is the second of four genes in an operon: *rpsF*, *priB*, *rpsR* and *rplI*. The three other genes encode ribosomal subunit proteins.

Proposed Models of DNA Replication Restart

DNA replication restart reloads the replicative helicase onto bacterial chromosomes on sites far removed from *oriC* in a DNA structure dependent, sequence independent manner. As such, the process has three overall goals that it must achieve. First, the RRP must recognize and be capable of binding diverse DNA structural intermediates that result from a wide variety of repair processes. Second, remodeling of the DNA structure present at abandoned replication forks is required to expose ssDNA, the preferred substrate, for the replicative helicase to load on to. Lastly, the RRP aids in reloading the replicative helicase by protein-protein interactions mediated by DNA binding. PriA, PriB, PriC, and DnaT work together to achieve the goal of loading DnaB. Genetic and biochemical studies have delineated three distinct pathways in *E. coli* (Figure 1.2) that can be classified as either PriA or PriC mediated defined by the first protein that binds to the replication fork in order to begin restart processes. The functional redundancy

of these pathways allows for bacteria to confront a vast array of cellular situations that might arrest DNA replication and highlights the essential importance of these proteins for bacterial survival.

PriA-Mediated DNA Replication Restart

PriA recognizes both D-loop (99) and abandoned replication forks that contain a 3' OH group in close proximity to the branch point of the fork (100), though the minimum gap size that PriA is capable of recognizing has recently come under question (23). PriA's interaction with the replication fork has the potential to occur in two different modes, one dependent on binding and stabilization of the fork via PriA's N-terminus to the 3' OH while the other independent of 3' OH fork recognition and involves fork destabilization via helicase activity (44, 71). PriA is also capable of binding to replication forks coated with SSB and reshaping the substrate via SSB binding mode remodeling to expose a ssDNA substrate for subsequent reloading activities (51, 101).

PriA binding and fork remodeling begins a cascade of protein-protein interactions that involves the coordinated effort of PriA, PriB, and DnaT to reload the replicative helicase DnaB onto the replication fork in a proposed "hand-off mechanism" (79). Fluorescence polarization (FP) studies with full length and fragments of PriA in the presence or absence of DNA and PriB highlighted interactions of PriA to PriB stimulated by ssDNA. It is hypothesized that binding of PriA to DNA leads to a conformational change in PriA that exposes PriB's binding site on the PriA HD (79). PriB serves to stabilize the PriA-fork interaction, stimulates PriA's helicase activity (77) and facilitates formation of a ternary complex with PriA, DnaT, and DNA where PriB's binding sites partially overlap with these three components (58). Formation of this ternary complex readies the replication fork for the final steps to reload DnaB, though the exact

mechanisms by which this occurs still remain vague. Binding of DnaT leads to release of PriB from the complex, and thus it is thought that binding of DnaT leads to exposure of ssDNA for DnaB to be loaded by DnaC (79). Whether DnaT plays a role beyond this, such as directly recruiting DnaB by direct protein-protein interactions, is unknown and has not been shown as of this point.

PriC-Mediated DNA Replication Restart

PriC-mediated replication restart is involved in two of the three pathways seen in *E. coli* where it preferentially binds to replication forks with gap sizes larger than 7 nucleotides between the nascent leading strand and replication fork (22). Such substrates occur primarily as a result of blocked nascent strand replication and continued fork unwinding. PriC has been shown to load DnaB with the aid of DnaC *in vitro* on forks without a nascent lagging strand in the absence of any other restart proteins (22); however, the exact mechanisms by which DnaB is loaded onto these forks remains undefined at this point. Like PriA, PriC is also capable of remodeling SSB-coated forks, where PriC binding to SSB preferentially stabilizes the 35nt binding mode of SSB over the 65nt binding mode. This nucleoprotein complex remodeling is proposed to generate a stretch of ssDNA on to which DnaB can load (85).

The presence of a nascent lagging strand at a stalled fork with a large gap size presents a unique situation for the replication restart proteins that requires further fork remodeling. Since PriC lacks enzymatic activity on its own, it must recruit the aid of helicases to remodel the replication fork. PriC interacts with PriA or Rep helicases in two distinct pathways. The PriA/PriC pathway has been observed *in vivo* where a *priB/priA300* double mutant acts similar phenotypically to the PriA null mutant *priA2::kan* (31). PriA helicase activity is essential for

this pathway (22, 31), but the in-depth biochemical mechanisms of this pathway still remain unclear.

PriC and Rep helicase function together in a PriA-independent pathway of replication restart. This was first demonstrated when it was found that a *rep* deletion is synthetically lethal with *priA* null mutations (73, 102). PriC has been shown to stimulate the helicase activity of Rep *in vitro* (103). In the PriC/Rep pathway *in vivo*, the role of Rep may simply be to remove nascent lagging strand DNA to enable PriC-mediated loading of DnaB. Rep also interacts with DnaB and may play a role in recruitment of DnaB (104).

The understanding of this pathway of restart is complicated by the fact that Rep has a role in stabilizing the replication fork. Rep is able to remove proteins bound to DNA and plays a role in resolving DNA replication/transcription conflicts (105, 106). Deletions of *rep* also exhibit a slower DNA replication rate than wild type cells (107-109). Slower replication rates and poor resolution of transcription/replication conflicts could lead to an increase in DNA damage and the need for replication restart processes.

Replication Restart in Eukaryotes

DNA replication fork arrest in eukaryotes is a potentially dangerous situation that is involved in genomic instability (110, 111). Despite the apparent necessity for such mechanisms, studies of the process of replication restart have been historically confined to the bacterial kingdom. The presence of multiple licensed origins in eukaryotes allows for rescue of arrested DNA forks and would thus bypass the need for an origin independent loading of the replisome (112, 113). Furthermore, sequence orthologs of the bacterial RRP do not exist in eukaryotes and structural orthologs have not been identified.

It is becoming more and more evident though that replication fork breakdown and arrest still requires attention. Eukaryotic systems have evolved highly regulated, complex mechanisms to protect DNA forks and replication restart-like processes important for viability under replication stress conditions may exist. Several distinct pathways exist not only to protect replication forks, such as the Mec 1/ATR pathway (114, 115) but also to direct restart of replication following repair of genomic damage. Human cells exposed to hydroxyurea are capable of restarting DNA replication from paused forks through a Rad51-dependent mechanism independent of DSB repair (116). Recent studies have also highlighted the role of TopBP1 in recruiting Pol α-primase to ssDNA in *Xenopus* egg extracts (117). Pol α-primase binding leads to recruitment of the eukaryotic replisome (118-120) reminiscent of the RRP recruiting the bacterial replisome, though the exact mechanisms differ. Further studies of replication restart in eukaryotes are essential and will be greatly aided by increased knowledge from their bacterial cousins.

Future of DNA Replication Restart

After more than 40 years of research first pioneered by Arthur Kornberg and Jerard Hurwitz in the early 1970s, the study of DNA replication restart stands at an exciting point in time. Recent high resolution structures have not only confirmed the vast amount of biochemistry performed over the past four decades but also provided novel mechanistic insights into this essential process. Despite recent advances, several key questions remain in DNA replication restart. Models of PriA and PriC recognition of abandoned replication forks have been proposed based on the recently determined structures (both presented in this thesis and unpublished observations) that need to be further confirmed biochemically. Recruitment of DnaB and the protein-protein interactions that drive this final step and subsequent removal of the RRP from the

replication fork are currently unknown. PriA- and PriC-mediated replication restart is well conserved in the γ-proteobacterium clade (and indeed, PriA is well conserved across bacterial species), but PriB, PriC, and DnaT are less conserved. This observation suggests structural homologs (and not necessarily sequence homologs) could exist across bacteria families or that diverse mechanisms of replication restart must exist. Understanding diverse mechanisms of DNA replication restart will provide insights into eukaryotic systems that may employ similar mechanisms. Studies of DNA replication restart will not only provide clues to this process across all kingdoms of life, but will provide general mechanisms of genome stability employed by all organisms.

Figure 1.1

Wild type

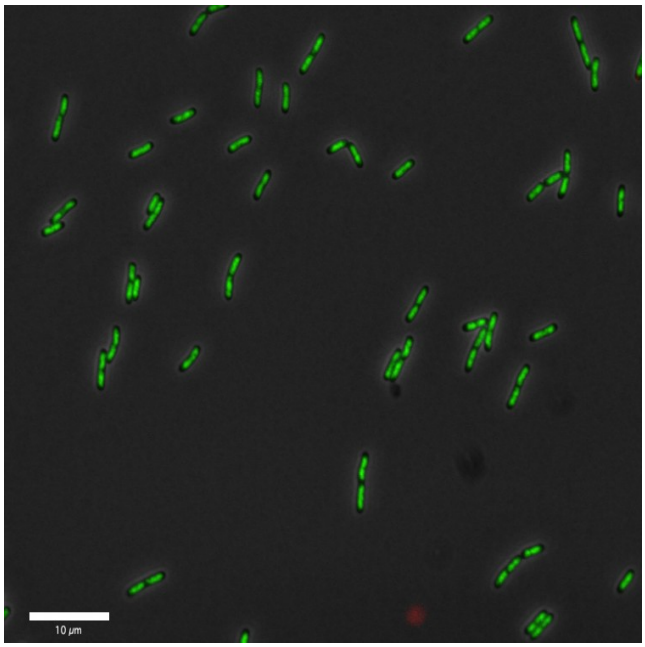

priA2::kan

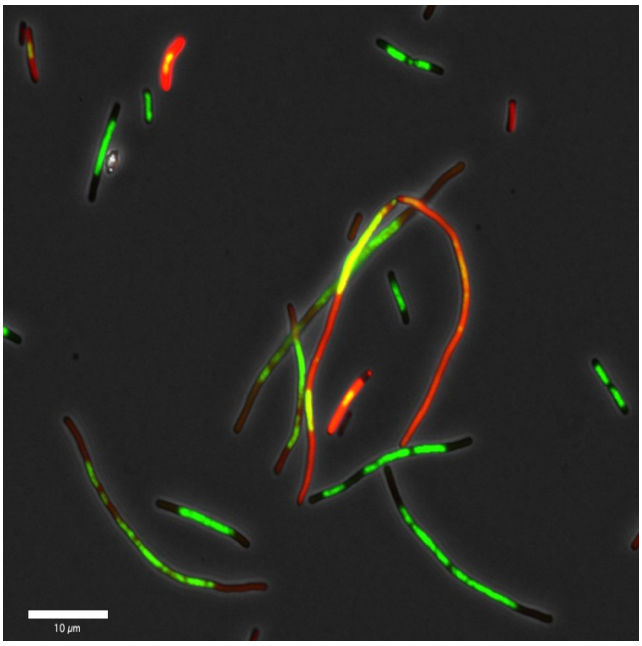

Figure 1.1 The Physiological Importance of DNA Replication Restart
Overlay of phase contrast, red (*sulAp-mcherry* , SOS induction) and green (*hupA-gfp,* nucleoids) for both a wild type strain and a *priA* null strain (*priA2::kan*). A marker for defects in DNA replication restart is induction of the SOS response, filamentation and poorly formed and partitioned nucleoids. *Images courtesy of Shawn Massoni and Steve Sandler (University of Massachusetts-Amherst).*

Figure 1.2

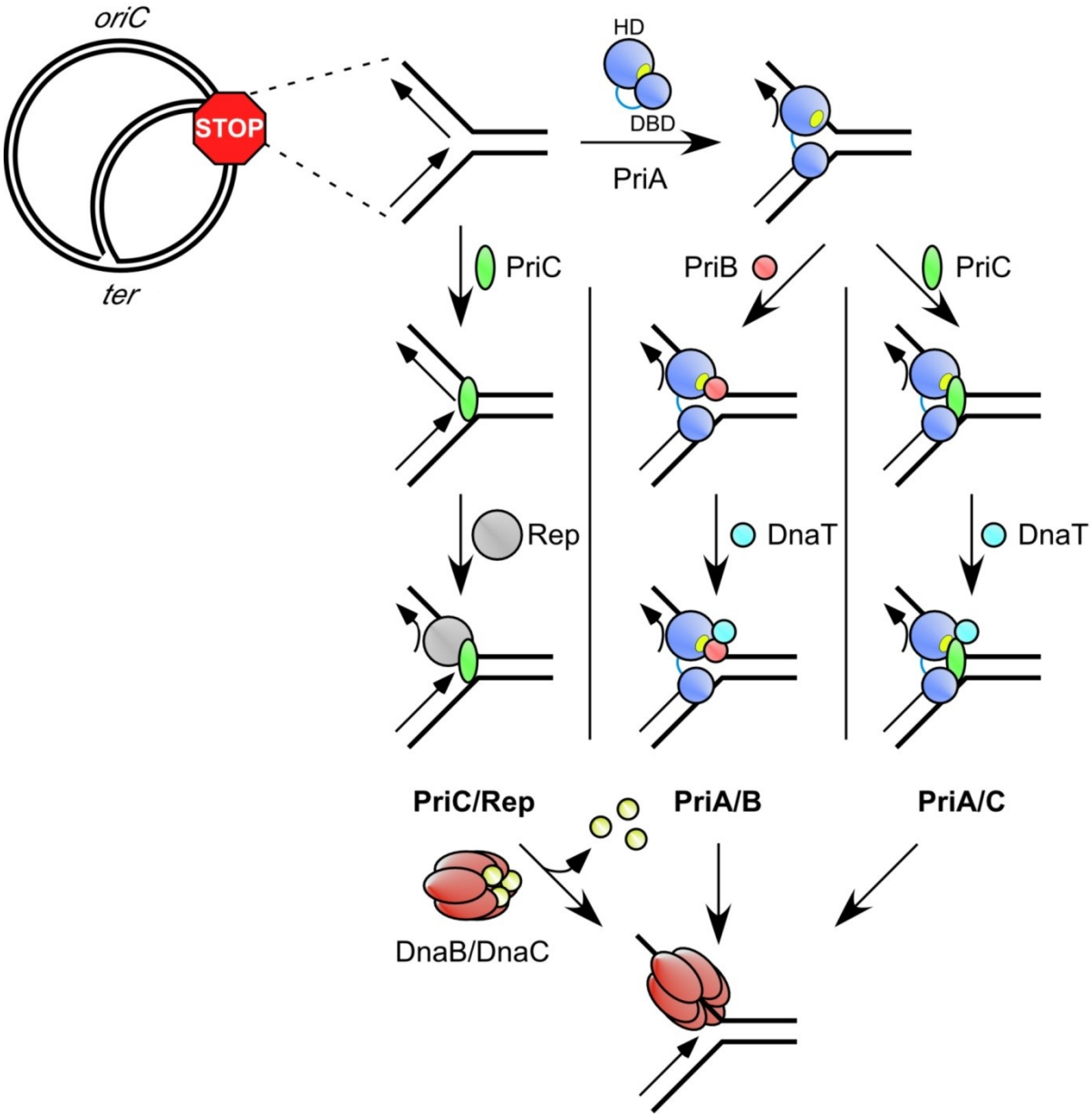
oriC
STOP
ter
HD
DBD
PriA
PriC
PriB
PriC
Rep
DnaT
DnaT
PriC/Rep
PriA/B
PriA/C
DnaB/DnaC

Figure 1.2 DNA Replication Restart Pathways in *Escherichia coli*
E. coli and related bacteria possess three functional pathways for DNA replication restart. All three pathways serve to reload the replicative helicase, DnaB, on sites far remove from the origin of replication (*oriC*) in a DNA structure dependent manner. Key steps in the process also include recognition of abandoned replication forks either by PriA or PriC as well as remodeling of the fork to allow for subsequent protein-protein interactions. Loss of all three pathways via gene deletion is lethal to *E. coli* and DNA replication restart is an essential, genome maintenance process.

References

1. Bramhill D & Kornberg A (1988) Duplex opening by dnaA protein at novel sequences in initiation of replication at the origin of the *E. coli* chromosome. *Cell* 52(5):743-755.

2. Grimwade JE*, et al.* (2007) Mutational analysis reveals *Escherichia coli* oriC interacts with both DnaA-ATP and DnaA-ADP during pre-RC assembly. *Mol Microbiol* 66(2):428-439.

3. Ludlam AV, McNatt MW, Carr KM, & Kaguni JM (2001) Essential amino acids of *Escherichia coli* DnaC protein in an N-terminal domain interact with DnaB helicase. *J Biol Chem* 276(29):27345-27353.

4. Marszalek J & Kaguni JM (1994) DnaA protein directs the binding of DnaB protein in initiation of DNA replication in *Escherichia coli*. *J Biol Chem* 269(7):4883-4890.

5. Wahle E, Lasken RS, & Kornberg A (1989) The dnaB-dnaC replication protein complex of *Escherichia coli*. I. Formation and properties. *J Biol Chem* 264(5):2463-2468.

6. Wahle E, Lasken RS, & Kornberg A (1989) The dnaB-dnaC replication protein complex of *Escherichia coli*. II. Role of the complex in mobilizing dnaB functions. *J Biol Chem* 264(5):2469-2475.

7. Mok M & Marians KJ (1987) The *Escherichia coli* preprimosome and DNA B helicase can form replication forks that move at the same rate. *J Biol Chem* 262(34):16644-16654.

8. Kim S, Dallmann HG, McHenry CS, & Marians KJ (1996) tau couples the leading- and lagging-strand polymerases at the *Escherichia coli* DNA replication fork. *J Biol Chem* 271(35):21406-21412.

9. Kim S, Dallmann HG, McHenry CS, & Marians KJ (1996) Tau protects beta in the leading-strand polymerase complex at the replication fork. *J Biol Chem* 271(8):4315-4318.

10. Kim S, Dallmann HG, McHenry CS, & Marians KJ (1996) Coupling of a replicative polymerase and helicase: a tau-DnaB interaction mediates rapid replication fork movement. *Cell* 84(4):643-650.

11. Hill TM & Marians KJ (1990) *Escherichia coli* Tus protein acts to arrest the progression of DNA replication forks in vitro. *Proc Natl Acad Sci U S A* 87(7):2481-2485.

12. McGlynn P & Lloyd RG (2002) Recombinational repair and restart of damaged replication forks. *Nat Rev Mol Cell Biol* 3(11):859-870.

13. Cox MM*, et al.* (2000) The importance of repairing stalled replication forks. *Nature* 404(6773):37-41.

14. Yeeles JT, Poli J, Marians KJ, & Pasero P (2013) Rescuing stalled or damaged replication forks. *Cold Spring Harb Perspect Biol* 5(5):a012815.

15. Marians KJ (1992) Prokaryotic DNA replication. *Annu Rev Biochem* 61:673-719.

16. Schekman R, Weiner A, & Kornberg A (1974) Multienzyme systems of DNA replication. *Science* 186(4168):987-993.

17. Schekman R, Weiner JH, Weiner A, & Kornberg A (1975) Ten proteins required for conversion of phiX174 single-stranded DNA to duplex form in vitro. Resolution and reconstitution. *J Biol Chem* 250(15):5859-5865.

18. Wickner S & Hurwitz J (1975) Association of phiX174 DNA-dependent ATPase activity with an *Escherichia coli* protein, replication factor Y, required for in vitro synthesis of phiX174 DNA. *Proc Natl Acad Sci U S A* 72(9):3342-3346.

19. Abarzua P, Soeller W, & Marians KJ (1984) Mutational analysis of primosome assembly sites. I. Distinct classes of mutants in the pBR322 *Escherichia coli* factor Y DNA effector sequences. *J Biol Chem* 259(22):14286-14292.

20. Soeller W, Abarzua P, & Marians KJ (1984) Mutational analysis of primosome assembly sites. II. Role of secondary structure in the formation of active sites. *J Biol Chem* 259(22):14293-14300.

21. Heller RC & Marians KJ (2006) Replisome assembly and the direct restart of stalled replication forks. *Nat Rev Mol Cell Biol* 7(12):932-943.

22. Heller RC & Marians KJ (2005) The disposition of nascent strands at stalled replication forks dictates the pathway of replisome loading during restart. *Mol Cell* 17(5):733-743.

23. Manhart CM & McHenry CS (2013) The PriA replication restart protein blocks replicase access prior to helicase assembly and directs template specificity through its ATPase activity. *J Biol Chem* 288(6):3989-3999.

24. Lee EH, Masai H, Allen GC, Jr., & Kornberg A (1990) The priA gene encoding the primosomal replicative n' protein of *Escherichia coli*. *Proc Natl Acad Sci U S A* 87(12):4620-4624.

25. Nurse P, DiGate RJ, Zavitz KH, & Marians KJ (1990) Molecular cloning and DNA sequence analysis of *Escherichia coli priA*, the gene encoding the primosomal protein replication factor Y. *Proc Natl Acad Sci U S A* 87(12):4615-4619.

26. Nurse P, Zavitz KH, & Marians KJ (1991) Inactivation of the *Escherichia coli* PriA DNA replication protein induces the SOS response. *J Bacteriol* 173(21):6686-6693.

27. Masai H, Asai T, Kubota Y, Arai K, & Kogoma T (1994) *Escherichia coli* PriA protein is essential for inducible and constitutive stable DNA replication. *Embo J* 13(22):5338-5345.

28. McCool JD & Sandler SJ (2001) Effects of mutations involving cell division, recombination, and chromosome dimer resolution on a *priA2::kan* mutant. *Proc Natl Acad Sci U S A* 98(15):8203-8210.

29. Boonsombat R, Yeh SP, Milne A, & Sandler SJ (2006) A novel *dnaC* mutation that suppresses *priB rep* mutant phenotypes in *Escherichia coli* K-12. *Mol Microbiol* 60(4):973-983.

30. McCool JD, Ford CC, & Sandler SJ (2004) A *dnaT* mutant with phenotypes similar to those of a *priA2::kan* mutant in *Escherichia coli* K-12. *Genetics* 167(2):569-578.

31. Sandler SJ, McCool JD, Do TT, & Johansen RU (2001) PriA mutations that affect PriA-PriC function during replication restart. *Mol Microbiol* 41(3):697-704.

32. Kushner SR, Nagaishi H, Templin A, & Clark AJ (1971) Genetic recombination in *Escherichia coli*: the role of exonuclease I. *Proc Natl Acad Sci U S A* 68(4):824-827.

33. Sandler SJ (1996) Overlapping functions for *recF* and *priA* in cell viability and UV-inducible SOS expression are distinguished by *dnaC809* in *Escherichia coli* K-12. *Mol Microbiol* 19(4):871-880.

34. Lee EH & Kornberg A (1991) Replication deficiencies in *priA* mutants of *Escherichia coli* lacking the primosomal replication n' protein. *Proc Natl Acad Sci U S A* 88(8):3029-3032.

35. Kogoma T (1997) Stable DNA replication: interplay between DNA replication, homologous recombination, and transcription. *Microbiol Mol Biol Rev* 61(2):212-238.

36. Camps M & Loeb LA (2005) Critical role of R-loops in processing replication blocks. *Front Biosci* 10:689-698.

37. Eykelenboom JK, Blackwood JK, Okely E, & Leach DR (2008) SbcCD causes a double-strand break at a DNA palindrome in the *Escherichia coli* chromosome. *Mol Cell* 29(5):644-651.

38. Meddows TR, Savory AP, & Lloyd RG (2004) RecG helicase promotes DNA double-strand break repair. *Mol Microbiol* 52(1):119-132.

39. Ivancic-Bacce I, Vlasic I, Cogelja-Cajo G, Brcic-Kostic K, & Salaj-Smic E (2006) Roles of PriA protein and double-strand DNA break repair functions in UV-induced restriction alleviation in *Escherichia coli*. *Genetics* 174(4):2137-2149.

40. Courcelle J, Belle JJ, & Courcelle CT (2004) When replication travels on damaged templates: bumps and blocks in the road. *Res Microbiol* 155(4):231-237.

41. Rangarajan S, Woodgate R, & Goodman MF (2002) Replication restart in UV-irradiated *Escherichia coli* involving pols II, III, V, PriA, RecA and RecFOR proteins. *Mol Microbiol* 43(3):617-628.

42. Shi Q, *et al.* (2008) DNA damage differentially activates regional chromosomal loci for Tn7 transposition in *Escherichia coli*. *Genetics* 179(3):1237-1250.

43. Sasaki K, *et al.* (2006) Crystallization and preliminary crystallographic analysis of the N-terminal domain of PriA from *Escherichia coli*. *Biochim Biophys Acta* 1764(1):157-160.

44. Tanaka T, Mizukoshi T, Sasaki K, Kohda D, & Masai H (2007) *Escherichia coli* PriA protein, two modes of DNA binding and activation of ATP hydrolysis. *J Biol Chem* 282(27):19917-19927.

45. Sasaki K, *et al.* (2007) Structural basis of the 3'-end recognition of a leading strand in stalled replication forks by PriA. *EMBO J* 26(10):2584-2593.

46. Lucius AL, Jezewska MJ, & Bujalowski W (2006) The *Escherichia coli* PriA helicase has two nucleotide-binding sites differing dramatically in their affinities for nucleotide cofactors. 1. Intrinsic affinities, cooperativities, and base specificity of nucleotide cofactor binding. *Biochemistry* 45(23):7202-7216.

47. Lucius AL, Jezewska MJ, Roychowdhury A, & Bujalowski W (2006) Kinetic mechanisms of the nucleotide cofactor binding to the strong and weak nucleotide-binding site of the *Escherichia coli* PriA helicase. 2. *Biochemistry* 45(23):7217-7236.

48. Lucius AL, Jezewska MJ, & Bujalowski W (2006) Allosteric interactions between the nucleotide-binding sites and the ssDNA-binding site in the PriA helicase-ssDNA complex. 3. *Biochemistry* 45(23):7237-7255.

49. Szymanski MR, Jezewska MJ, & Bujalowski W (2010) The *Escherichia coli* PriA helicase-double-stranded DNA complex: location of the strong DNA-binding subsite on the helicase domain of the protein and the affinity control by the two nucleotide-binding sites of the enzyme. *J Mol Biol* 402(2):344-362.

50. Sunchu B, Berg L, Ward HE, & Lopper ME (2012) Identification of a small molecule PriA helicase inhibitor. *Biochemistry* 51(51):10137-10146.

51. Bhattacharyya B, *et al.* (2014) Structural mechanisms of PriA-mediated DNA replication restart. *Proc Natl Acad Sci U S A* 111(4):1373-1378.

52. Zavitz KH & Marians KJ (1992) ATPase-deficient mutants of the *Escherichia coli* DNA replication protein PriA are capable of catalyzing the assembly of active primosomes. *J Biol Chem* 267(10):6933-6940.

53. Kogoma T, Cadwell GW, Barnard KG, & Asai T (1996) The DNA replication priming protein, PriA, is required for homologous recombination and double-strand break repair. *J Bacteriol* 178(5):1258-1264.

54. Sandler SJ, Samra HS, & Clark AJ (1996) Differential suppression of *priA2::kan* phenotypes in *Escherichia coli* K-12 by mutations in *priA, lexA, and dnaC*. *Genetics* 143(1):5-13.

55. Jones JM & Nakai H (1999) Duplex opening by primosome protein PriA for replisome assembly on a recombination intermediate. *J Mol Biol* 289(3):503-516.

56. Masai H, Deneke J, Furui Y, Tanaka T, & Arai KI (1999) *Escherichia coli* and *Bacillus subtilis* PriA proteins essential for recombination-dependent DNA replication: involvement of ATPase/helicase activity of PriA for inducible stable DNA replication. *Biochimie* 81(8-9):847-857.

57. Zavitz KH & Marians KJ (1993) Helicase-deficient cysteine to glycine substitution mutants of *Escherichia coli* replication protein PriA retain single-stranded DNA-dependent ATPase activity. Zn^{2+} stimulation of mutant PriA helicase and primosome assembly activities. *J Biol Chem* 268(6):4337-4346.

58. Liu J, Nurse P, & Marians KJ (1996) The ordered assembly of the phiX174-type primosome. III. PriB facilitates complex formation between PriA and DnaT. *J Biol Chem* 271(26):15656-15661.

59. Berges H, Oreglia J, Joseph-Liauzun E, & Fayet O (1997) Isolation and characterization of a *priB* mutant of *Escherichia coli* influencing plasmid copy number of delta rop ColE1-type plasmids. *J Bacteriol* 179(3):956-958.

60. Harinarayanan R & Gowrishankar J (2004) A *dnaC* mutation in *Escherichia coli* that affects copy number of ColE1-like plasmids and the PriA-PriB (but not Rep-PriC) pathway of chromosomal replication restart. *Genetics* 166(3):1165-1176.

61. Sandler SJ (2005) Requirements for replication restart proteins during constitutive stable DNA replication in *Escherichia coli* K-12. *Genetics* 169(4):1799-1806.

62. Morigen, Lobner-Olesen A, & Skarstad K (2003) Titration of the *Escherichia coli* DnaA protein to excess *datA* sites causes destabilization of replication forks, delayed replication initiation and delayed cell division. *Mol Microbiol* 50(1):349-362.

63. Flores MJ, Ehrlich SD, & Michel B (2002) Primosome assembly requirement for replication restart in the *Escherichia coli holDG10* replication mutant. *Mol Microbiol* 44(3):783-792.

64. Grompone G, Ehrlich SD, & Michel B (2003) Replication restart in *gyrB Escherichia coli* mutants. *Mol Microbiol* 48(3):845-854.

65. Skarstad K, von Meyenburg K, Hansen FG, & Boye E (1988) Coordination of chromosome replication initiation in *Escherichia coli*: effects of different *dnaA* alleles. *J Bacteriol* 170(2):852-858.

66. Grompone G, Bidnenko V, Ehrlich SD, & Michel B (2004) PriA is essential for viability of the *Escherichia coli* topoisomerase IV *parE10(Ts)* mutant. *J Bacteriol* 186(4):1197-1199.

67. Moore T, McGlynn P, Ngo HP, Sharples GJ, & Lloyd RG (2003) The RdgC protein of *Escherichia coli* binds DNA and counters a toxic effect of RecFOR in strains lacking the replication restart protein PriA. *EMBO J* 22(3):735-745.

68. Grompone G, Sanchez N, Dusko Ehrlich S, & Michel B (2004) Requirement for RecFOR-mediated recombination in *priA* mutant. *Mol Microbiol* 52(2):551-562.

69. Al-Deib AA, Mahdi AA, & Lloyd RK (1996) Modulation of recombination and DNA repair by RecG and PriA helicases of *Escherichia coli* K-12. *J. Bacteriol.* 178(23):6782-6789.

70. Gregg AV, McGlynn P, Jaktaji RP, & Lloyd RG (2002) Direct rescue of stalled DNA replication forks via the combined action of PriA and RecG helicase activities. *Molecular cell* 9(2):241-251.

71. Tanaka T & Masai H (2006) Stabilization of a stalled replication fork by concerted actions of two helicases. *J Biol Chem* 281(6):3484-3493.

72. Jaktaji RP & Lloyd RG (2003) PriA supports two distinct pathways for replication restart in UV-irradiated *Escherichia coli* cells. *Mol Microbiol* 47(4):1091-1100.

73. Sandler SJ (2000) Multiple genetic pathways for restarting DNA replication forks in *Escherichia coli* K-12. *Genetics* 155(2):487-497.

74. Heller RC & Marians KJ (2005) Unwinding of the nascent lagging strand by Rep and PriA enables the direct restart of stalled replication forks. *J Bio Chem* 280(40):34143-34151.

75. Allen GC, Jr. & Kornberg A (1991) The *priB* gene encoding the primosomal replication n protein of *Escherichia coli*. *J Biol Chem* 266(18):11610-11613.

76. Lopper M, Holton JM, & Keck JL (2004) Crystal structure of PriB, a component of the *Escherichia coli* replication restart primosome. *Structure* 12(11):1967-1975.

77. Cadman CJ, Lopper M, Moon PB, Keck JL, & McGlynn P (2005) PriB stimulates PriA helicase via an interaction with single-stranded DNA. *J Biol Chem* 280(48):39693-39700.

78. Ng JY & Marians KJ (1996) The ordered assembly of the phiX174-type primosome. II. Preservation of primosome composition from assembly through replication. *J Biol Chem* 271(26):15649-15655.

79. Lopper M, Boonsombat R, Sandler SJ, & Keck JL (2007) A hand-off mechanism for primosome assembly in replication restart. *Mol Cell* 26(6):781-793.

80. Boonsombat R, Yeh SP, Milne A, & Sandler SJ (2006) A novel *dnaC* mutation that suppresses *priB rep* mutant phenotypes in *Escherichia coli* K-12. *Mol Microbiol* 60(4):973-983.

81. Marinus MG (2000) Recombination is essential for viability of an *Escherichia coli dam* (DNA adenine methyltransferase) mutant. *J. Bacteriol.* 182(2):463-468.

82. Nowosielska A & Marinus MG (2005) Cisplatin induces DNA double-strand break formation in *Escherichia coli dam* mutants. *DNA repair* 4(7):773-781.

83. Courcelle CT, Landstrom AJ, Anderson B, & Courcelle J (2012) Cellular characterization of the primosome and rep helicase in processing and restoration of replication following arrest by UV-induced DNA damage in *Escherichia coli*. *J Bacteriol* 194(15):3977-3986.

84. Sandler SJ*, et al.* (1999) *dnaC* mutations suppress defects in DNA replication and recombination-associated functions in *priB* and *priC* double mutants in *Escherichia coli* K-12. *Mol Micro* 34(1):91-101.

85. Wessel SR*, et al.* (2013) PriC-mediated DNA replication restart requires PriC complex formation with the single-stranded DNA-binding protein. *J Biol Chem* 288(24):17569-17578.

86. Aramaki T*, et al.* (2013) Domain separation and characterization of PriC, a replication restart primosome factor in *Escherichia coli*. *Genes Cells* 18(9):723-732.

87. Aramaki T, Abe Y, Katayama T, & Ueda T (2013) Solution structure of the N-terminal domain of a replication restart primosome factor, PriC, in *Escherichia coli*. *Protein Sci* 22(9):1279-1286.

88. Hinds T & Sandler SJ (2004) Allele specific synthetic lethality between *priC* and $dnaA^{ts}$ alleles at the permissive temperature in *E. coli* K-12. *Biomedcentral Microbiology* 4:47-58.

89. Heller RC & Marians KJ (2005) Unwinding of the nascent lagging strand by Rep and PriA enables the direct restart of stalled replication forks. *J Biol Chem* 280(40):34143-34151.

90. Ng JY & Marians KJ (1996) The ordered assembly of the phiX174-type primosome. I. Isolation and identification of intermediate protein-DNA complexes. *J Biol Chem* 271(26):15642-15648.

91. Szymanski MR, Jezewska MJ, & Bujalowski W (2013) Energetics of the *Escherichia coli* DnaT protein trimerization reaction. *Biochemistry* 52(11):1858-1873.

92. Szymanski MR, Jezewska MJ, & Bujalowski W (2013) The *Escherichia coli* primosomal DnaT protein exists in solution as a monomer-trimer equilibrium system. *Biochemistry* 52(11):1845-1857.

93. Huang YH & Huang CY (2013) The N-terminal domain of DnaT, a primosomal DNA replication protein, is crucial for PriB binding and self-trimerization. *Biochem Biophys Res Commun* 442(3-4):147-152.

94. Huang YH, Lin MJ, & Huang CY (2013) DnaT is a single-stranded DNA binding protein. *Genes Cells* 18(11):1007-1019.

95. Lark CA, Riazi J, & Lark KG (1978) *dnaT*, dominant conditional-lethal mutation affecting DNA replication in *Escherichia coli*. *J. Bacteriol.* 1136(3):1008-1017.

96. Masai H & Arai K-I (1988) Operon structure of *dnaT* and *dnaC* genes essential for normal and stable DNA replication of *Escherichia coli* chromosome. *J Bio Chem* 263(29):15083-15093.

97. Naykayama N, Bond M, Miyajima A, Kobor J, & Arai K-i (1987) Structure of *Escherichia coli dnaC*. *J Bio Chem* 262(22):10475-10480.

98. Courcelle J, Khodursky A, Peter B, Brown PO, & Hanawalt PC (2001) Comparative gene expression profiles following UV exposure in wild-type and SOS-deficient *Escherichia coli*. *Genetics* 158(1):41-64.

99. McGlynn P, Al-Deib AA, Liu J, Marians KJ, & Lloyd RG (1997) The DNA replication protein PriA and the recombination protein RecG bind D-loops. *J Mol Biol* 270(2):212-221.

100. Jones JM & Nakai H (2001) *Escherichia coli* PriA helicase: fork binding orients the helicase to unwind the lagging strand side of arrested replication forks. *J Mol Biol* 312(5):935-947.

101. Cadman CJ & McGlynn P (2004) PriA helicase and SSB interact physically and functionally. *Nucleic Acids Res* 32(21):6378-6387.

102. Seigneur M, Bidnenko V, Ehrlich SD, & Michel B (1998) RuvAB acts at arrested replication forks. *Cell* 95(3):419-430.

103. Heller RC & Marians KJ (2007) Non-replicative helicases at the replication fork. *DNA Repair (Amst)* 6(7):945-952.

104. Guy CP*, et al.* (2009) Rep provides a second motor at the replisome to promote duplication of protein-bound DNA. *Mol Cell* 36(4):654-666.

105. Yancey-Wrona JE, Wood ER, George JW, Smith KR, & Matson SW (1992) *Escherichia coli* Rep protein and helicase IV. Distributive single-stranded DNA-dependent ATPases that catalyze a limited unwinding reaction in vitro. *Eur J Biochem* 207(2):479-485.

106. Boubakri H, de Septenville AL, Viguera E, & Michel B (2010) The helicases DinG, Rep and UvrD cooperate to promote replication across transcription units *in vivo*. *EMBO J* 29(1):145-157.

107. Lane HE & Denhardt DT (1975) The rep mutation. IV. Slower movement of replication forks in *Escherichia coli rep* strains. *J Mol Biol* 97(1):99-112.

108. Colasanti J & Denhardt DT (1987) The *Escherichia coli rep* mutation. X. Consequences of increased and decreased Rep protein levels. *Mol Gen Genet* 209(2):382-390.

109. Atkinson J, Gupta MK, & McGlynn P (2011) Interaction of Rep and DnaB on DNA. *Nucleic Acids Res* 39(4):1351-1359.

110. Aguilera A & Gomez-Gonzalez B (2008) Genome instability: a mechanistic view of its causes and consequences. *Nat Rev Genet* 9(3):204-217.

111. Hastings PJ, Ira G, & Lupski JR (2009) A microhomology-mediated break-induced replication model for the origin of human copy number variation. *PLoS Genet* 5(1):e1000327.

112. Ge XQ, Jackson DA, & Blow JJ (2007) Dormant origins licensed by excess Mcm2-7 are required for human cells to survive replicative stress. *Genes Dev* 21(24):3331-3341.

113. Ibarra A, Schwob E, & Mendez J (2008) Excess MCM proteins protect human cells from replicative stress by licensing backup origins of replication. *Proc Natl Acad Sci U S A* 105(26):8956-8961.

114. Lopes M, Foiani M, & Sogo JM (2006) Multiple mechanisms control chromosome integrity after replication fork uncoupling and restart at irreparable UV lesions. *Mol Cell* 21(1):15-27.

115. Tercero JA & Diffley JF (2001) Regulation of DNA replication fork progression through damaged DNA by the Mec1/Rad53 checkpoint. *Nature* 412(6846):553-557.

116. Petermann E, Orta ML, Issaeva N, Schultz N, & Helleday T (2010) Hydroxyurea-stalled replication forks become progressively inactivated and require two different RAD51-mediated pathways for restart and repair. *Mol Cell* 37(4):492-502.

117. Yan S & Michael WM (2009) TopBP1 and DNA polymerase alpha-mediated recruitment of the 9-1-1 complex to stalled replication forks: implications for a replication restart-based mechanism for ATR checkpoint activation. *Cell Cycle* 8(18):2877-2884.

118. Ricke RM & Bielinsky AK (2004) Mcm10 regulates the stability and chromatin association of DNA polymerase-alpha. *Mol Cell* 16(2):173-185.

119. Zhu W*, et al.* (2007) Mcm10 and And-1/CTF4 recruit DNA polymerase alpha to chromatin for initiation of DNA replication. *Genes Dev* 21(18):2288-2299.

120. Gambus A*, et al.* (2009) A key role for Ctf4 in coupling the MCM2-7 helicase to DNA polymerase alpha within the eukaryotic replisome. *EMBO J* 28(19):2992-3004.

Chapter 2

Structural Mechanisms of PriA-Mediated DNA Replication Restart

This chapter represents work that has been published:

Bhattacharyya B, George NP, Thurmes TM, Zhou R, Jani N, Wessel SR, Sandler SJ, Ha T, and Keck JL. (2014) Structural Mechanisms of PriA-Mediated DNA Replication Restart. *Proceedings of the National Academy of Sciences.* 111(4): 1373-8.

Abstract:

Collisions between cellular DNA replication machinery (replisomes) and damaged DNA or immovable protein complexes can dissociate replisomes prior to the completion of replication. This potentially lethal problem is resolved by cellular "replication restart" reactions that recognize the structures of prematurely abandoned replication forks and mediate replisomal reloading. In bacteria, this essential activity is orchestrated by the PriA DNA helicase, which identifies replication forks via structure-specific DNA binding and interactions with fork-associated single-stranded DNA-binding proteins (SSBs). However, the mechanisms by which PriA binds replication fork DNA and coordinates subsequent replication restart reactions have remained unclear due to the dearth of high-resolution structural information available for the protein. Here we describe the crystal structures of full-length PriA and PriA bound to SSB. The structures reveal a modular arrangement for PriA in which several novel DNA binding domains surround its helicase core in a manner that appears poised for binding to branched replication fork DNA structures while simultaneously allowing complex formation with SSB. PriA interaction with SSB is shown to modulate SSB/DNA complexes in a manner that exposes a potential replication initiation site. From these observations, a model emerges to explain how PriA links recognition of diverse replication forks to replication restart.

Significance:

This study describes the crystal structures of the full-length PriA DNA helicase, a multifunctional enzyme that mediates the essential process of restarting prematurely terminated DNA replication reactions in bacteria. Our findings reveal how PriA is able to recognize replication restart substrates through structure-specific DNA binding and interactions with the single-stranded DNA-binding protein and how it exposes single-stranded DNA that could be used to reload the replisome and reinitiate replication. These observations shed new light on the physical mechanisms that allow cells to survive the common and potentially lethal problems posed by incomplete genome replication.

Introduction

Replisomes frequently encounter obstructions such as impassable DNA damage or frozen protein complexes that can arrest replication and/or eject the replisome prior to completion of replication (1-4). Left unrepaired, these events lead to incomplete chromosome duplication, genomic instability, and cell death. All proliferating cells must contend with these clashes since replication blockades can arise from essential endogenous cellular processes. Replication restart, the process by which replisomes are reloaded onto abandoned replication forks, has been observed in both bacteria and eukaryotes. However, only the bacterial factors that mediate this process have been identified. The bacterial replication restart proteins thus serve as models for understanding the general mechanisms of replication restart in all cells (4).

Replication restart in bacteria is orchestrated by the multifunctional PriA DNA helicase (5, 6). The process is initiated by PriA binding to abandoned DNA replication forks or other appropriate replication re-initiation sites in a structure-specific manner. In this recognition step, PriA binds to duplex parental DNA and can accommodate either duplex or gapped leading- and lagging-strand DNA in branched replication fork structures (7-10). PriA's ability to recognize multiple DNA structures appears to provide the flexibility needed for replication restart to be initiated on structures ranging from simple replication forks to D-loops that are produced by recombinational repair of double-stranded DNA breaks (5, 6, 10). However, the structural mechanism by which PriA manages to bind to this array of substrates is unknown. In addition to structure-specific DNA binding, PriA also takes advantage of a direct protein interaction with single-stranded (ss) DNA-binding protein (SSB) tetramers to target its activity to replication forks. SSBs coat the lagging strand template when it is single stranded and form a complex with PriA that stimulates PriA's helicase activity (11-15). In this interaction PriA binds to the

extreme C-terminus of SSB (SSB-Ct), which is a known docking site for numerous genome maintenance proteins that process ssDNA within SSB/ssDNA nucleoprotein complexes (16). Once bound to an appropriate replication restart substrate, PriA remodels the lagging-strand arm to expose ssDNA by either unwinding DNA (if the lagging strand is duplex) or altering the SSB-bound template DNA (if the lagging strand is ssDNA) (17-19). The structural mechanisms underlying lagging-strand remodeling by PriA have not been well defined. PriA then recruits additional replication restart proteins (PriB and DnaT in *E. coli*) to complete formation of the PriA/PriB/DnaT "primosome" complex that is competent to mediate the first step of replication restart – loading of the replicative helicase (DnaB in *E. coli*) onto the remodeled replication fork (20-24). Assembly of the full replisome is then mediated by DnaB activities and protein interactions.

Biochemical studies have identified a two-domain architecture for PriA that includes a DNA-binding domain (DBD, N-terminal ~200 residues) and a helicase domain (HD, C-terminal ~530 residues) (18, 21, 25) (Figure 2.1a). However, despite decades of genetic and biochemical research, the lack of high-resolution structural information for full-length PriA has left the molecular mechanisms underlying abandoned replication fork recognition and processing unresolved. To better understand the roles and mechanisms of PriA in replication restart, we have determined the X-ray crystal structures of full-length PriA and of the PriA/SSB-Ct complex, and have examined the biochemical consequences of PriA/SSB complex formation using a single-molecule approach. The structures reveal a modular arrangement for PriA in which its central helicase core is surrounded by an array of DNA-binding elements. These elements include two domains within the DBD (a 3' DNA-binding domain (3' BD) and an unusual circularly-permuted winged-helix domain (WH)) and two domains within the HD (a

Cys-rich region (CRR) that binds two Zn^{2+} ions, and a C-terminal domain (CTD) with unanticipated similarity to the S10 subunit of the bacterial ribosome). The positioning of these domains coupled with their known or anticipated roles in DNA binding and replication fork remodeling leads to a model that explains how PriA binds to branched DNA replication fork structures in a specific manner. SSB binds to PriA at a site formed at the interface of the 3' BD, CTD and helicase core that appears to be positioned to allow simultaneous PriA binding to both DNA and SSB. PriA interaction with SSB through this site modulates the SSB/ssDNA complex in a manner that exposes ssDNA that could be used to reload DnaB onto abandoned replication forks. Together with the PriA DNA-binding model, these findings produce a molecular view of initial steps of PriA-mediated replication restart.

Results and Discussion

PriA DNA helicase X-ray crystal structure determination.

Several bacterial PriA proteins were initially selected as targets in our crystallographic effort to determine the structure of full-length PriA. Among these proteins, PriA from *Klebsiella pnuemoniae* (KpPriA) crystallized in a form that diffracted X-rays to 2.65 Å resolution (Table 2.1). KpPriA shares 88% sequence identity with the prototypical *E. coli* PriA protein (EcPriA) and the two proteins display very similar DNA binding and DNA-dependent ATPase activities with a synthetic forked DNA substrate (Figure 2.5). Moreover, expression of the *K. pneumoniae priA* gene complements the filamentation and constitutive SOS phenotypes of *priA- E. coli* cells (Figure 2.5). Thus KpPriA and EcPriA are structural and functional homologs.

Single-wavelength anomalous diffraction data from a selenomethionine-substituted KpPriA crystal were used to calculate a 3.76-Å resolution experimental electron density map that allowed building of a partial model of the KpPriA structure. This partial structure was then used as a search model to solve the 2.65-Å resolution native KpPriA structure via molecular replacement (Table 2.1).

The KpPriA structure comprises six subdomains that cluster together (Figure 2.1). Two of these subdomains (3' BD and WH) comprise the N-terminal DBD and the remaining four (two lobes of the helicase core, CRR, and CTD) comprise the HD. The 3' BD, helicase core, CRR and CTD interact with one another to form a shallow cup shape whereas the WH domain projects away from the rest of KpPriA in a position that is stabilized by interactions with symmetrically-related PriA proteins in the crystal lattice (Figure 2.1b). Since the WH lacks direct contacts with the rest of KpPriA, its position is likely to be dynamic in the PriA monomer in solution, which may have led to conformational heterogeneity that prevented crystallization of other full-length

PriA proteins. The electrostatic surface of PriA includes prominent basic patches presented by the 3' BD, WH, helicase, and CTD elements on its concave surface (Figure 2.1c). A significant portion of the concave surface and more scattered patches on the convex surface are evolutionarily well conserved among PriA proteins (Figure 2.1d).

PriA structure reveals two subdomains within the DBD.

The structure of KpPriA showed that the DBD is subdivided into two DNA-binding elements. The first is the 3' BD, which has been shown previously to bind the 3' end of the leading-strand arm of replication fork structures (26). This recognition is thought to help direct PriA replisomal reloading activity to appropriate DNA structures (25-28). The 3' BD structure from full-length KpPriA is strikingly similar to the previously determined structure of the isolated 3' BD from EcPriA (26) (rmsd = 1.8 Å for 90 common C_α atoms). Residues that are known to bind the 3' end of nascent leading-strand DNA in EcPriA (26) form an exposed pocket in full-length KpPriA, making it available for leading strand recognition in the apo structure (Figure 2.1). A leading-strand binding role for this site within full-length PriA is described further below in our model of the PriA/replication fork structure complex.

The second DBD element is a WH domain, which has an unusual circularly-permuted topology that distinguishes it from the classic WH fold. Typical WH domains are defined by core helix-turn-helix folds with β-hairpin "wing" elements; these motifs bind the major and minor grooves of duplex DNA, respectively, in many WH domains (29) (Figure 2.6). The helix-turn-helix fold is present within the PriA WH domain, however the β-hairpin "wing" element has been split open and serves as the connection between the WH domain and the rest of PriA (Figures 2.1b and 2.6). This β-hairpin splitting also alters the order of secondary structural

elements in the PriA domain relative to other WH folds. This difference is accommodated by circular permutation in which the elements that serve as N- and C-terminal ends in most WH domains are directly linked (Figure 2.6). In spite of these differences, an EcPriA fragment comprising just the WH domain is able to bind partial duplex DNA *in vitro* and a longer fragment that includes both the 3' BD and WH domains binds DNA replication fork structures with higher affinity than either domain alone, indicating that the two domains functionally cooperate (9). The most conserved surface of the WH domain presents a highly basic patch from the helix-turn-helix motif on the concave face of PriA that we speculate is important in replication fork DNA binding (below).

The PriA HD includes a helicase core and unusual Zn^{2+}-binding and C-terminal domains with roles in DNA binding and unwinding.

The PriA HD is comprised of a bilobed helicase core region that is buttressed by CRR and CTD elements (Figures 2.1 and 2.2). The PriA helicase core shares significant similarity with other helicases, with canonical helicase motifs lining the interface between the two lobes. An ADP molecule is bound at this interface (Figure 2.2a). Two features were identified within the helicase core that could provide important auto-regulatory elements that restrict PriA ATPase activity in the absence of DNA. The first is a conserved aromatic-rich loop (ARL) in the N-terminal helicase lobe that extends from the helicase core to bind both the 3' BD and CTD (Figure 2.2a). Similar ARLs in RecQ and PcrA DNA helicases bind directly to ssDNA and couple binding to structural changes that stimulate ATPase and helicase activities (30, 31). Mutations within this region of EcPriA block binding to D-loop DNA structures (25), which is consistent with the ARL having a direct role in DNA binding in PriA. The second feature is an

extended helicase motif V that positions the side chain of Lys543 between the β phosphate of ADP and the carboxyl group of Asp319 from helicase motif II (Figure 2.2a). This carboxyl group coordinates an active site Mg^{2+} in other helicases. In the PcrA DNA helicase, a similar Lys modulates ATPase kinetics in a manner that appears to stabilize the ADP product complex (32). Both the ARL and Lys543 are highly conserved among PriA proteins (Figure 2.5) and we predict that they help coordinate PriA DNA binding and ATPase activities.

An unusual feature of the PriA HD is the presence of a CRR embedded within the C-terminal helicase lobe (Figure 2.2b). This 50-residue insertion forms a structure on the surface of the helicase core in which two Zn^{2+} ions are coordinated by invariant Cys residues. A portion of the PriA CRR bears an unexpected structural similarity to the N-terminal domain of the Rpb9 subunit of eukaryotic RNA polymerase II (rmsd = 2.3 Å for 39 common C_α atoms (33)), although the analogous Rpb9 domain only binds a single Zn^{2+} ion. The functional significance of this structural similarity is not known. Previous biochemical experiments have shown that sequence changes to Zn^{2+}-binding Cys residues in the EcPriA CRR can eliminate helicase, but not ATPase, activity and can block assembly of PriB onto DNA-bound PriA (24, 34), implicating the CRR in multiple functions in PriA. Interestingly, a β-hairpin within the CRR is in a similar position relative to the PriA helicase core to "wedge" elements that are critical for DNA strand separation in other related helicases (Figure 2.7). Given the position of the CRR and noted defects of EcPriA CRR Cys variants in DNA unwinding, the β-hairpin within the CRR is an excellent candidate to function as a DNA unwinding wedge in PriA. In this activity, the helicase core would directionally translocate on a ssDNA tail of a partial duplex DNA and pull the duplex into the β-hairpin wedge, which would split the duplex into two strands. Given the 3'-5' translocase and helicase activity of PriA and its preference for unwinding the lagging strand of

replication fork structures (11-13, 35, 36), this model suggests that lagging strand template ssDNA would be engaged by the helicase core while the duplex portion of the lagging strand would be unwound by the CRR. This arrangement could create a PriA/DNA structure onto which PriB can dock during primosome assembly and may be important for creating ssDNA that acts as a loading site for DnaB.

The final element of the HD is the CTD, which forms a central core in PriA that directly contacts all domains but the WH (Figure 2.2c). The CTD is unexpectedly similar to the S10 ribosomal subunit (rmsd = 2.2 Å for 68 common C_α atoms), which binds branched rRNA within the bacterial ribosome (37) (Figure 2.2d). Several basic residues within the CTD project toward the helicase domain near where ssDNA is predicted to bind and are positioned similarly to RNA-binding residues in S10, highlighting their possible roles in DNA binding in PriA. To test the DNA binding properties of the PriA CTD, a recombinant EcPriA CTD was constructed based on the KpPriA structure and tested for its ability to bind to fluorescein-labeled DNA structures. The isolated CTD was able to bind to a variety of DNA structures *in vitro*, including ssDNA, duplex DNA, and a replication fork mimic (duplex DNA with 3' and 5' ssDNA tails) (Figure 2.2e), consistent with roles for the CTD in DNA binding in the context of full-length PriA.

Structure and function of the PriA/SSB complex.

In addition to structure-specific DNA binding, PriA interacts with the SSB C-terminus (SSB-Ct) at replication forks (13-15). To identify the SSB-Ct binding site on PriA, we determined the 4.1-Å-resolution structure of KpPriA bound to an SSB-Ct peptide (Table 2.1). Although the resolution of the structure was modest, clear electron density for the SSB-Ct peptide was observed in the F_o-F_c maps that permitted fitting of the peptide (Figure 2.3a). The

SSB-Ct binds at an evolutionarily conserved site formed at the junction of the CTD, helicase core, and 3' BD that is on the opposite face of PriA relative to the DNA binding surface (Figure 2.1). This partitioning would allow PriA to contact DNA and SSB simultaneously. The PriA SSB-Ct binding site shares similarity with binding pockets characterized in other SSB-interacting proteins, including the presence of a prominent basic residue (Arg697) near the α-carboxyl group of the C-terminal-most residue of the SSB-Ct (Figure 2.3a). In other proteins, sequence changes at the α-carboxyl interaction position dramatically destabilize their interactions with SSB (38-41).

Since SSB binding to ssDNA blocks reloading of DnaB (42), we used a single-molecule (sm) FRET assay to test whether direct binding of PriA to SSB could modulate SSB/DNA complexes in a manner that exposes a potential ssDNA replisome reloading site. *E. coli* SSB binds ssDNA in either a highly cooperative mode in which 35 nucleotides are bound per tetramer (SSB_{35}) or a less cooperative mode that binds 65 nucleotides per tetramer (SSB_{65}) (43); these modes can be distinguished in our assay by their differing FRET efficiencies between the fluorescence donor/acceptor pair (Cy3/Cy5) on the DNA substrate (44) (Figure 2.3b). When a single SSB tetramer is bound in the SSB_{65} mode, Cy3/Cy5 are in close proximity (FRET efficiency ~0.4) but when two SSB tetramers are bound to the DNA in the SSB_{35} mode, Cy3/Cy5 are further apart (FRET efficiency ~0.2) (Figure 2.3b) (44, 45). In the absence of SSB, the labeled DNA molecule is unconstrained, which leads to a very low FRET efficiency (efficiency ~0.1, Figure 2.3). Our experimental conditions, which include excess free SSB, allowed spontaneous interconversion between the SSB_{35} and SSB_{65} modes (Figure 2.3b, lower).

Interestingly, the addition of EcPriA had two effects on SSB/DNA complexes in the smFRET assay: PriA strongly stabilized the SSB_{35} binding mode over the SSB_{65} mode and PriA

modestly reduced the SSB_{35} mode FRET efficiency (Figure 2.3c). These changes are consistent with PriA exposing ssDNA (due to the SSB_{65}-to-SSB_{35} transition) and with PriA binding to the newly exposed ssDNA, which results in the slightly lower FRET efficiency state. In a simple model of this PriA/SSB/DNA ternary complex, PriA could associate at the single strand/duplex junction in the smFRET substrate and slide the two SSB tetramers to the end of the ssDNA tail. Interestingly, an Arg697Ala EcPriA variant, in which a key SSB-binding residue is neutralized, fails to alter the SSB_{35}/SSB_{65} distribution (Figure 2.3c). This variant retains DNA binding and unwinding activities and can still alter the FRET efficiencies of both SSB modes, suggesting that the observed modulation of SSB/DNA binding modes is dependent upon a functional PriA/SSB interaction and not due to differential DNA binding abilities of the PriA variant (Figures 2.3c, 2.8, and 2.9). These data indicate that PriA complex formation with SSB induces structural changes in the SSB/DNA complex that expose ssDNA that can be captured by PriA. A recent study showed that the PriC protein, which initiates a parallel replication restart pathway in *E. coli* and a small number of closely related bacterial species, also preferentially stabilizes the SSB_{35} mode (46). These findings suggest that SSB binding mode remodeling could be a general requirement for DNA replication restart.

Model for PriA-mediated replication restart.

A model emerges from our data to explain how PriA can recognize diverse DNA replication fork structures (Figure 2.4). The arrangement of DNA-binding domains within the PriA structure complements the positions of the three DNA arms of branched replication fork and D-loops structures, which could facilitate structure-specific DNA binding by PriA. Within this array of domains, we propose that the 3' BD would recognize the 3' end of the leading-strand

as has been observed previously (26) whereas the HD would preferentially bind to lagging-strand DNA. Lagging-strand binding by the HD in this model is consistent with PriA's noted 3' - 5' translocase and helicase activities and its preference for unwinding the nascent lagging strand of replication fork structures (11-13, 35, 36). This arrangement places the unreplicated parental DNA in an ideal position to be bound by the highly basic surface presented by the helix-turn-helix fold in the PriA WH domain (Figure 2.1c and Figure 2.4). The isolated EcPriA WH domain has been shown to bind partial duplex DNA (9), further supporting its suggested role in parental DNA binding. Finally, given the ability of the CTD to bind to a variety of DNA structures (Figure 2.2e), it could contribute to binding single stranded, duplex or branched DNA that is presented by the helicase core and/or the 3' BD. Our binding model thus explains how the structure of PriA is adapted to specifically recognize appropriate substrates for replication restart.

Following recognition of an abandoned replication fork, PriA must alter the lagging-strand to expose a ssDNA site for reloading the replicative helicase. Depending upon whether the lagging strand is duplex or single-stranded, this step requires DNA unwinding or remodeling of SSB-coated ssDNA, respectively. As described above, unwinding of the lagging strand could be accomplished by translocation of the core helicase domain along the lagging-strand template DNA with the CRR acting as a wedge to unwind duplex DNA (Figure 2.4, top). For SSB/DNA remodeling, the smFRET studies presented in Figure 2.3 support a model in which PriA acts by directly interacting with SSB bound to the lagging strand. Formation of the PriA/SSB complex exposes ssDNA from SSB to which PriA can then bind, leading to formation of a PriA/SSB/DNA ternary complex where PriA holds ssDNA in preparation for reloading of the replicative DnaB helicase. Additionally, PriA translocase activity could possibly "push" SSB along the lagging-strand template to expose additional ssDNA to which primosome components

(PriB and DnaT) can bind and that will ultimately serve as a binding site for DnaB. A similar "pushing" mechanism in which SSB is promoted along DNA by a directional enzyme has been demonstrated for the RecA recombinase *in vitro* (47).

Taken together, these models provide insights into the molecular mechanisms that govern the initial steps of replication restart in bacteria. Through a combination of its structure-specific DNA binding and unwinding properties and its ability to manipulate SSB/DNA complexes, PriA appears to have adapted to function on a variety of abandoned DNA replication forks structures that could form in response to diverse challenges during replication in cells. We speculate that these mechanistic features allow PriA to act selectively on *bona fide* sites for replication restart while avoiding the potential problems that would arise from non-selective replication restart in other loci throughout the genome. Similar core biochemical activities may form minimal functional requirements that could aid in the identification of eukaryotic replication restart factors.

Materials and Methods

Detailed experimental procedures used in this study can be found in SI Materials and Methods and in Tables 2.2 and 2.3. A summary of the experimental procedures follows.

Structure determination. KpPriA and selenomethionine-substituted KpPriA were crystallized using the hanging-drop vapor diffusion method and the structure of apo KpPriA was determined by a combination of single-wavelength anomalous dispersion and molecular replacement phasing. The structure of the KpPriA/SSB-Ct peptide complex was determined by molecular replacement using the apo KpPriA structure as a search model. Coordinate and structure factor files for apo KpPriA and the KpPriA/SSB-Ct peptide complex crystal structures are available at the RCSB Protein Data Bank (PDB codes: 4NL4 and 4NL8, respectively).

DNA-binding experiments. Equilibrium DNA binding by PriA proteins or domains was measured as protein-dependent changes in fluorescence anisotropy of fluorescein-labeled DNA.

smFRET experiments. Partial duplex DNA with donor (Cy3) and acceptor (Cy5) labels was immobilized on a quartz slide and first bound by SSB and then subsequently by EcPriA or an EcPriA variant. A total internal fluorescence microscope measured time-resolved FRET of individual molecules and FRET efficiency histograms were generated from >5000 molecules each.

Acknowledgements:

The authors thank Kenneth Satyshur and staff at the Advanced Photon Source (LS-CAT) for assistance with data collection. We thank James Berger, Matthew Lopper, and members of the Keck lab for manuscript review. This work was supported by the National Institutes of Health (GM098885 to JLK and SJS, and GM065367 to TH) and the National Science Foundation (0822613 to TH). TH is an employee of the Howard Hughes Medical Institute. BB and SRW were supported in part by an NIH training grant in Molecular Biosciences (GM07215). JLK is cofounder of Replisoma, Inc.

Figure 2.1

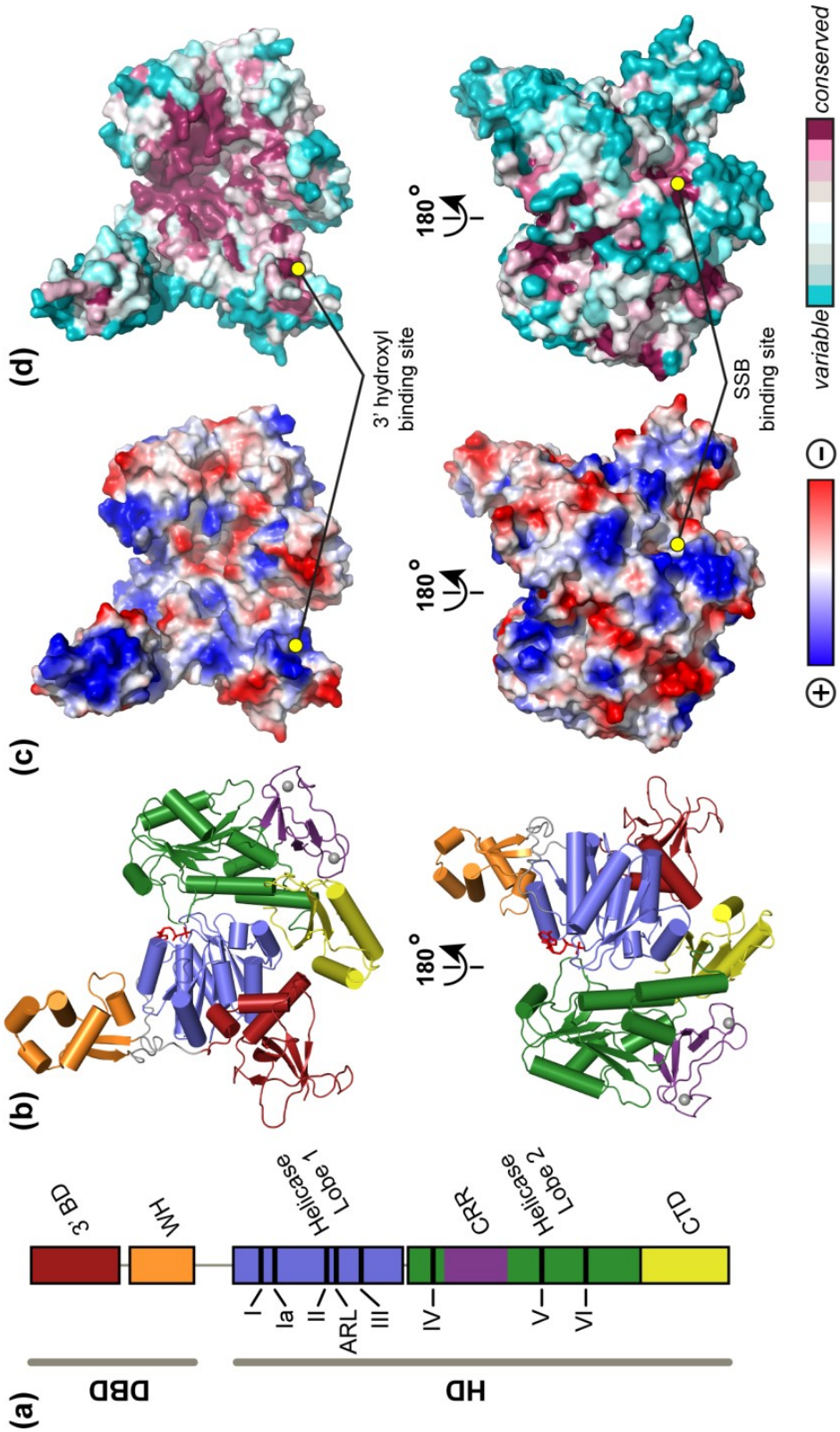
(a)
DBD
HD
3' BD
WH
Helicase Lobe 1
CRR
Helicase Lobe 2
CTD
I
Ia
II
ARL
III
IV
V
VI
(b)
(c)
(d)
180°
3' hydroxyl binding site
SSB binding site
conserved
variable
⊖
⊕

Figure 2.1. Structure of PriA DNA Helicase.
(a) Schematic diagram of PriA domain structure. DBD, DNA-binding domain; HD, helicase domain; 3' BD, 3' DNA-binding domain; CRR, Cys-rich region; CTD, C-terminal domain; ARL, aromatic-rich loop. **(b)** Crystal structure of KpPriA. Domains are colored as in (a). ADP (red sticks) is bound within the helicase core and two Zn^{2+} ions (grey spheres) are bound to the CRR. **(c)** Electrostatic surface features of KpPriA (blue, electropositive; red, electronegative; white, neutral). **(d)** Evolutionary conservation of KpPriA (conservation scale, from variable to invariant among 150 PriA protein sequences, is shown below the structure).

Figure 2.2

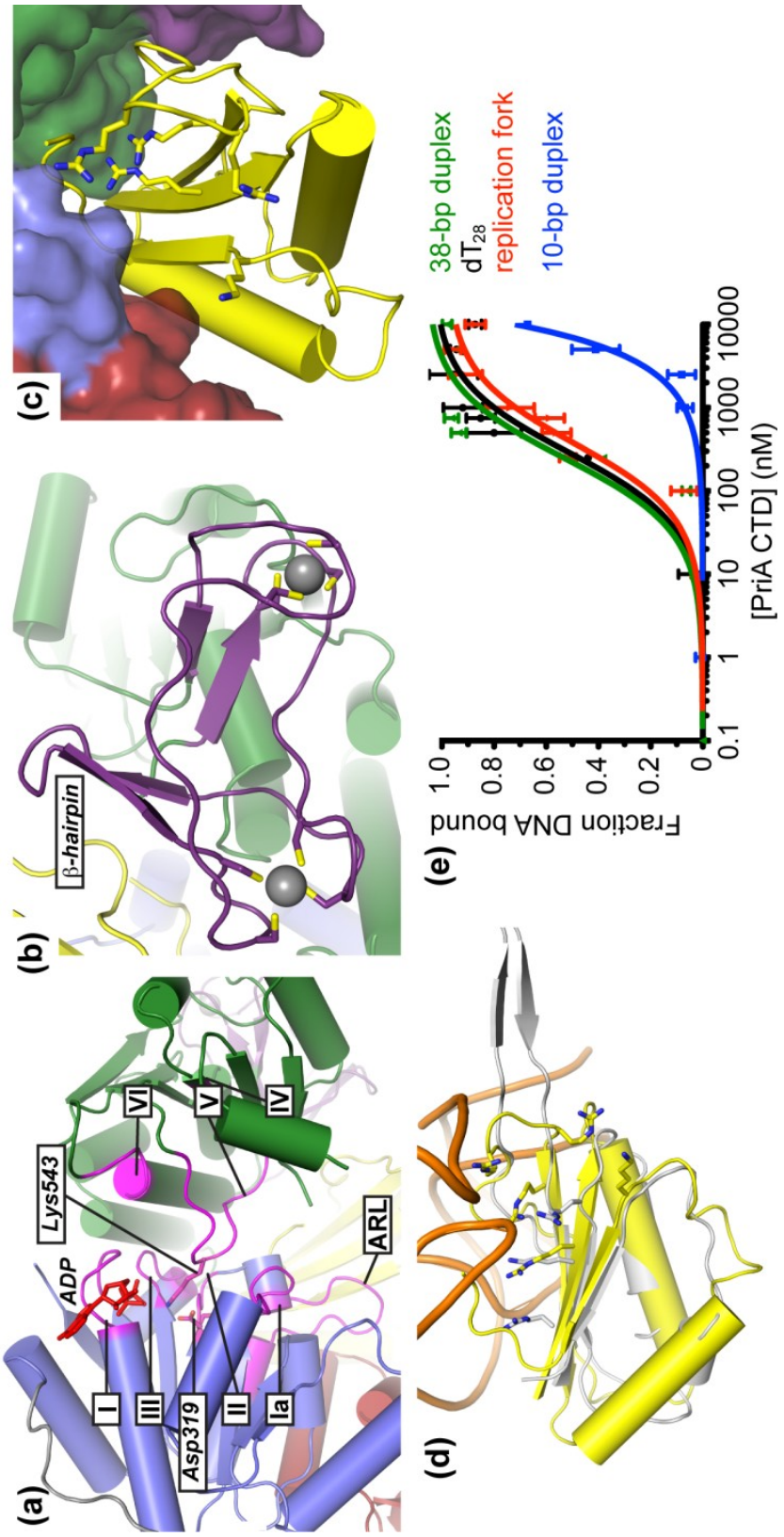
(a)
ADP
Lys543
Asp319
I
III
II
Ia
VI
V
IV
ARL
(b)
β-hairpin
(c)
(d)
(e)
38-bp duplex
dT28
replication fork
10-bp duplex
Fraction DNA bound
1.0
0.8
0.6
0.4
0.2
0
0.1
1
10
100
1000
10000
[PriA CTD] (nM)

Figure 2.2. PriA Domain Features.
(a) Core helicase motifs and the ARL (magenta, labeled) line the interface between the bilobed helicase domain. An ADP molecule (red sticks) is shown. **(b)** The PriA CRR binds two Zn^{2+} ions (grey spheres) and positions a β-hairpin that is proposed to act as a DNA unwinding wedge. **(c)** Close-up of the CTD (yellow) with basic residues displayed as sticks. The surfaces of the 3' BD, helicase core, and CRR are rendered to highlight the extensive contacts made between the CTD and each domain. **(d)** Overlay of KpPriA CTD (yellow) with the S10 ribosomal subunit (grey, with rRNA shown in orange (37)). RNA-binding basic residues from S10 and similarly positioned residues from the KpPriA CTD are shown (sticks). **(e)** EcPriA CTD binding to fluorescently labeled dT_{28} (black), 10-bp duplex (blue), 38-bp duplex (green), and replication fork (red) DNA. Data are the mean of three independent experiments with error bars representing 1 standard deviation.

Figure 2.3

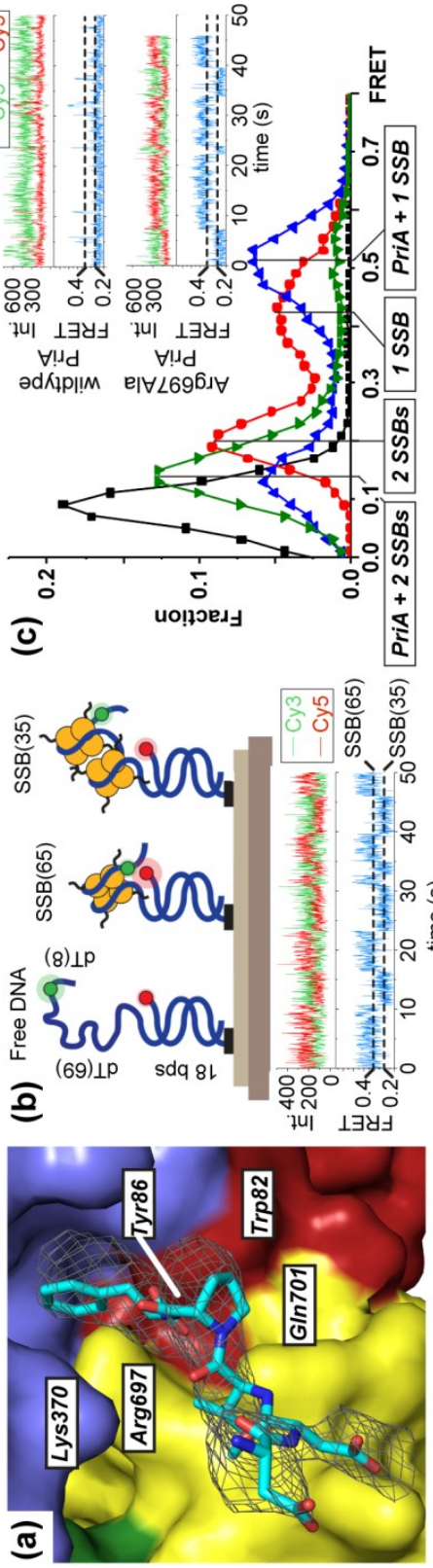
(a)
Lys370
Arg697
Tyr86
Trp82
Gln701
(b)
Free DNA
dT(69)
18 bps
dT(8)
SSB(65)
SSB(35)
Cy3
Cy5
Int.
FRET
SSB(65)
SSB(35)
time (s)
(c)
Fraction
FRET
PriA + 2 SSBs
2 SSBs
1 SSB
PriA + 1 SSB
Arg697Ala PriA
wildtype PriA
Cy3
Cy5
time (s)

Figure 2.3. PriA/SSB Complex Structure and Function.
(a) F_o-F_c omit electron density (1.7-σ contour) identifies the SSB-Ct peptide binding site on PriA. Invariant PriA residues are labeled. **(b)** (top) Schematic of the smFRET assay that distinguishes free DNA, SSB_{65}-bound DNA, and SSB_{35}-bound DNA (44). (bottom) Trace of an individual DNA molecule transitioning between SSB_{65} and SSB_{35} binding modes. Cy3 (green), Cy5 (red) and FRET (blue) intensities fluctuate over time due to mode interconversion. **(c)** smFRET-efficiency histograms of DNA alone (black), DNA with 20 nM SSB (red), 20 nM SSB with 1 μM PriA (green), or 20 nM SSB with 1 μM Arg697Ala PriA (blue). Representative single molecule time traces are shown for PriA and Arg697PriA experiments (inset).

Figure 2.4

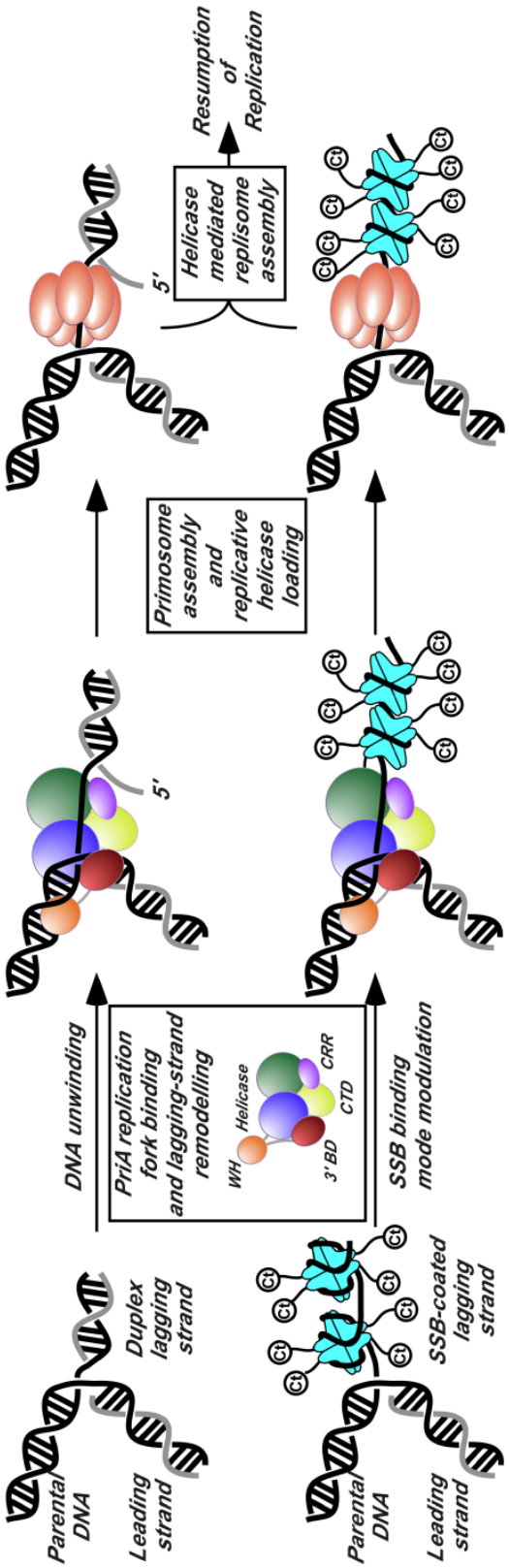
Parental DNA
Leading strand
Duplex lagging strand
SSB-coated lagging strand
DNA unwinding
PriA replication fork binding and lagging-strand remodelling
SSB binding mode modulation
WH
Helicase
3' BD
CRR
CTD
5'
Primosome assembly and replicative helicase loading
Helicase mediated replisome assembly
Resumption of Replication

Figure 2.4. PriA Replication Restart Initiation Models.
PriA recognizes abandoned DNA replication forks with either duplex (top) or SSB-bound ssDNA (bottom) lagging strands and processes these to expose ssDNA necessary for full primosome assembly and reloading of the replicative helicase. Nascent DNA strands are colored grey. Replisomal reassembly proceeds spontaneously after replicative helicase loading.

References:

1. Cox MM*, et al.* (2000) The importance of repairing stalled replication forks. *Nature* **404**:37-41.

2. Heller RC & Marians KJ (2006) Replisome assembly and the direct restart of stalled replication forks. *Nat Rev Mol Cell Biol* **7**:932-943.

3. Merrikh H, Zhang Y, Grossman AD, & Wang JD (2012) Replication-transcription conflicts in bacteria. *Nat Rev Microbiol* **10**:449-458.

4. Yeeles JT, Poli J, Marians KJ, & Pasero P (2013) Rescuing stalled or damaged replication forks. *Cold Spring Harb Perspect Biol* **5**:a012815.

5. Gabbai CB & Marians KJ (2010) Recruitment to stalled replication forks of the PriA DNA helicase and replisome-loading activities is essential for survival. *DNA Repair* **9**:202-209.

6. Masai H, Tanaka T, & Kohda D (2010) Stalled replication forks: making ends meet for recognition and stabilization. *BioEssays* **32**:687-697.

7. McGlynn P, Al-Deib AA, Liu J, Marians KJ, & Lloyd RG (1997) The DNA replication protein PriA and the recombination protein RecG bind D-loops. *J Mol Biol* **270**:212-221.

8. Nurse P, Liu J, & Marians KJ (1999) Two modes of PriA binding to DNA. *J Biol Chem* **274**:25026-25032.

9. Tanaka T, Mizukoshi T, Sasaki K, Kohda D, & Masai H (2007) *Escherichia coli* PriA protein, two modes of DNA binding and activation of ATP hydrolysis. *J Biol Chem* **282**:19917-19927.

10. Manhart CM & McHenry CS (2013) The PriA replication restart protein blocks replicase access prior to helicase assembly and directs template specificity through its ATPase activity. *J Biol Chem* **288**:3989-3999.

11. Lee MS & Marians KJ (1987) *Escherichia coli* replication factor Y, a component of the primosome, can act as a DNA helicase. *Proc Natl Acad Sci* **84**:8345-8349.

12. Lasken RS & Kornberg A (1988) The primosomal protein n' of *Escherichia coli* is a DNA helicase. *J Biol Chem* **263**:5512-5518.

13. Cadman CJ & McGlynn P (2004) PriA helicase and SSB interact physically and functionally. *Nucleic Acids Res* **32**:6378-6387.

14. Lecointe F*, et al.* (2007) Anticipating chromosomal replication fork arrest: SSB targets repair DNA helicases to active forks. *EMBO J* **26**:4239-4251.

15. Kozlov AG, Jezewska MJ, Bujalowski W, & Lohman TM (2010) Binding specificity of *Escherichia coli* single-stranded DNA binding protein for the chi subunit of DNA pol III holoenzyme and PriA helicase. *Biochemistry* **49**:3555-3566.

16. Shereda RD, Kozlov AG, Lohman TM, Cox MM, & Keck JL (2008) SSB as an organizer/mobilizer of genome maintenance complexes. *Critical reviews in biochemistry and molecular biology* **43**:289-318.

17. Jones JM & Nakai H (2001) *Escherichia coli* PriA helicase: fork binding orients the helicase to unwind the lagging strand side of arrested replication forks. *J Mol Biol* **312**:935-947.

18. Chen HW, North SH, & Nakai H (2004) Properties of the PriA helicase domain and its role in binding PriA to specific DNA structures. *J Biol Chem* **279**:38503-38512.

19. Shlomai J & Kornberg A (1980) A prepriming DNA replication enzyme of *Escherichia coli*. II. Actions of protein n': a sequence-specific, DNA-dependent ATPase. *J Biol Chem* **255**:6794-6798.

20. Low RL, Shlomai J, & Kornberg A (1982) Protein n, a primosomal DNA replication protein of *Escherichia coli*. Purification and characterization. *J Biol Chem* **257**:6242-6250.

21. Lopper M, Boonsombat R, Sandler SJ, & Keck JL (2007) A hand-off mechanism for primosome assembly in replication restart. *Mol Cell* **26**:781-793.

22. Ng JY & Marians KJ (1996) The ordered assembly of the phiX174-type primosome. I. Isolation and identification of intermediate protein-DNA complexes. *J Biol Chem* **271**:15642-15648.

23. Ng JY & Marians KJ (1996) The ordered assembly of the phiX174-type primosome. II. Preservation of primosome composition from assembly through replication. *J Biol Chem* **271**:15649-15655.

24. Liu J, Nurse P, & Marians KJ (1996) The ordered assembly of the phiX174-type primosome. III. PriB facilitates complex formation between PriA and DnaT. *J Biol Chem* **271**:15656-15661.

25. Tanaka T*, et al.* (2002) DNA binding of PriA protein requires cooperation of the N-terminal D-loop/arrested-fork binding and C-terminal helicase domains. *J Biol Chem* **277**:38062-38071.

26. Sasaki K*, et al.* (2007) Structural basis of the 3'-end recognition of a leading strand in stalled replication forks by PriA. *EMBO J* **26**:2584-2593.

27. Tanaka T & Masai H (2006) Stabilization of a stalled replication fork by concerted actions of two helicases. *J Biol Chem* **281**:3484-3493.

28. Mizukoshi T, Tanaka T, Arai K, Kohda D, & Masai H (2003) A critical role of the 3' terminus of nascent DNA chains in recognition of stalled replication forks. *J Biol Chem* **278**:42234-42239.

29. Gajiwala KS & Burley SK (2000) Winged helix proteins. *Curr Opin Struct Biol* **10**:110-116.

30. Dillingham MS, Soultanas P, & Wigley DB (1999) Site-directed mutagenesis of motif III in PcrA helicase reveals a role in coupling ATP hydrolysis to strand separation. *Nucleic Acids Res* **27**:3310-3317.

31. Zittel MC & Keck JL (2005) Coupling DNA-binding and ATP hydrolysis in *Escherichia coli* RecQ: role of a highly conserved aromatic-rich sequence. *Nucleic Acids Res* **33**:6982-6991.

32. Soultanas P, Dillingham MS, Velankar SS, & Wigley DB (1999) DNA binding mediates conformational changes and metal ion coordination in the active site of PcrA helicase. *J Mol Biol* **290**:137-148.

33. Liu X, Bushnell DA, Silva DA, Huang X, & Kornberg RD (2011) Initiation complex structure and promoter proofreading. *Science* **333**:633-637.

34. Zavitz KH & Marians KJ (1993) Helicase-deficient cysteine to glycine substitution mutants of *Escherichia coli* replication protein PriA retain single-stranded DNA-dependent ATPase activity. Zn^{2+} stimulation of mutant PriA helicase and primosome assembly activities. *J Biol Chem* **268**:4337-4346.

35. Heller RC & Marians KJ (2005) Unwinding of the nascent lagging strand by Rep and PriA enables the direct restart of stalled replication forks. *J Biol Chem* **280**:34143-34151.

36. Lee MS & Marians KJ (1990) Differential ATP requirements distinguish the DNA translocation and DNA unwinding activities of the *Escherichia coli* PRI A protein. *J Biol Chem* **265**:17078-17083.

37. Demeshkina N, Jenner L, Westhof E, Yusupov M, & Yusupova G (2012) A new understanding of the decoding principle on the ribosome. *Nature* **484**:256-259.

38. Lu D & Keck JL (2008) Structural basis of *Escherichia coli* single-stranded DNA-binding protein stimulation of exonuclease I. *Proc Natl Acad Sci* **105**:9169-9174.

39. Marceau A*, et al.* (2011) Structure of the SSB-DNA polymerase III interface and its role in DNA replication. *EMBO J* **30**:4236-4247.

40. Ryzhikov M, Koroleva O, Postnov D, Tran A, & Korolev S (2011) Mechanism of RecO recruitment to DNA by single-stranded DNA binding protein. *Nucleic Acids Res* **39**:6305-6314.

41. Inoue J*, et al.* (2011) A mechanism for single-stranded DNA-binding protein (SSB) displacement from single-stranded DNA upon SSB-RecO interaction. *J Biol Chem* **286**:6720-6732.

42. LeBowitz JH & McMacken R (1986) The E*scherichia coli* dnaB replication protein is a DNA helicase. *J Biol Chem* **261**:4738-4748.

43. Bujalowski W & Lohman TM (1986) *Escherichia coli* single-strand binding protein forms multiple, distinct complexes with single-stranded DNA. *Biochemistry* **25**:7799-7802.

44. Roy R, Kozlov AG, Lohman TM, & Ha T (2007) Dynamic Structural Rearrangements Between DNA Binding Modes of *E. coli* SSB Protein. *J Mol Biol* **369**:1244-1257.

45. Zhou R*, et al.* (2011) SSB functions as a sliding platform that migrates on DNA via reptation. *Cell* **146**:222-232.

46. Wessel SR*, et al.* (2013) PriC-mediated DNA replication restart requires PriC complex formation with the single-stranded DNA-binding protein. *J Biol Chem* **288**:17569-17578.

47. Roy R, Kozlov AG, Lohman TM, & Ha T (2009) SSB diffusion on single stranded DNA stimulates RecA filament formation. *Nature* **461**:1092-1097.

Supplemental text:

SI materials and methods

Tables 2.1-2.3

Figures 2.5-2.9

SI references

SI materials and methods

Oligonucleotides and DNA substrates

All oligonucleotides (Table 2.2) were purchased from the University of Wisconsin Biotechnology Center. The following molecules were used in DNA binding, DNA-dependent ATPase and/or helicase studies: dT_{28}, dT_{70}, 10-bp duplex (BB130 and FP_10mer_5'fluor-dsDNA), 38-bp duplex (11b-38 and oML225_rc_5'fluor), and replication fork substrate (described in (10), 1b-98, 3L-98, and 11b-38). Fluorescently labeled DNAs include a 5' fluorescein moiety. Branched DNA substrate was made by annealing oligonucleotides 3L-98 (^{32}P labeled using T4 polynucleotide kinase prior to annealing) and 1b-98. Oligonucleotides comprising the duplex, replication fork, and branched substrates were combined in equimolar rations in 20 mM Tris, pH 8.0, 100 mM NaCl, and 20 mM $MgCl_2$ and annealed by heating at 95°C for 5 minutes followed by slow cooling to room temperature.

Plasmid construction

The *K. pnuemoniae priA* open reading frame was PCR amplified from genomic DNA (strain MGH 78578, American Type Culture Collection) and subcloned into pET28b (Novagen), creating pET28-KpPriA. The gene encodes a His_6 affinity purification tag and thrombin cleavage site fused onto the N-terminus of KpPriA. The EcPriA CTD-encoding DNA sequence (for residues 633-732 of EcPriA) was amplified from plasmid pML100 (11) and subcloned in frame into pET15a, creating plasmid vector pET15-EcPriACTD. The open reading frame sequence of both plasmids was confirmed by DNA sequencing.

Protein purification

E. coli Rosetta2 were transformed with pET28-KpPriA or pET15-EcPriACTD and grown at 37°C in Luria broth supplemented with 50 μg/mL kanamycin and 37 μg/mL chloramphenicol. Cells at mid log phase ($OD_{600\ nm}$ of ~0.6) were induced to express KpPriA or the EcPriA CTD by the addition of 1 mM isopropyl β-D-1-thiogalactopyranoside and cells were harvested by centrifugation (8,000 rpm, 10 minutes, 4°C) after an additional 3 hours of growth. Cell pellets were resuspended in 47 mL lysis buffer (10 mM HEPES-HCl, pH 7.0, 10% glycerol, 500 mM NaCl, 100 mM glucose, 20 mM imidazole, 1 mM β-mercaptoethanol, 1 mM phenylmethylsulfonyl fluoride, 1 mM benzamidine, and 1 EDTA-free protease inhibitor tablet (Roche)), lysed by sonication on ice and clarified by centrifugation (18,000 rpm, 30 minutes, 4°C). Supernatants were incubated with Ni-NTA resin (Qiagen) for 1 hour at 4°C followed by washing with excess lysis buffer and elution in elution buffer (10 mM HEPES-HCl, pH 7.0, 10% glycerol, 500 mM NaCl, 300 mM imidazole, 1 mM β-mercaptoethanol). Eluted protein was dialyzed at 4°C against low-salt buffer (10 mM HEPES-HCl, pH 7.0, 10% glycerol, 150 mM NaCl, 10 mM dithiothreitol). Dialysates were further purified via ion exchange and size exclusion chromatography. KpPriA and EcPriACTD were >97% pure as judged by denaturing polyacrylamide gel electrophoresis. Selenomethionine-incorporated KpPriA was overexpressed according to previously published protocols (12) and purified using the same protocol as for the native protein. EcPriA was purified as described earlier (11). Protein concentrations were determined by measuring UV absorbance at 280 nm and using calculated extinction coefficients of 105,870 $M^{-1}cm^{-1}$ for EcPriA, 110,160 $M^{-1}cm^{-1}$ for KpPriA and 22,760 $M^{-1}cm^{-1}$ for the EcPriA CTD.

KpPriA structure determination

Native and selenomethionine-incorporated KpPriA were dialyzed against minimal buffer (10 mM Tris-HCl, pH 8.0, 500 mM ammonium acetate) and TCEP-HCl was added to 10 mM after dialysis. KpPriA (5 mg/mL) was mixed with mother liquor (10 mM Tris-HCl, pH 8.0, 5% MPD, and 6% PEG6000) and 0.6 mM ATPγS at a 0.9:0.9:0.2 ratio and crystallized by hanging drop vapor diffusion at 22°C. Five microliters of buffer containing 10 mM Tris-HCl, pH 8.0, 6% PEG6000, and 25% glycerol was added directly to drops with crystals, which were subsequently frozen in liquid nitrogen. Crystals had one KpPriA molecule per asymmetric unit.

The KpPriA structure was initially solved using single-wavelength anomalous dispersion (SAD) phasing to 3.76-Å resolution. Data were indexed and scaled using HKL2000 (13). Selenium positions were identified and refined using SHARP (14) and an initial model was obtained using COOT (15) and refined using Refmac5 (16). The initial model was then refined against a 2.65-Å native dataset and the final model was obtained through successive model building and TLS refinement (17). Final statistics for data collection and refinement are shown in Table 2.1. Phi and psi backbone angles for the final model were 87.7%, 10.8%, 0.3%, and 1.2% within the most favored, allowed, generously allowed, and disallowed regions of Ramachandran space, respectively.

Crystals of the SSB-Ct bound form of PriA were obtained essentially in the same manner as the ADP-bound crystals except KpPriA (5 mg/mL) was mixed with mother liquor (0.1 M ammonium acetate, 0.015 M magnesium acetate tetrahydrate, 0.05 M sodium cacodylate trihydrate pH 6.5, and 10% v/v 2-propanol) and 1.2 mM SSB-Ct peptide (Trp-Met-Asp-Phe-Asp-Asp-Asp-Ile-Pro-Phe) at a 0.9:0.9:0.2 ratio and crystallized by hanging drop vapor diffusion

at 22°C. Five microliters of buffer containing 0.1 M ammonium acetate, 0.015 M magnesium acetate tetrahydrate, 0.05 M sodium cacodylate trihydrate pH 6.5, and 25% glycerol was added directly to drops with crystals, which were subsequently frozen in liquid nitrogen. Crystals had three KpPriA/SSB-Ct complexes per asymmetric unit. The SSB-Ct bound form of KpPriA was solved to 4.1-Å resolution using the high resolution ADP bound structure as a model for molecular replacement in Phaser (18). The WH domain was not resolved in the crystal structure (likely due to dynamics) and was omitted from the search model and the final refined model. Data collection refinement statistics are shown in Table 2.1. Phi and psi backbone angles for the final model were 87.5%, 10.7%, 1.0%, and 0.8% within the most favored, allowed, generously allowed, and disallowed regions of Ramachandran space, respectively. Domain structure comparisons were carried out using DALI (19).

Fluorescence anisotropy DNA-binding assays

KpPriA, EcPriA or EcPriA-CTD was dialyzed against 20 mM HEPES-HCl, pH 7.0, 75 mM potassium glutamate, 5% glycerol and 10 mM DTT. Fluorescein-labeled DNA (1 nM (molecules) dT_{28}, 10 bp duplex, 38 bp duplex, or a replication fork substrate with 38 bp leading strand, 38 base single-stranded lagging strand and 60 bp duplex parental (10)) was incubated with varying concentrations of protein for 30 min at room temperature and fluorescence anisotropy was measured was measured using a Beacon 2000 fluorescence polarization instrument. Data were fit to a single binding site model and apparent K_d was determined on values converted from anisotropy data to fraction of protein bound to DNA using GraphPad (PRISM). Data represent average of three trials and error bars represent one standard deviation.

Single-molecule FRET experiments

All smFRET experiments were performed at 22 ± 1°C using a total internal reflection fluorescence microscope (20). Sample assembly, data acquisition, and FRET efficiency calculations were performed as described previously (20-22). Briefly, 50-100 pM of partial duplex DNA substrates ($(dT)_{69+8}$) were immobilized on a quartz slide surface coated with polyethylene glycol (mPEG-SC, Laysan Bio) in order to eliminate nonspecific surface adsorption of proteins. The immobilization was mediated by biotin-Neutravidin binding between biotinylated DNA, Neutravidin (Pierce), and biotinylated polymer (Bio-PEG-SC, Laysan Bio). All measurements were performed in an imaging buffer containing 50 mM HEPES (pH 7.0), 100 mM NaCl, 5 mM $MgCl_2$, 1 mM DTT, 0.1 mg/ml BSA, 5% (vol/vol) glycerol, 0.5% (wt/vol) D-glucose, 165 U/ml glucose oxidase, 2170 U/ml catalase and 3 mM Trolox with indicated protein concentrations. Single-molecule FRET-time traces were recorded with a time resolution of 30 ms and the single molecule FRET efficiency histograms were generated by averaging 300 ms from > 5000 molecules each.

DNA-dependent ATPase assays

Purified EcPriA or KpPriA (50 nM) was incubated with 200 nM DNA replication fork substrate in a buffer containing 20 mM HEPES-HCl, pH 8.0, 50 mM NaCl, 1 mM β-mercaptoethanol, 5 mM $MgCl_2$, 0.1 g/L bovine serum albumin, 1 mM ATP in the presence of an ATP regeneration system (23). ATP hydrolysis is measured spectrophotmetrically at $A_{340\ nm}$ by measuring the oxidation of NADH (conversion of NADH to NAD^+ is coupled to the conversion of ADP to ATP (23)). Steady-state $\Delta A340/\Delta t$ was measured and converted to $\Delta[ATP]/\Delta t$ to determine the rate of ATP hydrolysis.

Complementation assays

The complementation analysis presented here tests three *priA* phenotypes: high levels of SOS expression, partitioning defect and filamentation. Quantitation of SOS expression are described in detail elsewhere (24). Briefly cells (Table 2.2) were grown in minimal medium to mid-log phase and then 3 microlitres of cells were placed on a 1% agarose (made in minimal medium) slab (25). A coverslip was then applied on the top of the cells. Cells were then imaged under identical settings to gain a phase, red and green image. The data combines nine different fields of view taken on three different days for each strain. These phase contrast and *gfp* images were analyzed by a combination of MicrobeTracker (26) software and Matlab R2010a (Mathworks, Inc.) software. The relative fluorescence intensity (RFI) for each cell was normalized to the average fluorescence intensity of a JC13509 strain (no *gfp*).

Helicase assays

Helicase reactions included 1 nM branched DNA substrate (molecules) and were performed in a buffer containing 50 mM HEPES-HCl, pH 8.0, 40 mg/L BSA, 2 mM DTT, 2 mM ATP, and 4 mM $MgOAc_2$. Reactions were started by the addition of PriA (or PriA Arg697Ala) to the desired concentration and incubated at 37°C for 25 min. Unwinding was terminated by the addition of 20 mM EDTA, 0.5% SDS, 0.2 mg/mL proteinase K, and 2.5 ng/μL oligonucleotide 3L-98 (final concentrations) and incubated at 37°C for 30 minutes. Samples were resolved on a 10% native polyacrylamide gel. The gels were then fixed in 10% methanol, 7% acetic acid, and 5% glycerol, dried, exposed to a phosphorimager screen and imaged on a Typhoon FLA 9000. Band intensities were quantified using ImageQuant (GE Healthcare) and percent unwinding was

determined by dividing the intensity of the single strand product band by the total intensity in the lane.

Table 2.1. X-ray data collection and structure determination statistics

	Native PriA (ADP Bound)	SeMet PriA	PriA/SSB-Ct complex
Data Collection			
Wavelength, Å	1.008	0.97934	0.97872
Resolution Range (high resolution bin), Å	50-2.65 (2.70-2.65)	50-3.76 (3.83-3.76)	50-4.10 (4.17-4.10)
Space Group	$P3_2$	$P3_2$	$P2_12_12_1$
Unit Cell (a, b, c (Å))	85.53, 85.53, 111.62	86.35, 86.35, 109.75	106.61, 153.25, 192.37
(α, β, γ (°))	90, 90, 120	90, 90, 120	90, 90, 90
Completeness, %	100	100	85.1
Total/Unique Reflections	194,349/26,591	223,136/9,710	97,950/21,752
Redundancy	7.3 (7.1)	23.0 (23.0)	4.5 (4.2)
$\langle I/\sigma I \rangle$	15.4 (2.34)	32.3 (7.2)	10.3 (1.9)
R_{sym}, %	0.072 (0.838)	0.115 (0.643)	0.108 (0.495)
Refinement			
Resolution, Å	35-2.65		50-4.10
R_{work}/R_{free}	0.2176/0.2540		0.2441/0.3035
Rms deviations			
Bonds, Å	0.005		0.009
Angles, °	1.00		1.34
Number of atoms			
protein	5,490		13,376
solvent	28		0
<B factor>, $Å^2$			
Protein	63.7		151.7
Solvent	64.0		N/A

Table 2.2. Oligonucleotides used in this study

Name	Sequence (5' to 3')	Notes
BB23	TATATCATATGTCCGTCGCCCACGTTGC	Forward primer to clone KpPriA ORF into pET28b
BB24	GTCACGGATCCTTATCCTTCAATCGGATCGAC	Reverse primer to clone KpPriA ORF into pET28b
BB130	CGCACGTCAG	Reverse complement of FP_10mer_5' fluor-dsDNA
BB141	TTCTGCATATGACCAGCCATGTGATTGTG	Forward primer to clone EcPriA 633-732 into pET15a
BB142	TCCTGGGATCCTTAACCCTCAATCGGATC	Reverse primer to clone EcPriA 633-732 into pET15a
1b-98	GCAAGCCTTCTACAGGTCGACCGTCCATGGCGACTCGAGACC GCAATACGGATAAGGGCTGAGCACGCCGACGAACATTCACCA CGCCAGACCACGTA	Oligonucleotide to form model fork substrate. From(1).
3L-98	GACTATCTACGTCCGAGGCTCGCGCCGCAGACTCATTTAGCCC TTATCCGTATTGCGGTCTCGAGTCGCCATGGACGGTCGACCTG TAGAAGGCTTGC	Oligonucleotide to form model fork substrate. From(1).
11b-38	TACGTGGTCTGGCGTGGTGAATGTTCGTCGGCGTGCTC	Oligonucleotide to form model fork substrate. From(1).
FP_10mer_5'fluor-dsDNA	CTGACGTGCG	Fluorescently labeled oligonucleotide for 10 bp dsDNA substrate
oML225_rc_5'fluor	GAGCACGCCGACGAACATTCACCACGCCAGACCACGTA	Fluorescently labeled oligonucleotide for 38 bp dsDNA substrate

Table 2.3. Strains used in this study

Strain	*priA*	Other relevant genotype	Origin or Reference
JC13509[a]	+		Laboratory stock
SS8510	+	*Ωgfp*[b]	Purified colony derived from SS996(2)
SS6321	+	*Ωgfp hupA::mcherry*	SS6279→SS996[c,d]
SS8994	*304*	*Ωgfp hupA::mcherry*	SS421→SS6321[e]
SS8995	*304*	*Ωgfp hupA::mcherry*	pPriA(Klb)→SS8994[f]
SS8997	*304*	*Ωgfp hupA::mcherry*	pSJS1108→SS8994[g]

[a] JC13509 has the following partial genotype: *sulB103 lacMS286 Φ80dIIlacBK1 argE3 his-4 thi-1 xyl-5 mtl-1 rplS31 tsx*. The *lacMS286 Φ80dIIlacBK1* codes for two partial non-overlapping deletions of the lac operon (see (3, 4)).

[b] *attλ::sulAp Ωgfp-mut2* is abbreviated *Ωgfp*.

[c] Select Minimal Kan^R

[d] Kanamycin marker flipped out using pCP20

[e] Select Minimal Cam^R

[f] pPriA(Klb) expresses KpPriA protein. Select Min Kan^R.

[g] pSJS1108 expresses EcPriA protein. Select Min Kan^R.

Figure 2.5

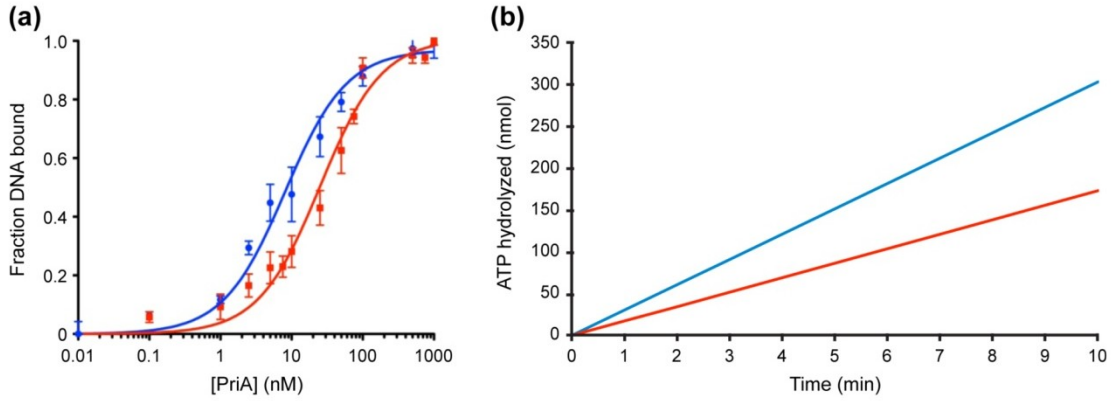

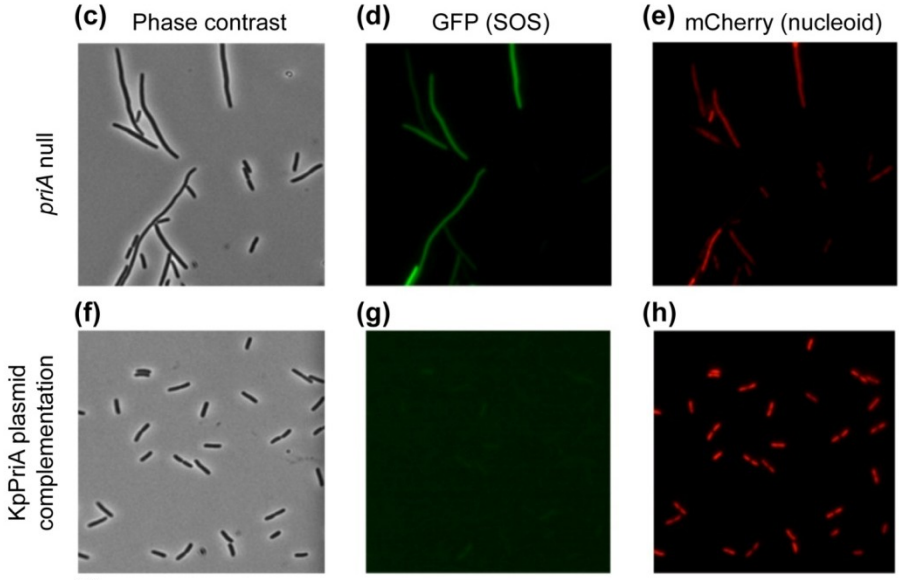

(i)

Strain	Chromosomal *priA*	Plasmid *priA*	RFI	% of cells expressing SOS[c]	Average cell area	Cells Counted
SS6321	+	-	1.7 ± 0.6	1.4	584 ± 56	3857
SS8994	*304*	-	27.2 ± 7.8	78	1194 ± 176	757
SS8995	*304*	*priA(Kp)*	1.9 ± 0.6	1.6	682 ± 39.8	1679
SS8997	*304*	*priA (Ec)*	1.3 ± 0.2	0.9	697 ± 65	1578

(j)

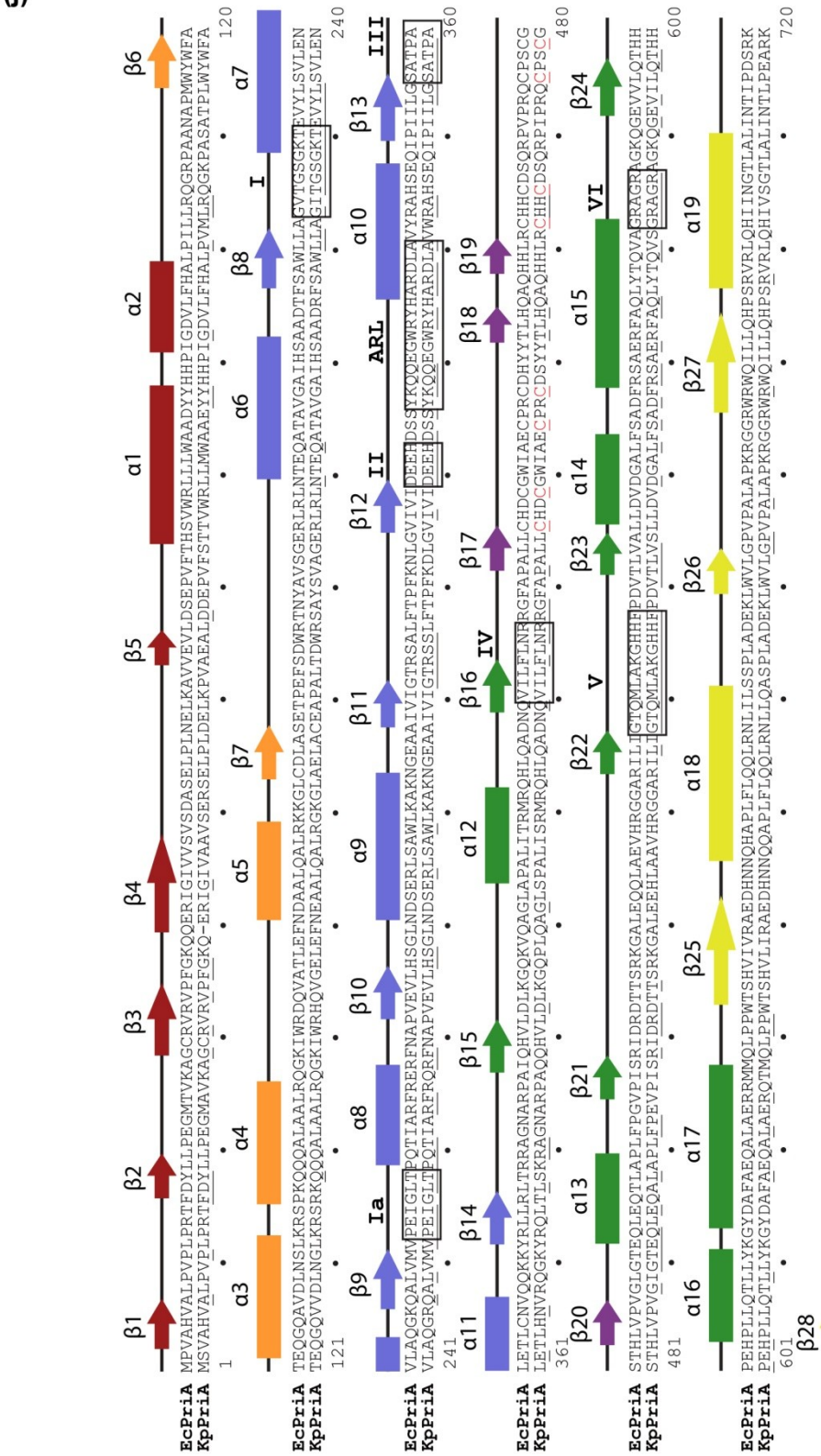
EcPriA MPVAHVALPVPLPRTFDYLLPEGMTVKAGCRVRVPFGKQQERIGIVVSVSDASELPLNEILKAVVEVLDSEPVFTHSVWRLLLWAADYYHHPIGDVLFHALPILLRQGRPAANAPMWYWFA
KpPriA MSVAHVALPVPLPRTFDYLLPEGMAVKAGCRVRVPFGKQ-ERIGIVAAVSERSELPLDELKPVAEALDDEPVFSTTVWRLLMWAAEYYHHPIGDVLFHALPVMLRQGKPASATPLWYWFA
EcPriA TEQGQAVDLNSLKRSPKQQQALAALRQGKIWRDQVATLEFNDAALQALRKKGLCDLASETPEFSDWRTNYAVSGERLRLNTEQATAVGAIHSAADTFSAWLLAGVTGSGKTEVYLSVLEN
KpPriA TEQGQVVDLNGLKRSRKQQQALAALRQGKIWRHQVGELEFNEAALQALRGKGLAELACEAPALTDWRSAYSVAGERLRLNTEQATAVGAIHSAADRFSAWLLAGITGSGKTEVYLSVLEN
EcPriA VLAQGKQALVMVPEIGLTPQTIARFRERFNAPVEVLHSGLNDSERLSAWLKAKNGEAAIVIGTRSALFTPFKNLGVIVIDEEHDSSYKQQEGWRYHARDLAVVRAHSEQIPIILGSATPA
KpPriA VLAQGRQALVMVPEIGLTPQTIARFRQRFNAPVEVLHSGLNDSERLSAWLKAKNGEAAIVIGTRSSLFTPFKDLGVIVIDEEHDSSYKQQEGWRYHARDLAVWRAHSEQIPIILGSATPA
EcPriA LETLCNVQQKKYRLLLRLITRRAGNARPAIQHVLDLKGQKVQAGLAPALITRMRQHLQADNQVILFLNRRGFAPALLCHDCGWIAECPRCDHYYTLHQAQHHLRCHHCDSQRPVPRQCPSCG
KpPriA LETLHNVRQGKYRQLTLSKRAGNARPAQQHVLDLKGQPLQAGLSPALISRMRQHLQADNQVILFLNRRGFAPALLCHDCGWIAECPRCDSYYTLHQAQHHLRCHHCDSQRPIPRQCPSCG
EcPriA STHLVPVGLGTEQLEQTLAPLFPGVPISRIDRDTTSRKGALEQQLAEVHRGGARILIGTQMLAKGHHFPDVTLVALLDVDGALFSADFRSAERFAQLYTQVAGRAGKQGEVVLQTHH
KpPriA STHLVPVGIGTEQLEQALAPLFPEVPISRIDRDTTSRKGALEEHLAAVHRGGARILIGTQMLAKGHHFPDVTLVSLLDVDGALFSADFRSAERFAQLYTQVSGRAGRQGEVILQTHH
EcPriA PEHPLLQTLLYKGYDAFAEQALAERRMMQLPPWTSHVIVRAEDHNNQHAPLFLQQLRNLILSSPLADEKLWVLGPVPALAPKRGGRWRWQILLQHPSRVRLQHIINGTLALINTIPDSRK
KpPriA PEHPLLQTLLYKGYDAFAEQALAERQTMQLPPWTSHVLIRAEDHNNQQAPLFLQQLRNLLQASPLADEKLWVLGPVPALAPKRGGRWRWQILLQHPSRVRLQHIVSGTLALINTLPEARK
EcPriA VKWVLDVDPIEG
KpPriA VKWVLDVDPIEG

Figure 2.5. Biochemical, Cellular and Sequence Comparison of KpPriA and EcPriA.
(a) EcPriA (blue) and KpPriA (red) binding to fluorescently labeled replication fork DNA was assessed by fluorescence anisotropy. Data are the mean of three independent experiments with error bars of 1 standard deviation. **(b)** Time-resolved DNA-dependent ATP hydrolysis activities of EcPriA (blue) and KpPriA (red) were measured using the same replication fork DNA in (a). Rates of hydrolysis were 30±3 nmol/min for EcPriA and 17±4 nmol/min for KpPriA. **(c-e)** Strain SS8994 encodes *priA304* on the chromosome. The strain produces an EcPriA variant (Cys479Tyr within the CRR) that leads to filamentation and increased constitutive SOS (SOS^c) expression in *E. coli*. **(e-h)** Strain SS8995 encodes *priA304* on the chromosome and expresses KpPriA from a plasmid. KpPriA is capable of restoring wild-type phenotypes. There is no vector-only control for the *priA304* strain because *colEI* plasmids do not replicate in a *priA* mutant (5, 6). Phase contrast images of cells are shown in (c) and (f). SOS induction is measured using a GFP fusion to SulA (d and g) whereas nucleoid segregation is monitored with a mCherry fusion to HupA (e and h). **(i)** Quantitation of complementation studies. RFI = relative fluorescence intensity. The percentage of cells in SOS is the percentage of the population 9-fold over background. The uncertainties represent the uncertainties found in the measurements with data collected on three different days. **(j)** Sequence alignment of KpPriA and EcPriA. Sequences of EcPriA (top) and KpPriA (bottom) were aligned and the secondary structure of KpPriA is displayed above the sequence to indicate the positions of helices (boxes) and strands (arrows). Domain color-coding is as shown in Figure 2.1 from the main paper. Helicase sequence elements are enclosed in boxes and labeled and invariant residues shared among PriA proteins are underlined. Zn^{2+}-binding Cys residues are colored red.

Figure 2.6

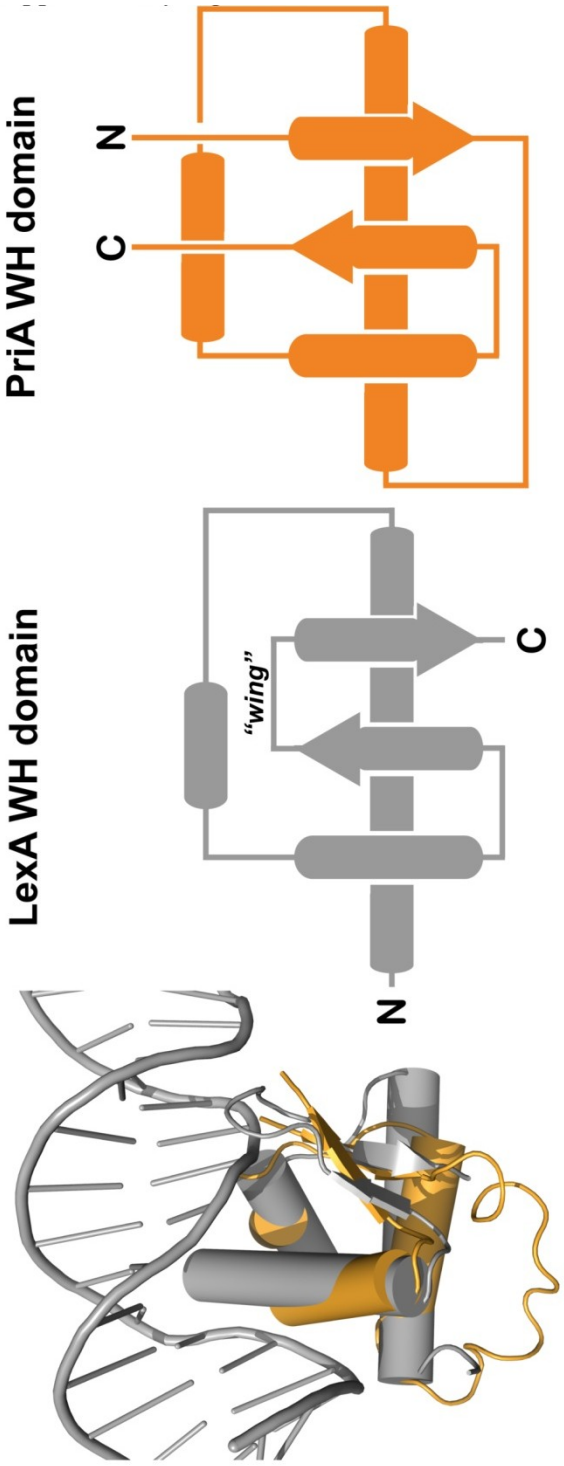

Figure 2.6. Comparison of PriA and LexA WH domains.
WH domains of KpPriA (orange) and LexA (grey, PDB 3JSO, (7)) are superimposed (left) and the topology of the two domains is compared (right). Although the domains share a related fold their topology differs.

Figure 2.7

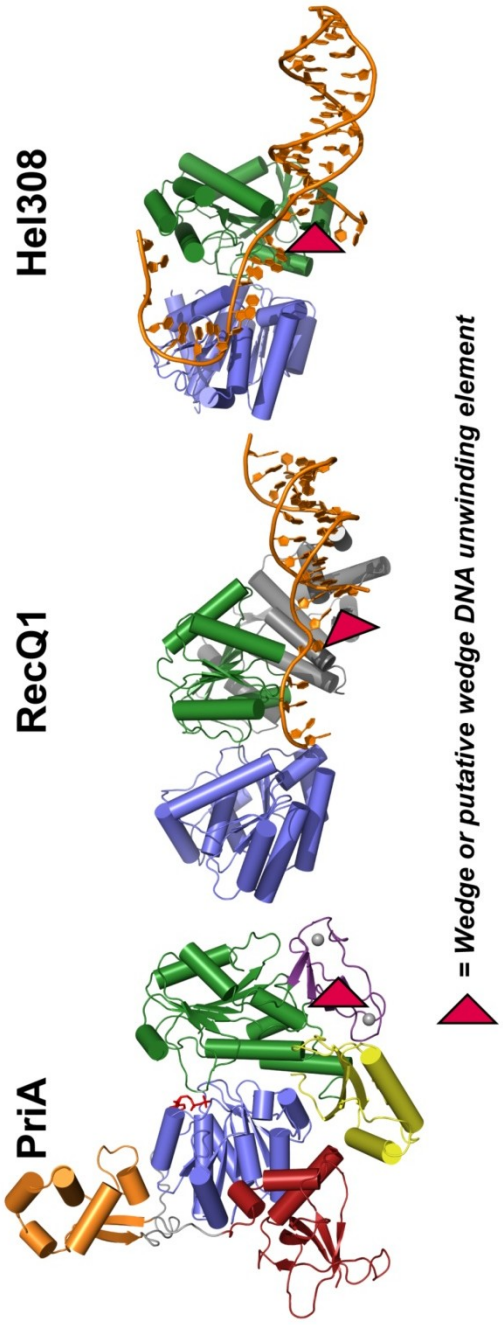
Hel308
RecQ1
PriA
= Wedge or putative wedge DNA unwinding element

Figure 2.7. Comparison of the Putative PriA DNA Unwinding Wedge to Wedge Elements in other Superfamily II DNA Helicases.
The helicase domains (blue and green) of PriA (left), human RecQ1 (middle, PDB 2WWY, (8)), and Hel308 (right, PDB 2P6R, (9)) are aligned. The DNA unwinding wedge elements for RecQ1 and Hel308 and the putative wedge element in PriA are indicated with arrows. Portions of the Hel308 structure were removed for clarity.

Figure 2.8

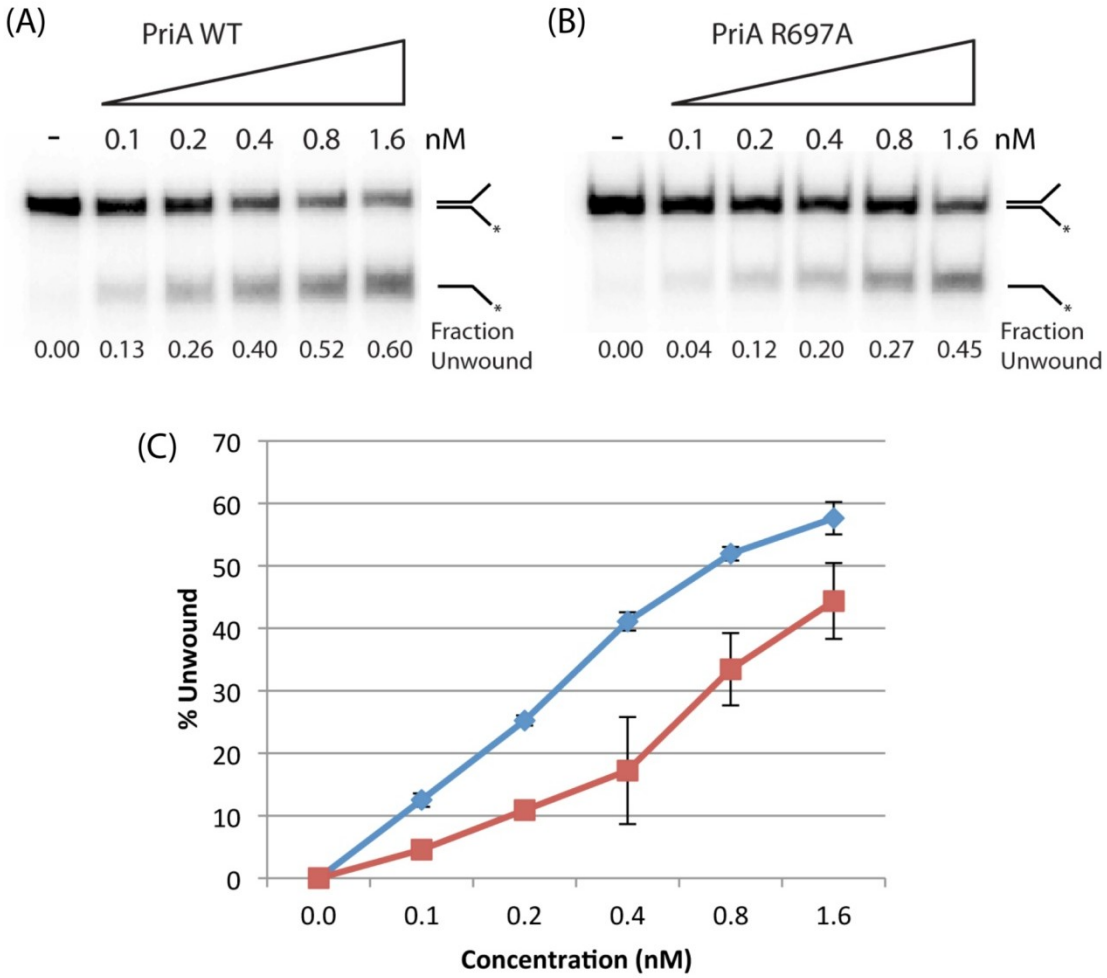
(A)
PriA WT
- 0.1 0.2 0.4 0.8 1.6 nM
0.00 0.13 0.26 0.40 0.52 0.60
Fraction Unwound
(B)
PriA R697A
- 0.1 0.2 0.4 0.8 1.6 nM
0.00 0.04 0.12 0.20 0.27 0.45
Fraction Unwound
(C)
% Unwound
0 10 20 30 40 50 60 70
0.0 0.1 0.2 0.4 0.8 1.6
Concentration (nM)

Figure 2.8. DNA Unwinding by EcPriA and the Arg697Ala EcPriA Variant.
(a) Gel analysis of EcPriA unwinding of branched DNA as a function of enzyme concentration. Fraction unwinding was calculated using the intensities of substrate and product (fraction unwound = product intensity/(substrate intensity + product intensity)). **(b)** Gel analysis of Arg697Ala EcPriA variant unwinding of replication fork DNA as a function of enzyme concentration. **(C)** Quantitation of DNA unwinding experiments for EcPriA (blue) and Arg697Ala EcPriA variant (red) performed in triplicate. Percent unwinding values (fraction unwound x 100%) are the mean of three independent experiments with error base representing 1 standard deviation.

Figure 2.9

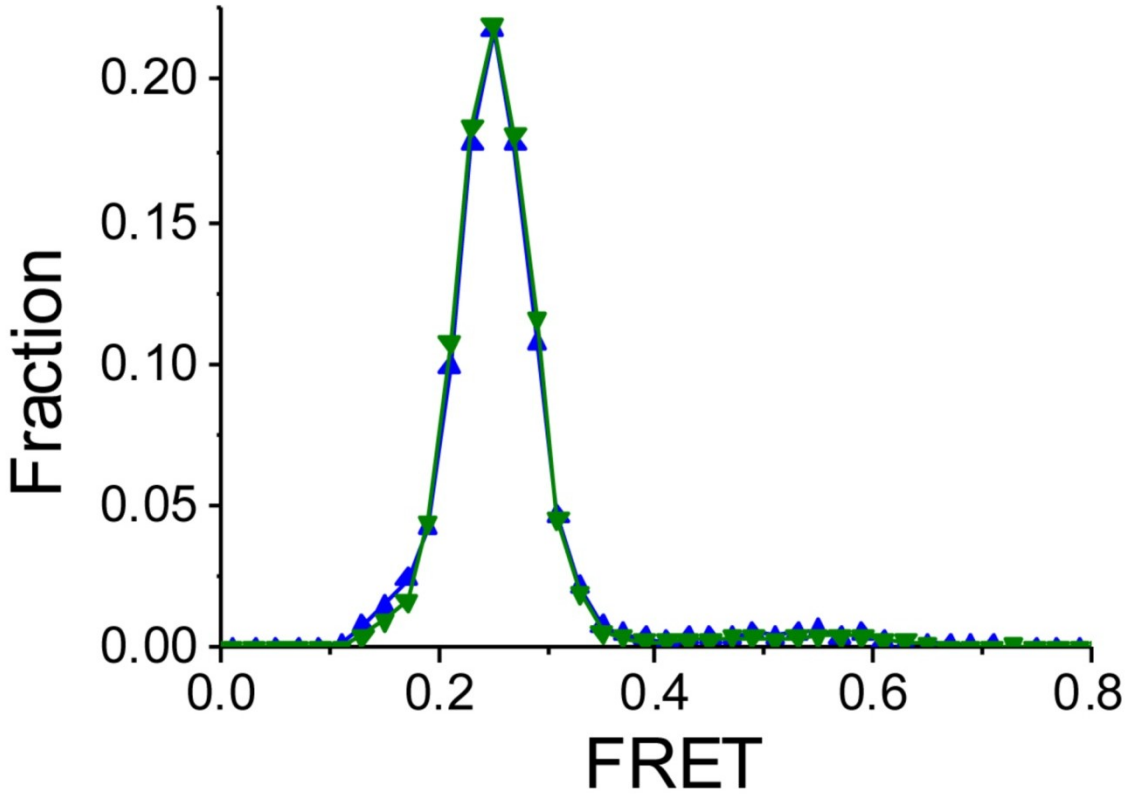

Figure 2.9. smFRET analysis of DNA binding by EcPriA and the Arg697Ala EcPriA variant.
smFRET-efficiency histograms of 1 μM PriA (green)1 or 1 μM Arg697Ala PriA (blue).

SI references.

1. Heller RC & Marians KJ (2005) The disposition of nascent strands at stalled replication forks dictates the pathway of replisome loading during restart. *Mol Cell* **17**:733-743.

2. McCool JD*, et al.* (2004) Measurement of SOS expression in individual *Escherichia coli* K-12 cells using fluorescence microscopy. *Mol Microbiol* **53**:1343-1357.

3. Konrad EB (1977) Method for the isolation of *Escherichia coli* mutants with enhanced recombination between chromosomal duplications. *J Bact* **130**:167-172.

4. Zieg J & Kushner SR (1977) Analysis of genetic recombination between two partially deleted lactose operons of *Escherichia coli* K-12. *J Bact* **131**:123-132.

5. Masai H, Asai T, Kubota Y, Arai K, & Kogoma T (1994) *Escherichia coli* PriA protein is essential for inducible and constitutive stable DNA replication. *EMBO J* **13**:5338-5345.

6. Lee EH & Kornberg A (1991) Replication deficiencies in *priA* mutants of *Escherichia coli* lacking the primosomal replication n' protein. *Proc Natl Acad Sci* **88**:3029-3032.

7. Zhang AP, Pigli YZ, & Rice PA (2010) Structure of the LexA-DNA complex and implications for SOS box measurement. *Nature* **466**:883-886.

8. Vindigni A, Marino F, & Gileadi O (2010) Probing the structural basis of RecQ helicase function. *Biophys Chem* **149**:67-77.

9. Buttner K, Nehring S, & Hopfner KP (2007) Structural basis for DNA duplex separation by a superfamily-2 helicase. *Nat Struct Mol Biol* **14**:647-652.

10. Heller RC & Marians KJ (2005) The disposition of nascent strands at stalled replication forks dictates the pathway of replisome loading during restart. *Mol Cell* **17**:733-743.

11. Lopper M, Boonsombat R, Sandler SJ, & Keck JL (2007) A hand-off mechanism for primosome assembly in replication restart. *Mol Cell* **26**:781-793.

12. Van Duyne GD, Standaert RF, Karplus PA, Schreiber SL, & Clardy J (1993) Atomic structures of the human immunophilin FKBP-12 complexes with FK506 and rapamycin. *J Mol Biol* **229**:105-124.

13. Otwinowski Z & Minor W (1997) Processing of X-ray diffraction data collected in oscillation mode. *Methods Enzymol*, eds Carter CW & Sweet RM (Academic Press, New York), Vol 276A, pp 307-326.

14. Bricogne G, Vonrhein C, Flensburg C, Schiltz M, & Paciorek W (2003) Generation, representation and flow of phase information in structure determination: recent developments in and around SHARP 2.0. *Acta Cryst* D**59**:2023-2030.

15. Emsley P & Cowtan K (2004) Coot: model-building tools for molecular graphics. *Acta Cryst* D**60**:2126-2132.

16. Murshudov GN, Vagin AA, & Dodson EJ (1997) Refinement of Macromolecular Structures by the Maximum-Likelihood Method. *Acta Cryst* D**53**:240-255.

17. Winn MD, Isupov MN, & Murshudov GN (2001) Use of TLS parameters to model anisotropic displacements in macromolecular refinement. *Acta Cryst* D**57**:122-133.

18. McCoy AJ*, et al.* (2007) Phaser crystallographic software. *J Appl Crystallogr* **40**:658-674.

19. Holm L & Sander C (1993) Protein structure comparison by alignment of distance matrices. *J Mol Biol* **233**:123-138.

20. Zhou R*, et al.* (2011) SSB functions as a sliding platform that migrates on DNA via reptation. *Cell* **146**:222-232.

21. Wessel SR*, et al.* (2013) PriC-mediated DNA replication restart requires PriC complex formation with the single-stranded DNA-binding protein. *J Biol Chem* **288**:17569-17578.

22. Roy R, Kozlov AG, Lohman TM, & Ha T (2007) Dynamic Structural Rearrangements Between DNA Binding Modes of *E. coli* SSB Protein. *J Mol Biol* **369**:1244-1257.

23. Morrical SW, Lee J, & Cox MM (1986) Continuous association of *Escherichia coli* single-stranded DNA binding protein with stable complexes of recA protein and single-stranded DNA. *Biochemistry* **25**:1482-1494.

24. Massoni SC*, et al.* (2012) Factors limiting SOS expression in log-phase cells of *Escherichia coli*. *J Bact* **194**:5325-5333.

25. Levin PA (2002) *Light Microscopy Techniques for Bacterial Cell Biology* (Academic Press Ltd, London).

26. Sliusarenko O, Heinritz J, Emonet T, & Jacobs-Wagner C (2011) High-throughput, subpixel precision analysis of bacterial morphogenesis and intracellular spatio-temporal dynamics. *Mol Micro* **80**:612-627.

Chapter 3

Elucidating the Role of the Winged Helix Domain of *Escherichia coli* PriA

Abstract

DNA replication restart serves the essential function of reloading the replicative helicase DnaB onto abandoned replication forks in bacteria. In order to do this, the conserved replication restart primosome (RRP) protein PriA, a 3' to 5' superfamily 2 (SF2) helicase, must first recognize and bind to DNA in a structure specific manner. Previous work has highlighted the presence of two major domains in PriA, an N-terminal DNA binding domain (DBD) and a C-terminal helicase domain (HD). PriA truncations have identified that the DBD and HD act cooperatively in binding and unwinding replication forks. Further biochemical work defined two subdomains in the DBD with the first 105 amino acids recognizing the 3' OH hydroxyl group present at abandoned replication forks. Residues 106-182 of PriA form an accessory domain capable of binding double stranded DNA (dsDNA) that works in conjunction with the N-terminal subdomain in order to recognize specific fork structures. The full length structure of PriA revealed this accessory domain as a unique winged-helix (WH) domain, tethered to the core of the protein via two long loops. It was hypothesized that this domain had flexibility in its movement and bound parental duplex DNA and that a PriA variant with a WH deletion would inhibit replication restart processes. Here, we show that this variant possesses biochemical functions similar to wild-type PriA *in vitro*. However, this WH deletion displays phenotypes similar to a *priA* null mutant *in vivo*. These results provide further mechanistic insights into the role of the WH in DNA replication restart processes.

Introduction

It is predicted that up to once per cell cycle in bacteria, DNA replication is halted due to DNA damage or stalled protein complexes that dislodge the replication machinery (1). Overcoming this situation is made difficult by the presence of only one origin of replication (*oriC*) to initiate DNA replication, thus presenting a complex situation for the organism to restart replication independent of DNA sequence on a site far removed from *oriC*. In *E. coli*, this process occurs via the replication restart primosome (RRP), which serves to reload the replicative helicase DnaB. Binding of the replicative helicase leads to spontaneous reassembly of the replication machinery (replisome) and restart of DNA replication (2).

DNA replication restart is a unique DNA initiation process in that it requires structure specific recognition of templates in contrast to the DnaA mediated, sequence specific, initiation that occurs at *oriC*. Accomplishing the task are two core members of the RRP, PriA and PriC. These two proteins recognize diverse DNA structures that exist after DNA damage repair and/or other events that may lead to replication fork collapse and demise (3). PriA, a 3' to 5' superfamily 2 (SF2) helicase, is the most conserved of the RRP and is thought to represent the dominant mechanism by which replication restart occurs.

PriA was originally identified with the other proteins of the RRP in ΦX174 phage DNA replication (4, 5). Subsequent biochemical and genetic analysis identified PriA as a distinct member of the RRP and not a part of the core replisome that duplicates the bacterial genome (2). *In vitro* experiments identified PriA's preference for DNA substrates where a 3' OH group was available for binding. Such structures include D-loops and replication forks with small gap sizes between the nascent leading strand and the fork junction (3, 6).

Classical domain definitions of PriA describe two major domains: an N-terminal DNA binding domain (residues 1-181, DBD) and a C-terminal helicase domain (residues 182-732, HD). Recognition of the fork was predicted to occur solely through the DBD and the crystal structure of a fragment of the N-terminal DBD (residues 1-105) bound to a nucleotide provide a biochemical mechanism for recognition of the 3' OH group (7, 8). Recognition of the 3' OH is achieved by a binding pocket in PriA formed by Phe16, Asp17, Tyr18, Gly37, Leu55, and Lys61 and fluorescence correlation spectroscopy showed that this pocket was capable of binding DNA bases in a non-selective manner (8), highlighting PriA's sequence independent mechanism of DNA binding (Figure 3.1). Binding of the 3' OH group is predicted to orient PriA to bind to appropriate DNA structures (8-10).

Subsequent biochemical studies also identified a subdomain in the DBD. Both subdomains were shown to stimulate PriA's helicase activity and fragments containing both subdomains display higher affinity for DNA binding, suggesting cooperativity (9). The full length structure of PriA from *K. pneumoniae* identified this second subdomain in the DBD as a winged helix motif (WH) (Figure 3.1) (11). WH domains are common nucleic acid binding elements with a canonical helix-turn-helix (HTH) motif that allows for binding of the major and minor grooves of dsDNA (12). The WH domain of PriA is unique compared to the classical WH motifs of other nucleic acid binding domains—it contains a circularly permuted topology whereby the "wing" β-hairpin that typically binds the minor groove is split open into two loops that connect with the core of PriA (11).

Based on the full length structure and years of biochemical data, a model was proposed for how PriA recognizes the three arms of abandoned replication forks and D-loop structures. In this model, the 3' BD would recognize the hydroxyl group of the nascent leading strand arm and

position the HD to the lagging strand duplex where PriA's 3' to 5' helicase and translocase activity would allow for fork remodeling (3, 13-16). This positioned the parental duplex to be bound by the WH domain. To better understand the role of the WH in fork recognition and DNA binding, an in-frame deletion of this domain in *E. coli* PriA was created (PriA ΔWH). This chapter describes biochemical characterization of PriA ΔWH *in vitro* as well as genetic studies *in vivo*.

Methods and Materials

Oligonucleotides and DNA substrates

All oligonucleotides were purchased from the University of Wisconsin Biotechnology center. Replication forks used in DNA binding consisted of three oligonucleotides (1b-98, 3L-98, and 11b-38, described in (3)) annealed by combining equimolar ratios of all three oligonucleotides in 20 mM Tris, pH 8.0, 100 mM NaCl, and 20 mM $MgCl_2$, heating at 95°C for 5 minutes followed by slow cooling to room temperature. 3L-98 was fluorescently labeled with a 5' fluorescein moiety. For replication forks used in helicase assays, 3L-98 was ^{32}P labeled using T4 polynucleotide kinase and then annealed to 1b-98. The annealed product was purified on a 10% polyacrylamide gel and electroeluted into a 1X Tris Borate EDTA (TBE) buffer prior to dialysis in a buffer containing 10 mM Tris, pH 8.0 and 50 mM $MgCl_2$. All DNA substrates were stored at 4°C prior to use in assays.

Plasmid Construction

The *E. coli priA* open reading frame was PCR amplified out of pML100 (17) and subcloned into pET15a (Novagen) to create plasmid vector pET15-Eco-PriA. The gene encodes a His_6 affinity purification tag and thrombin cleavage site fused onto the N-terminus of PriA.

Deletion of the WH domain (amino acid residues 114-174) was accomplished by restriction enzyme digestion and ligation. Primers oML100 (5' GCG TAT TCC ATA TGC CCG TTG CCC ACG TTG CCT TG 3') and BB147 (5' TTA TTG ATA TCC GGC GCG TTC GCC GCA GG 3') were used to sub-clone out the N-terminus of PriA (encoding amino acid residues 1-113) from pML100. The C-terminus of PriA (encoding amino acid residues 175-732) was subcloned from pML100 using primers BB148 (5' GGC GGG GAT ATC GAT TTA GCA AGT GAA ACA CCA GAG 3') and oML101 (5' GTC ACG GAT CCT TAA CCC TCA ATC GGA TCA AC 3'). BB147 and BB148 add an EcoRV restriction site at the end of the PCR products. Sequential restriction enzyme digest of the N-terminus PCR product with 1 unit each NdeI and EcoRV (New England Biolabs) and the C-terminus PCR product with EcoRV and BamHI (New England Biolabs) was done at 37°C for one hour. Fragments were resolved on a 1% agarose/Tris Acetate EDTA (TAE) gel, purified and ligated using T4 DNA ligase overnight at 22°C. Products corresponding to the correct base pair length of the fusion product was resolved on a 1% agarose/TAE gel and subsequently purified. pET15a was incubated with 1 unit of NdeI and BamHI for one hour at 37°C and gel purified. One final ligation was performed using the stitched together PriA construct and pET15 to create vector pET15-Eco PriA ΔWH. All open reading frames were confirmed by DNA sequencing (University of Biotechnology Center).

Protein Purification

Purification of full length PriA was described previously (17). PriA ΔWH was purified in a similar manner to full length PriA. Briefly, *E. coli* Rosetta2 cells were transformed with either plasmid vector and grown at 37°C in Luria broth supplemented with 50 μg/mL ampicillin and 37 μg/mL chloramphenicol. 1 mM isopropyl β-D-1-thiogalactopyranoside was added at mid log phase ($OD_{600\ nm}$ of ~0.6) and cells were harvested by centrifugation (8,000 rpm, 10 minutes, 4°C) after an additional 3 hours of growth and induction of protein expression. Cell pellets were resuspended in 47 mL lysis buffer (10 mM HEPES-HCl, pH 7.0, 10% glycerol, 500 mM NaCl, 100 mM glucose, 20 mM imidazole, 1 mM β-mercaptoethanol, 1 mM phenylmethylsulfonyl fluoride, 1 mM benzamidine, and 1 EDTA-free protease inhibitor tablet (Roche)), lysed by sonication on ice and clarified by centrifugation (18,000 rpm, 30 minutes, 4°C). Supernatants were incubated with Ni-NTA resin (Qiagen) for 1 hour at 4°C followed by washing with excess lysis buffer and elution in elution buffer (10 mM HEPES-HCl, pH 7.0, 10% glycerol, 500 mM NaCl, 300 mM imidazole, 1 mM β-mercaptoethanol). Eluted protein was dialyzed at 4°C against low-salt buffer (10 mM HEPES-HCl, pH 7.0, 10% glycerol, 150 mM NaCl, 10 mM dithiothreitol). Dialysates were further purified via ion exchange and size exclusion chromatography. Full length PriA and PriA ΔWH were >97% pure as judged by denaturing polyacrylamide gel electrophoresis. Protein concentrations were determined by measuring UV absorbance at 280 nm and using calculated extinction coefficients of 105,870 $M^{-1}cm^{-1}$ for full length PriA and 87,520 $M^{-1}cm^{-1}$ for the PriA ΔWH.

Fluorescence Anisotropy DNA Binding Assays

Fluorescence anisotropy assays were performed as previously described (11). Briefly, proteins were dialyzed against 20 mM HEPES-HCl, pH 7.0, 75 mM potassium glutamate, 5% glycerol and 10 mM DTT. Fluorescein-labeled DNA (1 nM (molecules) of a replication fork substrate with 38 bp leading strand, 38 base single-stranded lagging strand and 60 bp duplex parental (18)) was incubated with varying concentrations of protein for 30 minutes at room temperature and fluorescence anisotropy was measured was measured using a Beacon 2000 fluorescence polarization instrument. Data were fit to a single binding site model and apparent K_d was determined on values converted from anisotropy data to fraction of protein bound to DNA using GraphPad (PRISM). Data represent average of three trials and error bars represent one standard deviation.

DNA-Dependent ATPase Assays

DNA-dependent ATPase assays were performed as previously described through a coupled spectrophotometric assay that measures NADH consumption as a direct correlation of ATP hydrolysis (11, 19). Purified full length PriA or PriA ΔWH (50 nM) was incubated with 200 nM DNA replication fork substrate in a buffer containing 20 mM HEPES-HCl, pH 8.0, 50 mM NaCl, 1 mM β-mercaptoethanol, 5 mM $MgCl_2$, 0.1 g/L bovine serum albumin, 1 mM ATPATP hydrolysis is measured spectrophotmetrically at $A_{340\,nm}$ by measuring the oxidation of NADH (conversion of NADH to NAD^+ is coupled to the conversion of ADP to ATP (19)). Steady-state ΔA340/Δt was measured and converted to Δ[ATP]/Δt to determine the rate of ATP hydrolysis.

Helicase Assays

Helicase reactions were performed as previously described (11). 1 nM branched DNA substrate (molecules) and were performed in a buffer containing 50 mM HEPES-HCl, pH 8.0, 40 mg/L BSA, 2 mM DTT, 2 mM ATP, and 4 mM $MgOAc_2$. Reactions were started by the addition of full length PriA or PriA ΔWH to the desired concentration and incubated at 37°C for 25 minutes. Unwinding was terminated by the addition of 20 mM EDTA, 0.5% SDS, 0.2 mg/mL proteinase K, and 2.5 ng/μL oligonucleotide 3L-98 (final concentrations) and incubated at 37°C for 30 minutes. Samples were resolved on a 10% native polyacrylamide gel. The gels were then fixed in 10% methanol, 7% acetic acid, and 5% glycerol, dried, exposed to a phosphorimager screen and imaged on a Typhoon FLA 9000. Band intensities were quantified using ImageQuant (GE Healthcare) and percent unwinding was determined by dividing the intensity of the single strand product band by the total intensity in the lane.

Complementation Assays and Microscopy

Strains (Table 3.1) incorporating *priA ΔWH* onto the chromosome in place of the open reading frame of *priA* was achieved through insertion with the pKO3 vector, which contains a temperature-sensitive origin of replication and markers for positive and negative selection for chromosomal integration and excision (20). To test the effect the role of the WH deletion on restart processes *in vivo,* two *priA* phenotypes were looked at: high levels of SOS expression (via a GFP fusion to SulA) and filamentation (by cell area). Quantitation of SOS expression are described in detail elsewhere (21). Briefly cells were grown in minimal medium to mid-log phase and then 3 microlitres of cells were placed on a 1% agarose (made in minimal medium) slab (22). A coverslip was then applied on the top of the cells. Cells were then imaged under

identical settings to gain a phase and green image. These phase contrast and *gfp* images were analyzed by a combination of MicrobeTracker (23) software and Matlab R2010a (Mathworks, Inc.) software. The relative fluorescence intensity (RFI) for each cell was normalized to the average fluorescence intensity of a JC13509 strain (no *gfp*).

Results

PriA ΔWH is Capable of Binding Abandoned Replication Forks in vitro

PriA is a 3' to 5' helicase that recognizes abandoned replication forks by interactions of domains that surround core helicase folds. Recognition of the fork is achieved by the N-terminus 3' BD while the PriA WH domain has been shown to bind dsDNA (9). A model of PriA-mediated replication restart proposes that this domain binds parental duplex DNA (11). To test this hypothesis, we created a deletion of the WH. We propose that deletion of this domain will affect both helicase and replication restart activities and thus began with an *in vitro* characterization of the PriA ΔWH variant. Using a fluorescence based anisotropy assay, a model fluorescently labeled replication fork with a 3' nascent leading strand labeled was incubated with both full length PriA and PriA ΔWH (Figure 3.2). PriA ΔWH (22 ± 3 nM) had a comparable apparent K_d for this fork structure compared to full length PriA (10 ± 2 nM). These data suggest that PriA ΔWH variant is folded and capable of binding a model replication fork.

PriA ΔWH Possesses ATPase Activity

We next tested the ability of the PriA ΔWH variant to hydrolyze ATP. PriA is a DNA dependent ATPase with canonical helicase motifs that line the interface between the two RecA-like folds (11). While PriA's WH domain is a flexible element attached via linkers to the core

helicase domain, deletion of the domain may affect ATPase rates. To confirm the role of the WH domain in ATP hydrolysis, we used a coupled spectrophotometric-based assay that monitors ATP consumption in direct correlation to a decrease in absorbance at 340 nm of NADH (19). The assay included a model replication fork with a nascent leading strand similar to the substrate used in the fluorescence anisotropy assays. An ATPase dead variant, PriA K230A (which mutates the Walker A lysine that coordinates the γ-phosphate of ATP) was also used. A modest defect in ATPase rate was observed with the PriA ΔWH variant (14±1 nmol/min) compared to full length PriA (30±3 nmol/min). PriA K230A has a baseline ATPase rate of 0.56±0.03 nmol/min. While not entirely dead for ATPase activity, the PriA ΔWH has reduced ATPase capabilities (Figure 3.3).

PriA ΔWH Maintains Robust Helicase Activities

Given the slight defects observed in ATPase rates of the PriA ΔWH variant, we next assayed the ability of the variant to unwind duplex DNA. Using a radiolabelled fork substrate with no nascent leading strand, DNA unwinding was tracked over a protein concentration gradient. Full length PriA achieves a maximum 72% substrate unwinding around 0.6 nM PriA. Despite a modest defect in ATP hydrolysis, PriA ΔWH achieves a similar ability to unwind duplex DNA reaching a maximum of 70% unwinding (Figure 3.4). Taken together, these data suggest that *in vitro*, the PriA ΔWH variant is biochemically active and capable of normal PriA activities (DNA binding, ATP hydrolysis, and DNA unwinding).

PriA ΔWH Displays Unique Phenotypes in vivo

PriA ΔWH displays biochemical activities comparable to full length PriA *in vitro*. We next looked at what effect deletion of this DNA binding element might have on viability *in vivo*. To test this, we looked at SOS induction and filamentation, two hallmarks of defects in PriA-mediated DNA replication restart (24). In frame substitutions of *priA ΔWH* in place of the open reading frame of *priA* were done in various backgrounds that knocked out other replication restart proteins. A quantification of the relative fluorescence intensity (a measure of SOS induction) and cell area (a measure of filamentation) is provided in Table 3.2 and Figure 3.5 shows representative phase contrast and fluorescence microscopy images. In frame substitution of *priA ΔWH* displays a wild-type phenotype in the presence of other replication restart proteins. Strains also harboring a *priC* deletion also retain wild-type phenotypes while deletion of *rep* has a modest affect in increasing SOS induction. The most dramatic effect of incorporation of *priA ΔWH* occurs in a *priB* knockout strain. Cells are highly filamented as well as highly induced for SOS comparable to a *priA* null strain (*priA2::kan*). A similar phenotype has been observed in a *priA K230R* which shows wild-type phenotypes, but a severe sickness phenotype in the presence of a *priB* deletion (25).

Discussion

DNA replication restart requires recognition and subsequent remodeling of DNA structures to allow for successful reloading of the replisome. Detailed mechanisms of how the replication restart helicase PriA achieves DNA recognition have been hindered by the absence of high resolution structural data. The recently solved high resolution structure of PriA reveals a multi-domain protein with DNA binding elements poised to recognize different DNA structures

(11). Two of these DNA binding elements exist at the N-terminus that was historically known as the DBD. The far N-terminus is responsible for fork recognition through the 3' OH group present near fork junctions (8). The second half of the classical DBD structurally resembles a WH motif, though the exact structure in PriA is a variation of the theme and is circularly permuted(11). To better understand the role of the WH domain in PriA fork recognition and replication restart processes, we created a deletion variant of this domain, PriA ΔWH. Biochemically, this domain retains the hallmarks of a fully functional PriA *in vitro*, maintaining DNA binding, ATPase and helicase activity.

Surprisingly, *in vivo*, this mutation displays a phenotype (and has subsequently been named *priA333*). Markers for filamentation and SOS induction demonstrate a capability of *priA333* to fully substitute the open reading frame of *priA* without any noticeable effect phenotypically. This seems to be a reasonable effect given the near wild-type levels observed biochemically of this variant *in vitro*. However, when expressed in *priB* deletion strains, the SOS response is highly induced and the cells are filamented, indicative of loss of replication restart functions within the cell. A similar phenotype is absent in a strain without *priC* and quite smaller in a *rep* deletion strain. The exact mechanisms for these *in vivo* observations are still vague but seem to suggest possible interference in protein-protein interactions possibly involving the sister PriC mediated replication restart pathways.

Understanding the mechanism of how PriA recognizes an abandoned replication fork is required to better understand replication restart processes as a whole. Specifically, understanding how and where the WH domain may bind to replications forks, its role in stabilizing protein-DNA interaction, as well as potentially its interaction with other replication

restart domains and pathways are needed. This will require a broader study, both biochemically and structurally, of the dynamics of this domain.

Figure 3.1

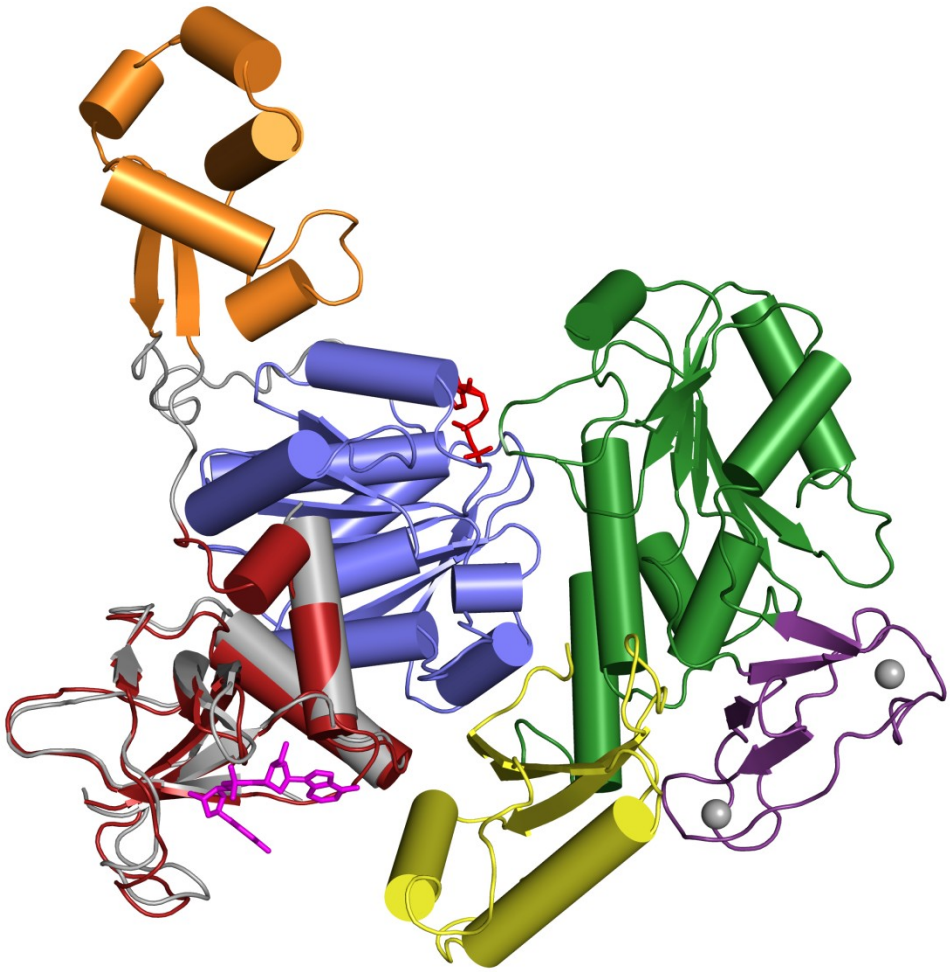

Figure 3.1. Recognition of Abandoned Replication Forks via the N-terminus of PriA
Shown is the full length structure of PriA from *K. pneumoniae* (11) as well as the previously determined structure of the first 105 amino acids from *E. coli* PriA (gray) bound to a nucleotide base (8). Recognition of abandoned replication forks occurs by this N-terminal domain. PriA also contains a flexible WH domain (orange) capable of binding dsDNA by itself (9).

Table 3.1 Relevant Strains used in this Study

Strain Name	Description
SS6321	Wild-type
SS9592	*priA::priA ΔWH*
SS9594	*priA::priA ΔWH, ΔpriB*
SS9595	*priA::priA ΔWH, ΔpriC*
SS9596	*priA::priA ΔWH, Δrep*
SS7064	*priA2::kan*
SS9116	*ΔpriB*
SS9114	*ΔpriC*
SS9112	*Δrep*

Figure 3.2

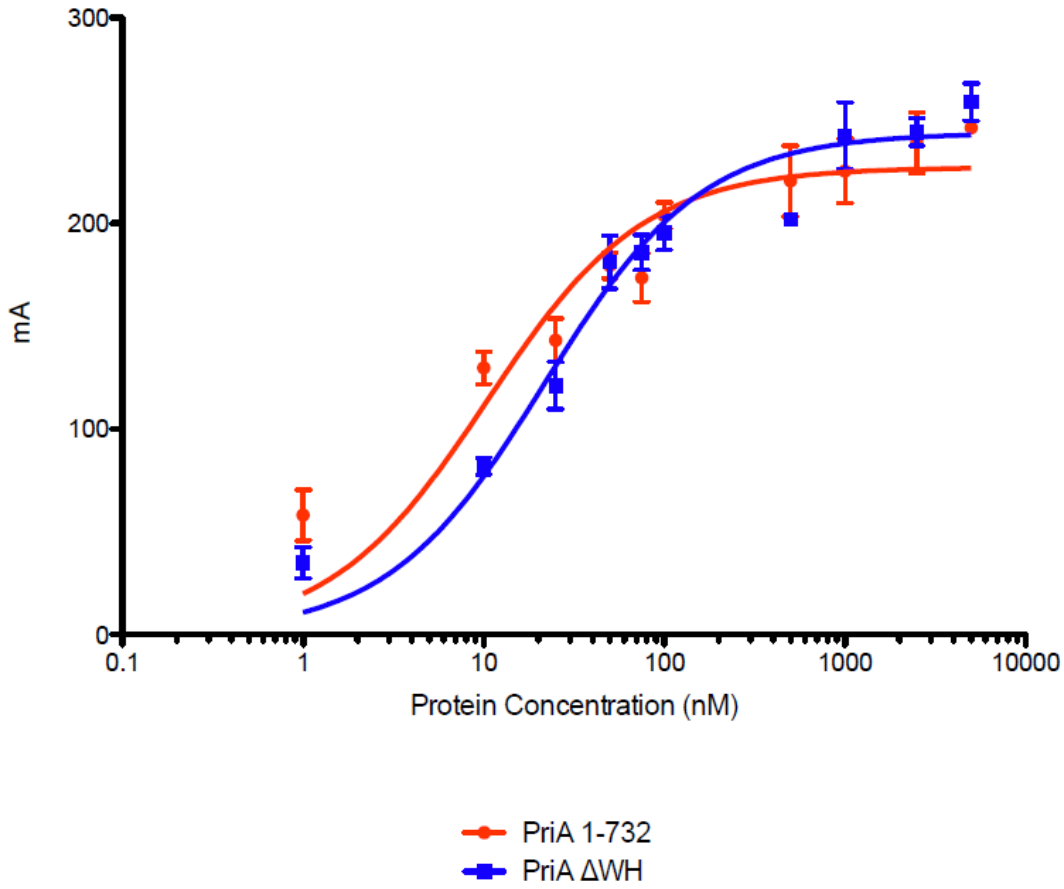
300
200
100
0
mA
0.1
1
10
100
1000
10000
Protein Concentration (nM)
PriA 1-732
PriA ΔWH

Figure 3.2. PriA ΔWH is Capable of Binding a Model Replication Fork
Fluorescence anisotropy based assay demonstrating similar binding affinities for a DNA replication fork with a nascent leading strand. Data are the mean of three independent experiments with error bars of 1 standard deviation.

Figure 3.3

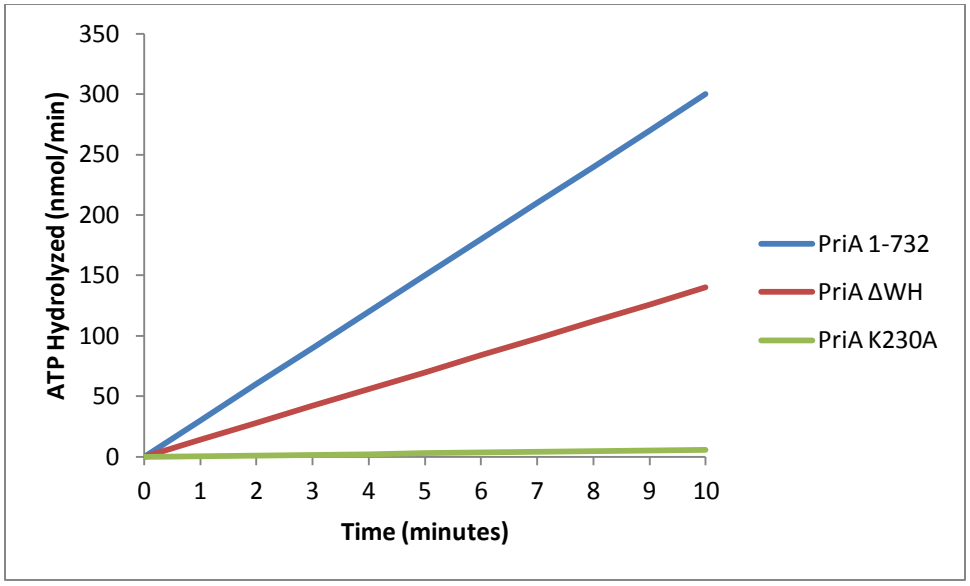
350
300
250
200
150
100
50
0
ATP Hydrolyzed (nmol/min)
0
1
2
3
4
5
6
7
8
9
10
Time (minutes)
PriA 1-732
PriA ΔWH
PriA K230A

Figure 3.3. PriAΔWH Displays Reduced ATPase Activity
Time-resolved DNA-dependent ATP hydrolysis activities of full length PriA (blue), PriA ΔWH (red), and PriA K230A (green) were measured using the same replication fork DNA in Figure 3.2. Deletion of the WH does not abolish ATPase activity, but modestly decreases it.

Figure 3.4

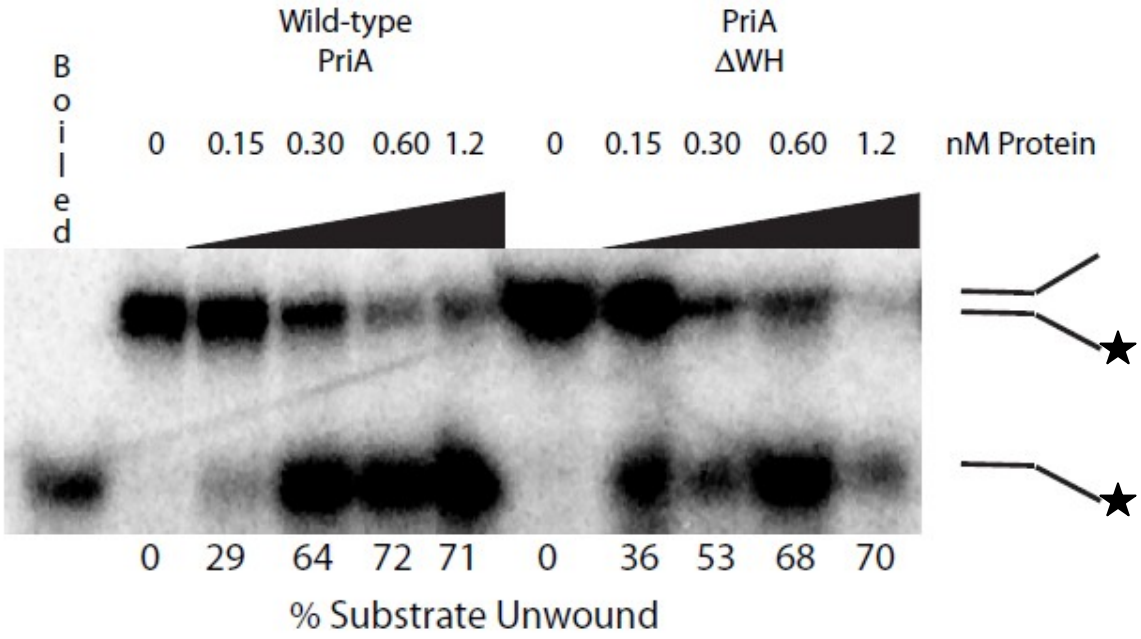
Wild-type
PriA
PriA
ΔWH
Boiled
0 0.15 0.30 0.60 1.2 0 0.15 0.30 0.60 1.2 nM Protein
0 29 64 72 71 0 36 53 68 70
% Substrate Unwound

Figure 3.4. PriA ΔWH Maintains Robust Helicase Activity
Gel analysis of unwinding of branched DNA as a function of enzyme concentration. Fraction unwinding was calculated using the intensities of substrate and product (fraction unwound = product intensity/(substrate intensity + product intensity)).

Figure 3.5

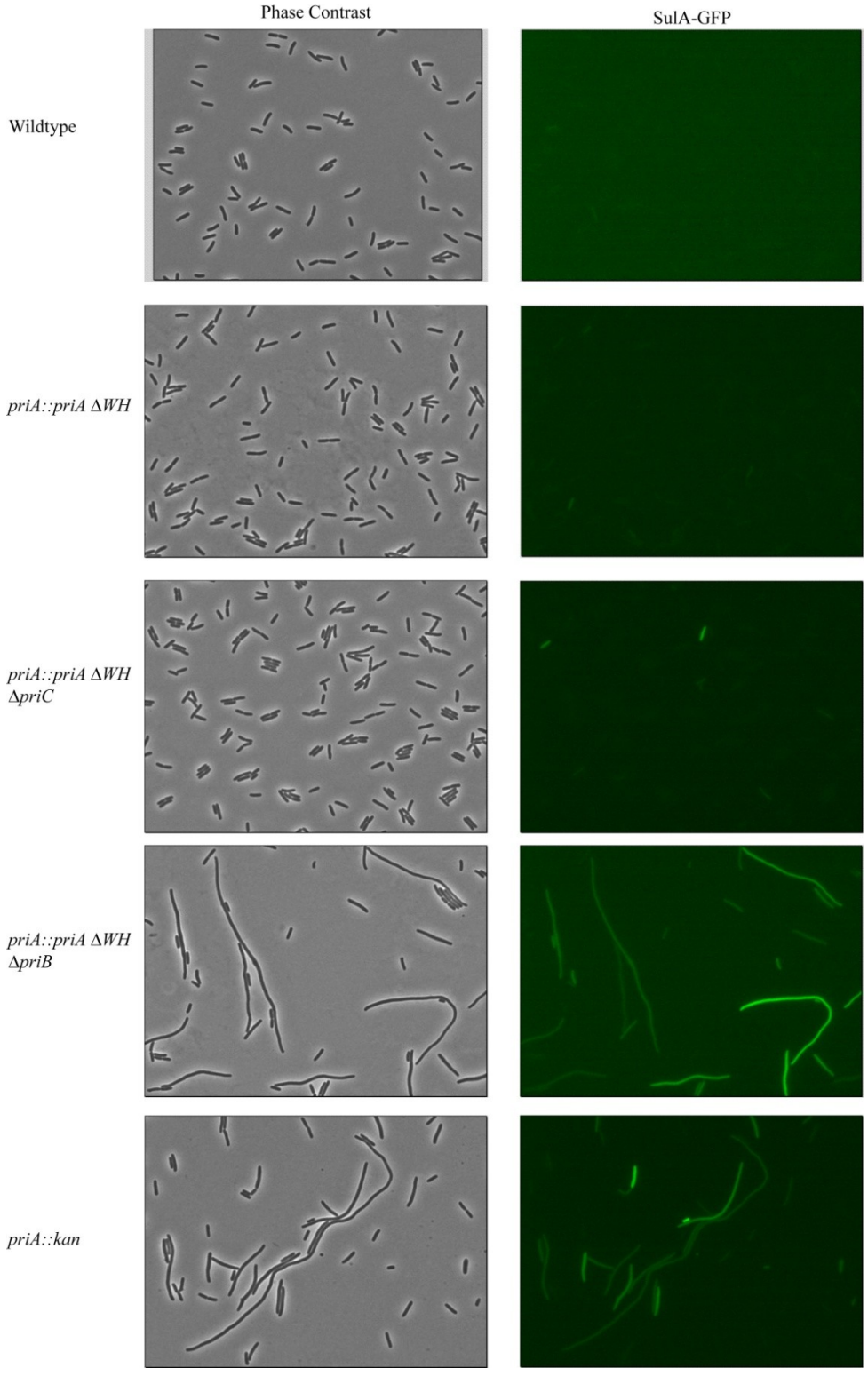
Phase Contrast
SulA-GFP
Wildtype
priA::priA ΔWH
priA::priA ΔWH ΔpriC
priA::priA ΔWH ΔpriB
priA::kan

Figure 3.5. PriA ΔWH Displays Unique Phenotypes *in vivo*
Representative microscopy images of in frame substitution of *priA ΔWH* onto the chromosome in various genetic backgrounds. Deletion of the WH domain has an effect in a *priB* deletion strain and is comparable to a *priA* null mutation.

Table 3.2. Quantification of Phenotypic Analysis of *priA ΔWH*

Strain	Strain Description	Relative Fluorescence Intensity	Cell Area
SS6321	Wild-type	1.12	732.9
SS9592	*priA::priA ΔWH*	0.84	637.7
SS9594	*priA::priA ΔWH, ΔpriB*	14.24	1399.45
SS9595	*priA::priA ΔWH, ΔpriC*	1.46	664.3
SS9596	*priA::priA ΔWH, Δrep*	3.03	996.2
SS7064	*priA2::kan*	9.11	1055
SS9116	*ΔpriB*	1.72	675.6
SS9114	*ΔpriC*	1.3	702
SS9112	*Δrep*	1.12	873.6

References

1. Cox MM, *et al.* (2000) The importance of repairing stalled replication forks. *Nature* 404(6773):37-41 .

2. Marians KJ (1992) Prokaryotic DNA replication. *Annu Rev Biochem* 61:673-719 .

3. Heller RC & Marians KJ (2005) The disposition of nascent strands at stalled replication forks dictates the pathway of replisome loading during restart. *Mol Cell* 17(5):733-743 .

4. Schekman R, Weiner JH, Weiner A, & Kornberg A (1975) Ten proteins required for conversion of phiX174 single-stranded DNA to duplex form in vitro. Resolution and reconstitution. *J Biol Chem* 250(15):5859-5865 .

5. Wickner S & Hurwitz J (1975) Association of phiX174 DNA-dependent ATPase activity with an *Escherichia coli* protein, replication factor Y, required for in vitro synthesis of phiX174 DNA. *Proc Natl Acad Sci U S A* 72(9):3342-3346 .

6. Liu J & Marians KJ (1999) PriA-directed assembly of a primosome on D loop DNA. *J Biol Chem* 274(35):25033-25041 .

7. Sasaki K, *et al.* (2006) Crystallization and preliminary crystallographic analysis of the N-terminal domain of PriA from *Escherichia coli*. *Biochim Biophys Acta* 1764(1):157-160 .

8. Sasaki K, *et al.* (2007) Structural basis of the 3'-end recognition of a leading strand in stalled replication forks by PriA. *EMBO J* 26(10):2584-2593 .

9. Tanaka T, Mizukoshi T, Sasaki K, Kohda D, & Masai H (2007) *Escherichia coli* PriA protein, two modes of DNA binding and activation of ATP hydrolysis. *J Biol Chem* 282(27):19917-19927 .

10. Tanaka T, *et al.* (2002) DNA binding of PriA protein requires cooperation of the N-terminal D-loop/arrested-fork binding and C-terminal helicase domains. *J Biol Chem* 277(41):38062-38071 .

11. Bhattacharyya B, *et al.* (2014) Structural mechanisms of PriA-mediated DNA replication restart. *Proc Natl Acad Sci U S A* 111(4):1373-1378 .

12. Aravind L, Anantharaman V, Balaji S, Babu MM, & Iyer LM (2005) The many faces of the helix-turn-helix domain: transcription regulation and beyond. *FEMS Microbiol Rev* 29(2):231-262 .

13. Lee MS & Marians KJ (1987) *Escherichia coli* replication factor Y, a component of the primosome, can act as a DNA helicase. *Proc Natl Acad Sci U S A* 84(23):8345-8349 .

14. Lasken RS & Kornberg A (1988) The primosomal protein n' of *Escherichia coli* is a DNA helicase. *J Biol Chem* 263(12):5512-5518 .

15. Cadman CJ & McGlynn P (2004) PriA helicase and SSB interact physically and functionally. *Nucleic Acids Res* 32(21):6378-6387 .

16. Lee MS & Marians KJ (1990) Differential ATP requirements distinguish the DNA translocation and DNA unwinding activities of the *Escherichia coli* PRI A protein. *J Biol Chem* 265(28):17078-17083 .

17. Lopper M, Boonsombat R, Sandler SJ, & Keck JL (2007) A hand-off mechanism for primosome assembly in replication restart. *Mol Cell* 26(6):781-793 .

18. Heller RC & Marians KJ (2005) The disposition of nascent strands at stalled replication forks dictates the pathway of replisome loading during restart. *Mol Cell* 17(5):733-743 .

19. Morrical SW, Lee J, & Cox MM (1986) Continuous association of *Escherichia coli* single-stranded DNA binding protein with stable complexes of RecA protein and single-stranded DNA. *Biochemistry* 25(7):1482-1494 .

20. Link AJ, Phillips D, & Church GM (1997) Methods for generating precise deletions and insertions in the genome of wild-type *Escherichia coli*: application to open reading frame characterization. *J Bacteriol* 179(20):6228-6237 .

21. Massoni SC*, et al.* (2012) Factors limiting SOS expression in log-phase cells of *Escherichia coli*. *Journal of bacteriology* 194(19):5325-5333 .

22. Levin PA (2002) *Light Microscopy Techniques for Bacterial Cell Biology* (Academic Press Ltd, London).

23. Sliusarenko O, Heinritz J, Emonet T, & Jacobs-Wagner C (2011) High-throughput, subpixel precision analysis of bacterial morphogenesis and intracellular spatio-temporal dynamics. *Molecular microbiology* 80(3):612-627.

24. McCool JD & Sandler SJ (2001) Effects of mutations involving cell division, recombination, and chromosome dimer resolution on a *priA2::kan* mutant. *Proc Natl Acad Sci U S A* 98(15):8203-8210.

25. Zavitz KH & Marians KJ (1992) ATPase-deficient mutants of the *Escherichia coli* DNA replication protein PriA are capable of catalyzing the assembly of active primosomes. *J Biol Chem* 267(10):6933-6940.

Chapter 4

Conclusions and Future Perspectives

Introduction

DNA replication restart is an essential genome maintenance process in *E. coli* and related bacteria that deals with the potentially lethal situation of abandoned replication forks. Such situations arise up to once per cell cycle (1) due to stalled protein complexes on the template or DNA damage. These impediments cause the replication machinery to be ejected prematurely. Bacteria have evolved multiple pathways to reload the replicative helicase, DnaB, in a DNA structure dependent manner. The replication restart primosome (RRP) in *E. coli* consists of four proteins: PriA, PriB, PriC, and DnaT that reload DnaB with the aid of the helicase loader DnaC. The three pathways in *E. coli* are delineated as being PriA-mediated or PriC-mediated depending on the DNA substrate encountered. PriA is the most well conserved of the RRP and likely represents the dominant DNA replication restart pathway. Despite over thirty years of biochemical studies of PriA-mediated DNA replication restart, much of the in-depth mechanistic understanding of the process has been hindered by the lack of high resolution data, especially with regards to PriA. This thesis addresses this limitation by providing the first high resolution structures of full length PriA. Models of PriA activity gleaned from the structures solved are tested biochemically and provide novel findings about how PriA recognizes abandoned replication forks and remodels the fork for subsequent RRP protein binding.

The Structure of PriA Reveals a Modular Domain Architecture Poised for DNA Binding

Chapter 2 described the first full length, high resolution (2.65 Å) structure of PriA from the Gram negative organism *Klebsiella pnuemoniae*. *K. pneumoniae* PriA is highly similar to *E. coli* PriA (89% identical, 95% similar) and studies confirmed *K. pnuemoniae* PriA's ability to complement a *priA* null mutant *in vivo* in *E. coli*. Furthermore, *in vitro* DNA binding and

ATPase activity assays confirmed similar modes of activity between the PriA orthologs of both species.

Classical domain definitions of PriA divided it into two major domains: the DNA binding domain (DBD) and the helicase domain (HD). The full length structure reveals six domains including a winged-helix (WH) domain, a conserved cysteine rich region (CRR), and a C-terminal domain (CTD) in addition to the previously described N-terminal DBD and the bilobed HD. PriA forms a bowl like shape with five of the core domains while the WH domain is connected to the core via two extended loops. Previous studies have identified that the WH domain is involved in DNA binding (2) and that the CRR region plays a role in helicase activity (3). The presence of the CTD was unexpected. Structural comparisons identified this as a possible nucleic acid binding domain and fluorescence polarization assays confirmed the ability of this domain to bind diverse DNA substrates (ssDNA, dsDNA, forked DNA). Given its location in the protein, the CTD serves as a keystone domain for the diverse DNA structures that may be present at an abandoned replication fork. The structure clearly provides mechanistic models of how PriA might bind to the three arms of an abandoned replication fork and use its helicase activity to remodel the fork for subsequent protein loading and represents an important step forward in the field as a model for studying PriA-mediated DNA replication restart.

Identification of the PriA-SSB Interaction Site Provides a Model for Fork Recognition

Based on the structure, models have been developed for how recognition of forks composed of solely dsDNA arms might occur. However, formation of D loops or other abandoned replication fork structures due to homologous recombination or uncoupling of DNA polymerases may lead to an abandoned replication fork that is composed of ssDNA. Such

scenarios lead to binding of SSB. This is an inherent challenge for restarting replication as DnaB is inhibited from loading onto DNA by SSB. PriA must overcome this SSB "barrier" and provide a ssDNA binding site for DnaB to reload. PriA binds to and is stimulated by SSB's conserved amphipathic C-terminal tail (4). But details of the exact mechanism of how PriA binds SSB and then remodels the fork to remove SSB have been lacking.

The low resolution (4.1 Å) structure of PriA bound to a peptide mimic of the SSB-CT (WMDFDDDIPF), with clear F_o-F_c omit density for the final four residues of the peptide, was also described in Chapter 2. The peptide binds on the opposite face of PriA compared to the 3' OH recognition binding pocket. The binding site of SSB on PriA contains conserved architecture observed in other SSB interacting proteins that includes the presence of a basic lip residue, a hydrophobic pocket for binding the invariant ultimate phenylalanine of SSB, and a basic ridge to coordinate the negatively charged aspartates. A conserved arginine, Arg697, serves as the basic lip residue. Mutation of basic lip residues to an alanine in other SSB interacting proteins abolishes the interaction (5). ITC confirmed a similar effect of the PriA variant Arg697Ala. Plasmid-based complementation studies preliminary suggest that this mutation *in vivo* does not affect viability of bacterial strains, potentially suggesting that this interaction is not essential for bacteria. However, further chromosome based studies are required to full understand the importance of the PriA-SSB interaction.

A single-molecule, FRET based assay (6) was also employed to understand the mechanism of PriA-SSB interactions and nucleoprotein complex formation. SSB is capable of binding ssDNA in two modes: either 35 nucleotides are bound per SSB tetramer (SSB_{35}) in a highly cooperative mode or 65 nucleotides are bound per SSB tetramer (SSB_{65}) in a less cooperative fashion. The assay can distinguish between these two binding modes through

measurement of FRET efficiencies and SSB-DNA complexes form a mixed population of both binding modes. Addition of wild-type PriA in the presence of excess SSB leads to two results: favoring of the SSB_{35} binding mode and a modest reduction of the FRET efficiency due to PriA-DNA interactions. The presence of PriA Arg697Ala with excess SSB resembles the SSB alone experiment, further validating this residue as the basic lip residue. The results of this experiment support a model in which the PriA-SSB interaction leads to remodeling of the nucleoprotein complex and PriA exposes ssDNA by the transition to a predominantly SSB_{35} binding mode. A similar result was reported in the parallel replication restart pathway mediated by PriC (7) suggesting that SSB binding mode remodeling may be a general mechanism required for DNA replication restart.

PriA's Winged Helix (WH) Domain Define Mechanisms of Replication Restart Functions

WH domains are nucleic acid binding motifs that possess a helix-turn-helix motif with β-hairpin "wing" motifs. The domain serves classically as a dsDNA binding motif that allows for simultaneous binding of the major and minor groove (8). PriA's WH actually contains a circularly permuted topology where the β-hairpin is split open and serves as the connection point for the WH to the core of the protein. The domain is capable of binding dsDNA *in vitro* and has functional cooperativity with the DBD (2). To better understand the role this domain plays in fork recognition and subsequent replication restart functions, a construct encoding a deletion of this domain was created and termed PriA ΔWH. *In vitro*, the domain displayed DNA binding, ATPase, and helicase activities similar to full length PriA. *In vivo*, *priA ΔWH* was able to fully complement a *priA* null mutation and displayed wild-type phenotypes in a *priC* deletion strain. When PriA ΔWH was expressed in a strain with *priA* and *priB* deleted, the strain was highly

filamented and induced for the SOS response, hallmarks of defects in DNA replication restart processes. These results suggest that PriA's WH domain may play a role in protein-protein interactions that mediate replication restart. Further biochemical studies will include a greater diversity of DNA substrates used for *in vitro* characterization as well as structural based experiments to better understand the role of the WH in DNA replication restart.

Future Perspectives

The proteins required for DNA replication restart were identified almost forty years ago (9, 10). In the intervening four decades, biochemical and genetic approaches have aimed to understand the mechanisms of this essential genome maintanence process. The structure of PriA and the results presented in this thesis confirm these results and have provided initial models of in-depth mechanisms of DNA replication restart. Future studies of PriA mediated, as well as general, DNA replication restart will build off the structure and explore areas of regulation of ATPase and helicase function, understanding the distinct mechanisms by which forks are remodeled, understanding the overall structure of the RRP, and exploring unique mechanisms of DNA replication restart.

Regulation of PriA ATPase Activity

PriA is a SF2 family 3' to 5' helicase that serves an important role in restarting DNA replication in response to prematurely terminated reactions. However, PriA activity must be regulated to prevent unnecessary replication reactions from occurring. The high resolution structure of PriA reveals two mechanisms of PriA auto-regulation in the absence of DNA. The

first key feature is a conserved aromatic rich loop (ARL) located in the N-terminal helicase lobe. More commonly found in SF1 family helicases, a similar loop is found in the SF2 family helicase RecQ. In RecQ, the loop couples ssDNA binding with ATPase activity in a regulatory fashion (11). In PriA, this loop exists at an interface between the 3' DBD, both helicase lobes, and the CTD. Mutations in this loop have been shown to inhibit D-loop binding (12). Initial studies with mutant variants Trp332Ala, Arg333Ala, and Tyr334Ala show a strong defect in ATPase activity suggesting that PriA may contain a similar mechanism to RecQ. Further studies into DNA binding and the role of this loop *in vivo* are currently being pursued.

The second putative auto-regulatory mechanism identified in the structure of PriA involves ATP binding and hydrolysis. The structure was solved with an ADP molecule bound. Lys543, a highly conserved residue that is part of an extended Motif V, is positioned such that its sidechain lies between the β phosphate of ADP and the carboxyl group of Asp319 from helicase motif II. This aspartate aids in magnesium coordination for ATP hydrolysis and given the position of Lys 543, we predict that this lysine may regulate ATP hydrolysis via a mechanism that stabilizes the ADP product, a mechanism similarly observed in PcrA helicase (13).

Mechanisms of PriA DNA Binding

The essential nature of DNA replication restart is the ability of the RRP to recognize diverse DNA structures in a sequence independent manner. Understanding the mechanisms by which this occurs is therefore paramount to truly understanding this core genome maintenance process. The high resolution structure of PriA combined with biochemical data, both previously published and novel data presented in this thesis, provide clues to how PriA binds to abandoned replication forks. However, the high resolution structure of PriA bound to its biologically

relevant DNA substrate would not only further confirm the models presented here, but would also provide insights into how PriA directs replication restart and the role of fork remodeling in this process. A structural based approach has already begun in which four PriA orthologues from *Cronobacter sakazakii, E. coli, K. pnuemoniae, and Neisseria gonorhoeae* have been set in sparse matrix crystal screens with fork substrates with arms of either 5, 10, or 15 base pair duplexes. An initial hit was obtained in a condition with the smallest fork substrate and *N. gonorhoeae* PriA that diffracted weakly to approximately 11 Å. UV scanning of the crystal provides support for the presence of DNA in the crystal and further crystal refinement and improvement is ongoing in order to improve diffraction quality of these crystals. Further crystallography experiments may include more orthologues of PriA and different DNA substrates with the thought that small differences on the protein surface may improve crystal packing. Should crystallography experiments fail to yield diffraction quality crystals, low resolution techniques may be employed. Initial experiments with small angle X-ray scattering (SAXS) have shown potential in defining DNA binding though further experiments with larger DNA substrates have shown a propensity to form multiple populations in solution, and have thus far proven more difficult to analyze. Further purification steps to isolate singular nucleoprotein complexes will need to be employed. Lastly, mapping techniques using unnatural amino acids may provide another alternative to classical structure based approaches to probing PriA-DNA interactions. Currently, four variants of PriA that encode *amber* mutations have been cloned targeting the 3' DBD, WH domain, and CRR. These variants will be expressed in the presence of a tRNA synthetase for incorporation of bisphenol A (BPA) at the sites of these stop codons. BPA will allow cross-linking experiments to be performed to map out specific protein-DNA

contacts (14-16). Should these initial experiments succeed, further BPA mapping will be performed targeting all domains of PriA.

Primosomal Structure: Putting it All Together

DNA replication restart in *E. coli* and related bacteria is orchestrated by a multi-protein complex with the specific goal of reloading the replicative helicase DnaB. The first step is the binding of PriA to fork substrates that may or may not be coated with SSB and subsequent remodeling of the substrate to allow protein-protein interactions to occur. In a hand-off fashion, PriB and DnaT are loaded on to form a ternary complex that primes subsequent binding of DnaB with the help of the helicase loader DnaC (17). For the first time since DNA replication restart was initially identified, the structures of all RRP proteins are known (PriA (18), PriB (19), PriC and DnaT (data unpublished)). The next step is to determine the macromolecular structure of the entire RRP, a process that will be aided by the knowledge of individual structures. Towards that end, low resolution structural approaches (cryo-EM, SAXS) are currently being pursued and constructs that fuse MBP to the RRP proteins have been cloned to aid in cryo-EM studies. Conditions for successful complex formation need to be determined and once that has been achieved, cryo-EM studies will be done in collaboration with the Berger Lab at Johns Hopkins University. BPA cross-linking may also provide invaluable insights into protein-protein interactions essential for DNA replication restart.

Unique Mechanisms of DNA Replication Restart

DNA replication restart is an essential process in *E. coli* whereby multiple pathways, delineated either as PriA- dependent or PriC-dependent, have evolved to deal with diverse abandoned replication forks that the cell may encounter during their life cycle. Despite the importance of DNA replication restart, conservation of mechanism does not seem to occur. Indeed, while PriA is well conserved across bacteria genera, other members of the RRP are less so, generally confined to the γ-proteobacter clade of Gram negative bacteria. Within PriA, diverse mechanisms may also exist. One example is the PriA from *Deinococcus radiodurans*, which contains a CRR, but appears to have lost its ATPase, and presumably, its helicase, activities as it lacks both clear Walker A and B motifs essential for nucleotide binding and hydrolysis. While helicase activity is not essential for DNA replication restart, the ability of *D. radiodurans* to deal with diverse DNA structures becomes a question of interest. Gram positive bacteria like *Bacillus subtilis* possess PriA orthologues, but also possess additional factors such as DnaD and DnaI which may serve similar functions to PriB and DnaT in *E. coli* as they function to load the replicative helicase (20), However, there is conflicting data that suggests that the helicase loader by itself can reload the replicative helicase (21). Clearly, a broader understanding of diverse mechanisms of DNA replication restart is required to fully understand this process in depth. Such an understanding will aid in understanding such mechanisms in other kingdoms of life, especially in eukaryotes, where slowly it is being accepted that DNA replication restart does occur even though the players that might be involved in such mechanisms are unknown.

References

1. Cox MM, *et al.* (2000) The importance of repairing stalled replication forks. *Nature* 404(6773):37-41 .

2. Tanaka T, Mizukoshi T, Sasaki K, Kohda D, & Masai H (2007) *Escherichia coli* PriA protein, two modes of DNA binding and activation of ATP hydrolysis. *J Biol Chem* 282(27):19917-19927 .

3. Zavitz KH & Marians KJ (1993) Helicase-deficient cysteine to glycine substitution mutants of *Escherichia coli* replication protein PriA retain single-stranded DNA-dependent ATPase activity. Zn^{2+} stimulation of mutant PriA helicase and primosome assembly activities. *J Biol Chem* 268(6):4337-4346 .

4. Cadman CJ & McGlynn P (2004) PriA helicase and SSB interact physically and functionally. *Nucleic Acids Res* 32(21):6378-6387 .

5. Shereda RD, Kozlov AG, Lohman TM, Cox MM, & Keck JL (2008) SSB as an organizer/mobilizer of genome maintenance complexes. *Crit Rev Biochem Mol Biol* 43(5):289-318 .

6. Zhou R, *et al.* (2011) SSB functions as a sliding platform that migrates on DNA via reptation. *Cell* 146(2):222-232 .

7. Wessel SR, *et al.* (2013) PriC-mediated DNA replication restart requires PriC complex formation with the single-stranded DNA-binding protein. *J Biol Chem* 288(24):17569-17578 .

8. Harami GM, Gyimesi M, & Kovacs M (2013) From keys to bulldozers: expanding roles for winged helix domains in nucleic-acid-binding proteins. *Trends Biochem Sci* 38(7):364-371 .

9. Schekman R, Weiner JH, Weiner A, & Kornberg A (1975) Ten proteins required for conversion of phiX174 single-stranded DNA to duplex form in vitro. Resolution and reconstitution. *J Biol Chem* 250(15):5859-5865 .

10. Wickner S & Hurwitz J (1975) Association of phiX174 DNA-dependent ATPase activity with an Escherichia coli protein, replication factor Y, required for in vitro synthesis of phiX174 DNA. *Proc Natl Acad Sci U S A* 72(9):3342-3346 .

11. Zittel MC & Keck JL (2005) Coupling DNA-binding and ATP hydrolysis in *Escherichia coli* RecQ: role of a highly conserved aromatic-rich sequence. *Nucleic Acids Res* 33(22):6982-6991.

12. Tanaka T, *et al.* (2002) DNA binding of PriA protein requires cooperation of the N-terminal D-loop/arrested-fork binding and C-terminal helicase domains. *J Biol Chem* 277(41):38062-38071 .

13. Soultanas P, Dillingham MS, Velankar SS, & Wigley DB (1999) DNA binding mediates conformational changes and metal ion coordination in the active site of PcrA helicase. *J Mol Biol* 290(1):137-148.

14. Chin JW, Martin AB, King DS, Wang L, & Schultz PG (2002) Addition of a photocrosslinking amino acid to the genetic code of *Escherichia coli*. *Proc Natl Acad Sci U S A* 99(17):11020-11024 .

15. Farrell IS, Toroney R, Hazen JL, Mehl RA, & Chin JW (2005) Photo-cross-linking interacting proteins with a genetically encoded benzophenone. *Nat Methods* 2(5):377-384 .

16. Ryu Y & Schultz PG (2006) Efficient incorporation of unnatural amino acids into proteins in Escherichia coli. *Nat Methods* 3(4):263-265 .

17. Lopper M, Boonsombat R, Sandler SJ, & Keck JL (2007) A hand-off mechanism for primosome assembly in replication restart. *Mol Cell* 26(6):781-793 .

18. Bhattacharyya B*, et al.* (2014) Structural mechanisms of PriA-mediated DNA replication restart. *Proc Natl Acad Sci U S A* 111(4):1373-1378 .

19. Lopper M, Holton JM, & Keck JL (2004) Crystal structure of PriB, a component of the *Escherichia coli* replication restart primosome. *Structure* 12(11):1967-1975 .

20. Velten M*, et al.* (2003) A two-protein strategy for the functional loading of a cellular replicative DNA helicase. *Mol Cell* 11(4):1009-1020 .

21. Soultanas P (2002) A functional interaction between the putative primosomal protein DnaI and the main replicative DNA helicase DnaB in *Bacillus*. *Nucleic Acids Res* 30(4):966-974 .